BOREFLOW SIMULATION AND ITS APPLICATION TO GEOTHERMAL WELL ANALYSIS AND RESERVOIR ASSESSMENT

Danilo C. Catigtig*
UNU Geothermal Training Programme
National Energy Authority
Grensasvegur 9, 108 Reykjavik
Iceland

*Permanent address:
Philippine National Oil Company (PNOC)
Energy Development Corporation (EDC)
Geothermal Division
PNOC Energy Companies Building
Merritt Road, Ft. Bonifacio
Makati, Metro Manila
PHILIPPINES

1983.12.12. JE/SPK/sá

Dr. Ingvar Birgir Fridleifsson,
Geothermal Project Co-ordinator,
UNU Geothermal Training Programme,
Reykjavík, Iceland.

Dear Sir.

This report is written by Mr. Danilo C. Catigtig, engineer of the PNOC, Energy Development Corporation, Philippines. It concludes his successful training as a UNU Fellow in Reservoir Engineering.

Prior to his work Mr. Catigtig has successfully completed the special course in which the Geothermal Reservoir Engineering Lecture Notes were used as a textbook (UNU Geothermal Training Programme Report No. 1983-2). We undersigned served as his supervisors on the research project that is described in this report. He also received tuition in reservoir engineering from Mr. Gísli Karel Halldórsson and Mr. Ómar Sigurdsson.

The objective of the work was to train Mr. Catigtig in computer simulation of the pressure and temperature profiles of blowing geothermal wells, and interpreting and using the results in the investigation and harnessing of geothermal reservoirs.

For this work we used data from the South Negros geothermal field in the Philippines, supplied by Mr. Catigtig. This data is not the complete data aquired in reservoir engineering investigations in South Negros. Missing data elements have been supplied by the instructors according to their own estimate, when this has been neccessary in course of the work.

This use of the South Negros data has the educational purpose only, to train the student in understanding and processing reservoir engineering data, as is the objective of the UNU Geothermal Training Programme. The results and conclusions in this report, therefore, may or may not be compatible or incompatible with South Negros reservoir engineering practice, without this having any effect whatsoever on Mr. Catigtig's successful completion of his training and study.

Yours sincerely,

Jónas Elíasson

Jónas Elíasson, lic. techn.,
Professor,
University of Iceland.

Snorri Páll Kjaran

Snorri Páll Kjaran, lic. techn.,
Managing Director,
VATNASKIL Consulting Engineers Ltd.

ABSTRACT

The simulation of flowing pressure profiles in geothermal wells is dealt with using a computer program. The validity of the program is tested against measured temperature and pressure profiles in the Southern Negros Geothermal Field (SNGF) in the Philippines. Various correlations to calculate the slip, void fraction occupied by the vapor phase, and the two-phase multiplier for the friction factor were tried in this program and are presented in Appendix B. The possible applications that can be derived from the simulation are discussed.

TABLE OF CONTENTS

LIST OF FIGURES

and

4

4

and

LIST OF TABLES

1 INTRODUCTION

1.1 Scope and objective of work

The Philippines is one of the many countries in the world located on a plate boundary, and for this reason it is endowed with enormous geothermal resources. The country is at present very much dependent on oil for its energy needs of which a significant portion is being used for power generation. The steady increase in oil prices prompted the Philippine government to explore alternative sources of energy. Presently, the government has embarked on an accelerated development program to harness geothermal energy as an indigenous power source. The development program calls for an estimated installed capacity of 1774 MW electricity at the end of 1985, which by that time is estimated to be about 12% of the total energy needs (Elizagaque and Tolentino, 1982). In line with this, the government has contracted foreign experts in geothermal technology for assistance in the exploration, development, and utilization of the geothermal resources. Selected Filipinos are also sent abroad for training in this field of technology. To mention a few, some of these countries are New Zealand, Iceland, and Japan.

The author in particular was awarded a UNU Fellowship and a place in the 1983 UNU Geothermal Training Programme held in the National Energy Authority in Reykjavik, Iceland. He attended a specialized training course in Reservoir Engineering.

The training programme as a whole included introductory lectures in various disciplines of geothermal technology such as; drilling, surface and borehole geophysics, surface and borehole geology, surface and borehole geochemistry, production and utilization, and reservoir engineering, for approximately six weeks. The next six weeks were spent on specialized lectures in borehole geophysics and reservoir engineering. Before commencing the specialized training in reservoir engineering, a one week excursion and seminar on the various geothermal fields of Iceland was held. The specialized studies started in the second half of the 6-month training course. The author also obtained a brief training in the use of the computer installed in the NEA.

The computer program used in this paper was initially written by G.K. Halldorsson of Vatnaskil Ltd., a geothermal consulting firm in Iceland, and modified by the author. The modifications made into the program involved the use of steam table correlations, and taking into consideration the effects of more than one feed zone and the fluid salinity and non-condensible gases. The specialized training was mostly centered on the simulation of flowing temperature and pressure profiles in geothermal wells and the interpretation of the results relative to the geothermal field considered.

2 THE SOUTHERN NEGROS GEOTHERMAL FIELD

2.1 General background

The Southern Negros Geothermal Field (SNGF) is located on the southern part of the Negros Island (Fig. 1). The field is specifically located in a valley formed between two dormant andesitic volcanoes, namely the Cuernos de Negros to the south, and Mount Balinsasayao to the north (Bagamasbad, 1979). The whole field is dissected by a series of NW-NNW trending right lateral faults, NE trending left lateral faults, and a system of step faults striking WNW, NW and NE (Fig. 2).

The SNGF consists of two promising geothermal areas, the Palinpinon field located on the eastern side of the valley, and the Baslay-Dauin field situated at the southern slope of the Cuernos volcano. The two fields are characterized by various surface thermal manifestations such as hot springs, fumaroles, and altered ground. The most intense surface manifestations are located in the Palinpinon area and that area is presently at an advanced stage of development, whereas the Baslay Dauin field is yet at an early stage of exploration drilling.

Geophysical surveys conducted in the area, with electrode spacings of AB/2 of 250 and 500 m (Bagamasbad, 1979), identified four significant anomalies (5, 10, 20, and 50 ohm-m), all converging towards the Cuernos volcano (Fig. 3). Isothermal contours drawn for the Palinpinon field at aquifer depths (Figs. 4,5,6,7), also indicated high temperatures towards the Cuernos volcano. This may indicate that the probable heat source of the SNGF geothermal system is the Cuernos volcano.

Early geochemical investigations and borehole production geochemistry are well summarized by O.T. Jordan (1982). Both the results obtained from geochemistry and flow

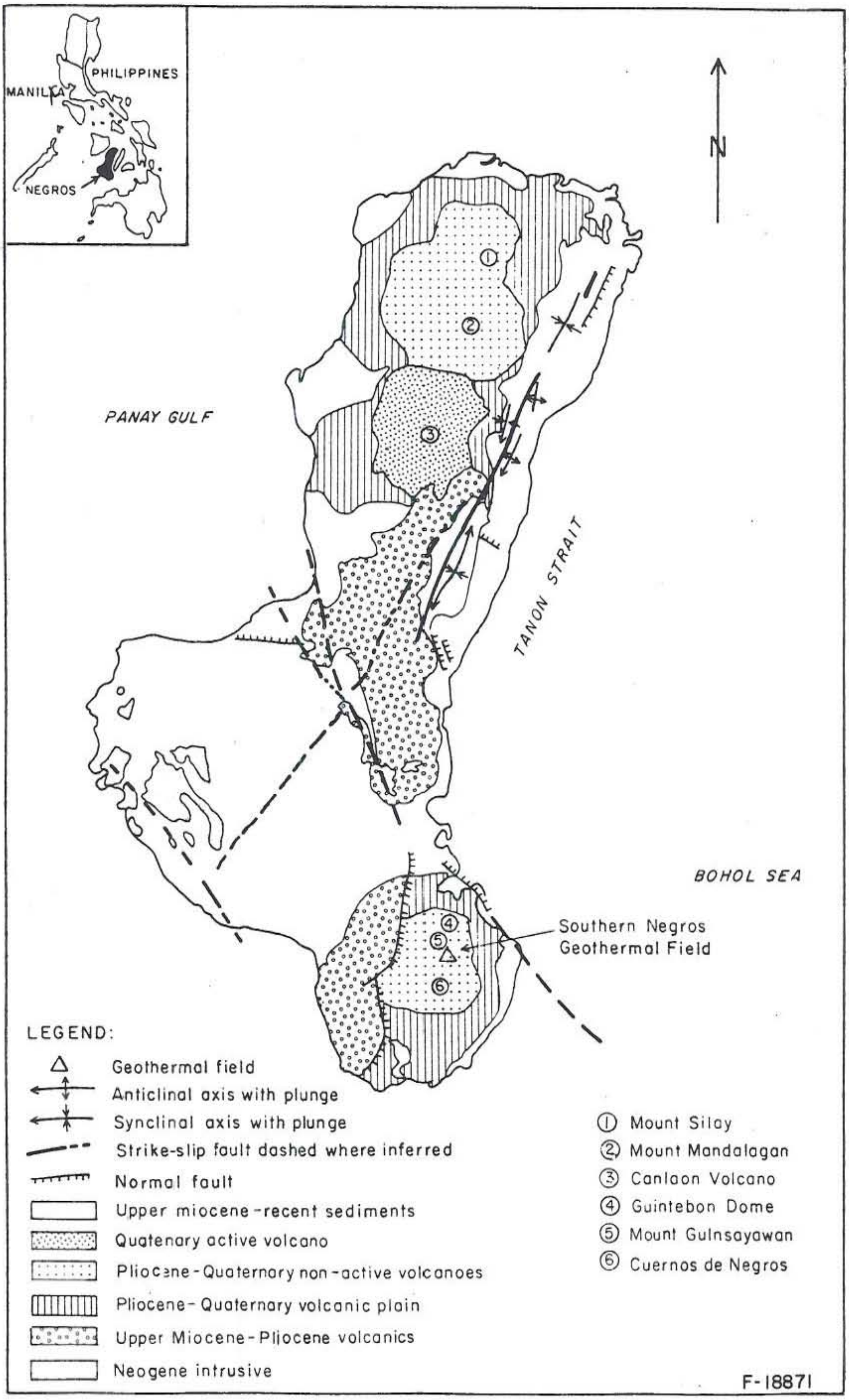

FIGURE 1 Map of Negros Island showing general geology and structures (after Jordan,1982)

JHD-HSP-9000-DCC
83-09-1195

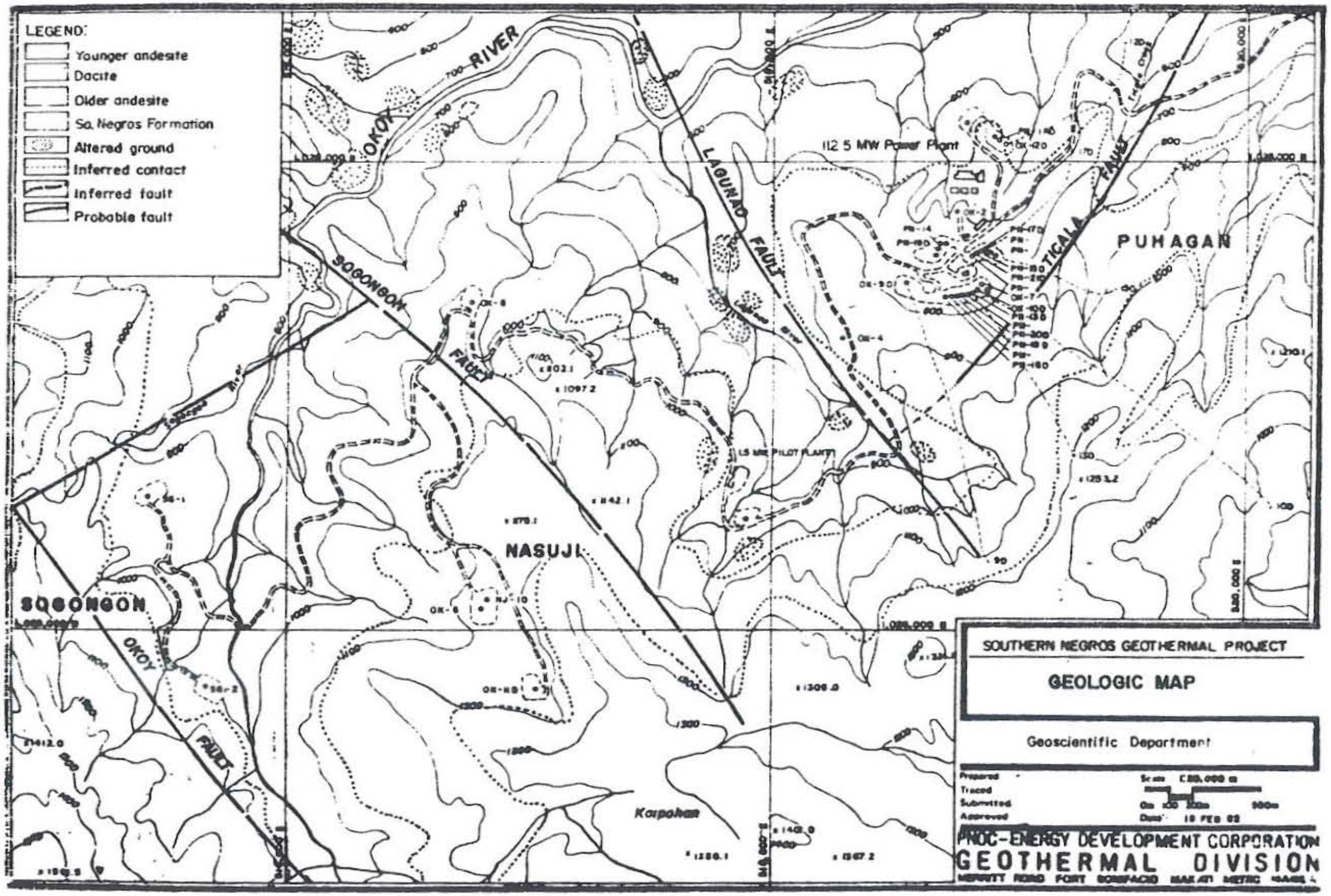

Fig. 2 Map showing faults intersecting the Southern Negros Geothermal Field

JHD-HSÞ-9000-OJ,
82.09.1108 AA

Figure 3 Map of Palinpinon field showing resistivity contours, distribution of thermal springs, and location of boreholes

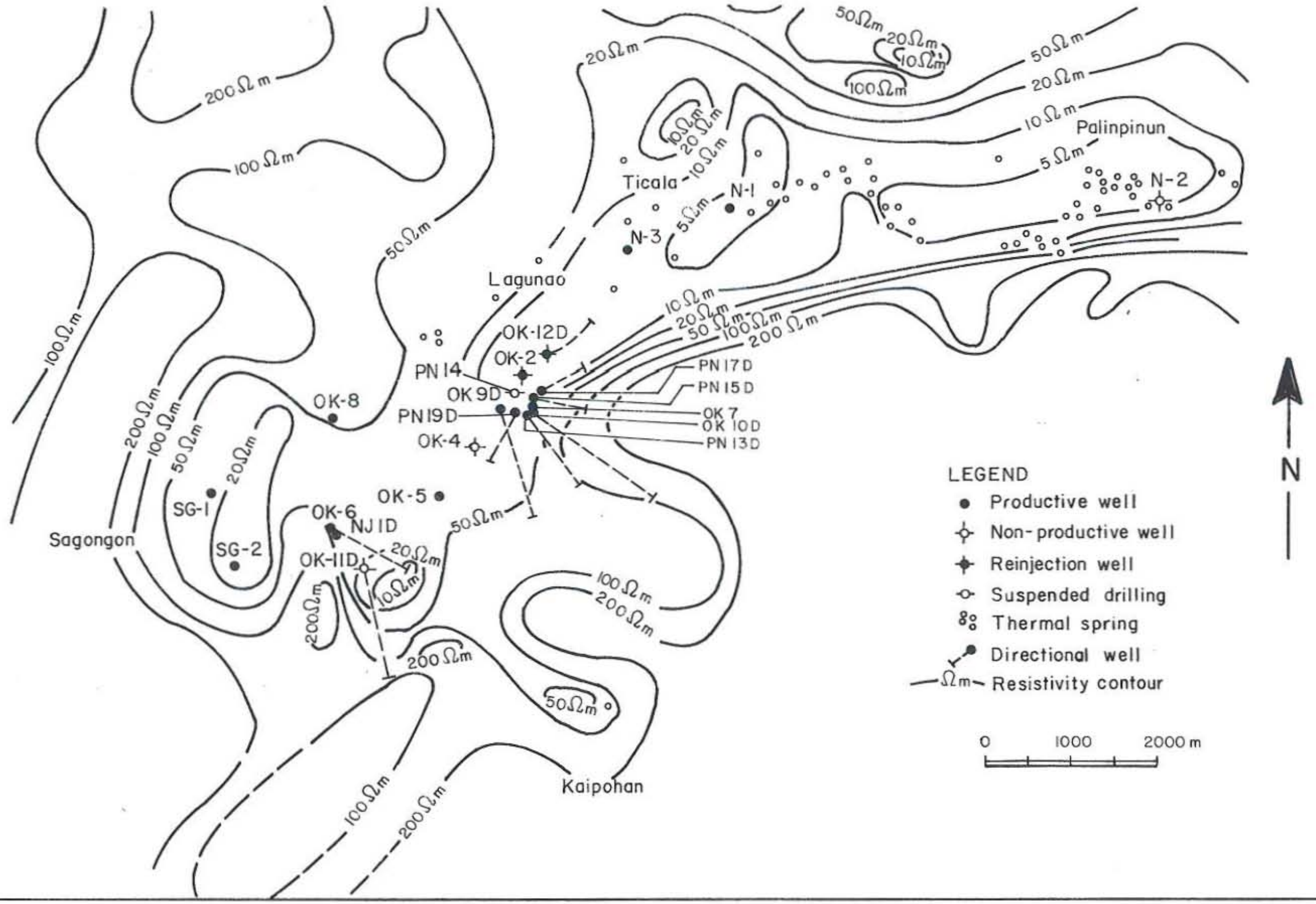

JHD-HSP-9000-DCC
83-09-1193

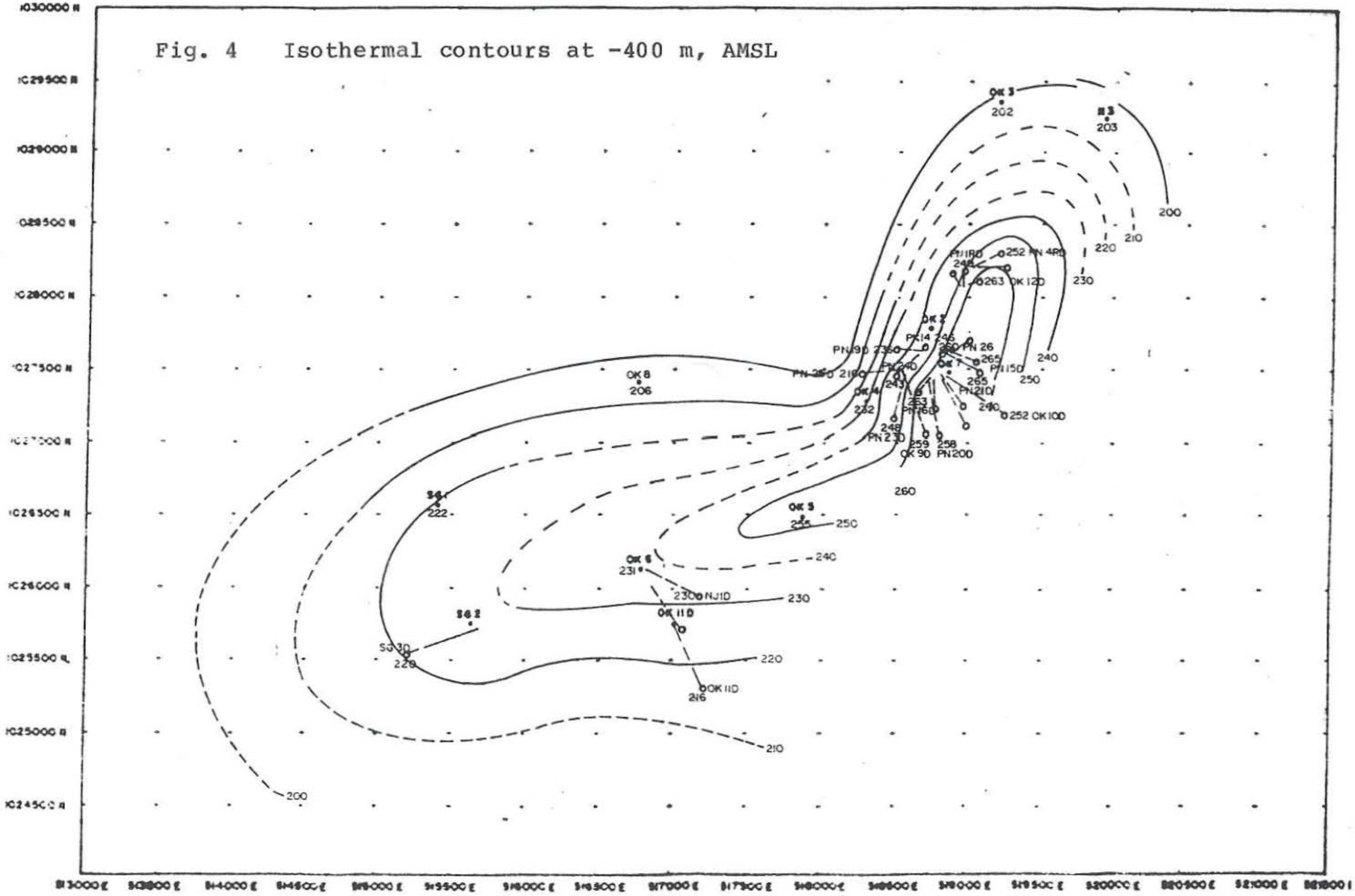

Fig. 4 Isothermal contours at -400 m, AMSL

JHD-HSP-9000-DCC
83-09-1192

Fig. 5 Isothermal contours at -800 m, AMSL

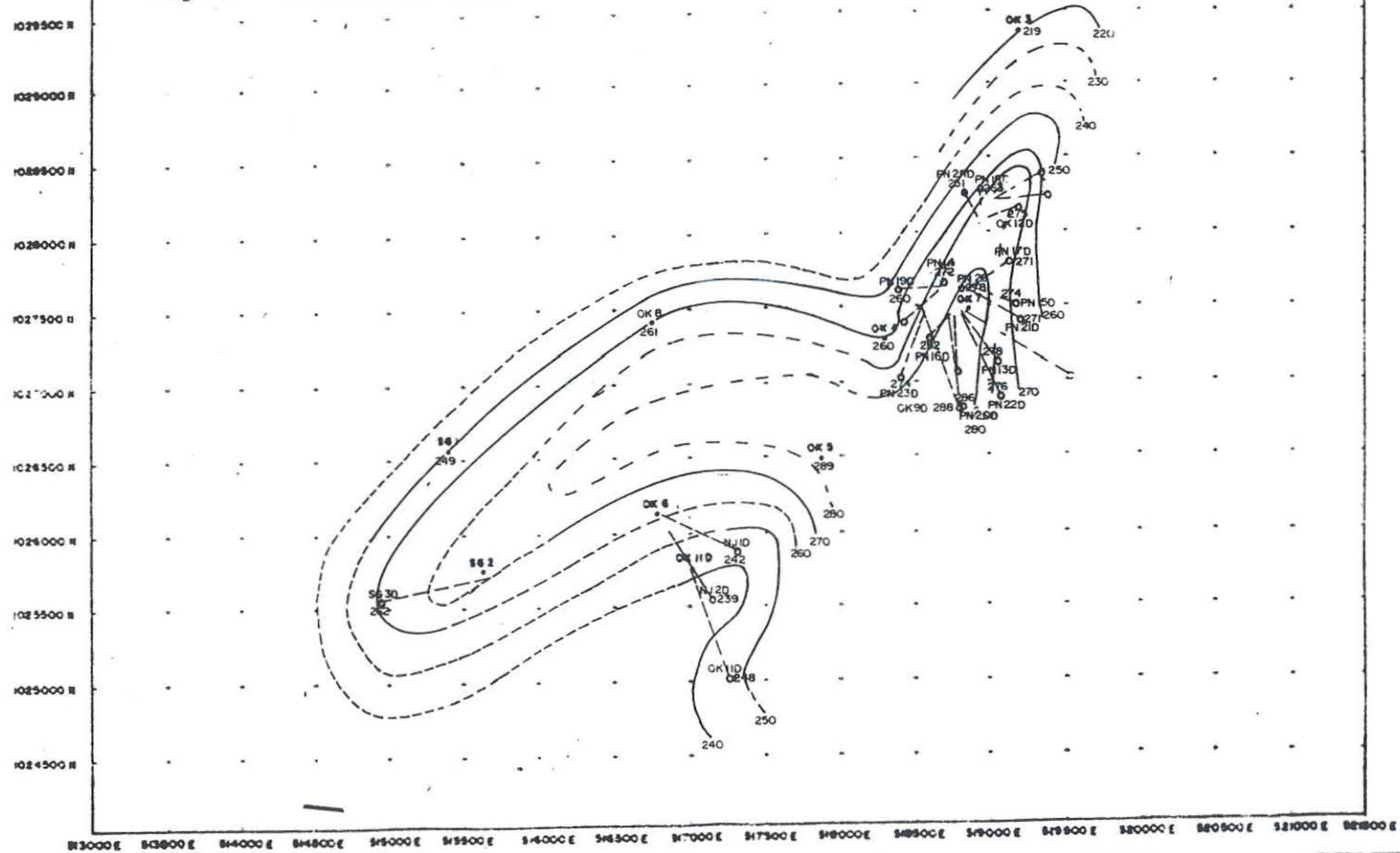

JHD-HSI 9000-DCC
83-09-1196

Fig. 6 Isothermal contours at -1200 m, AMSL

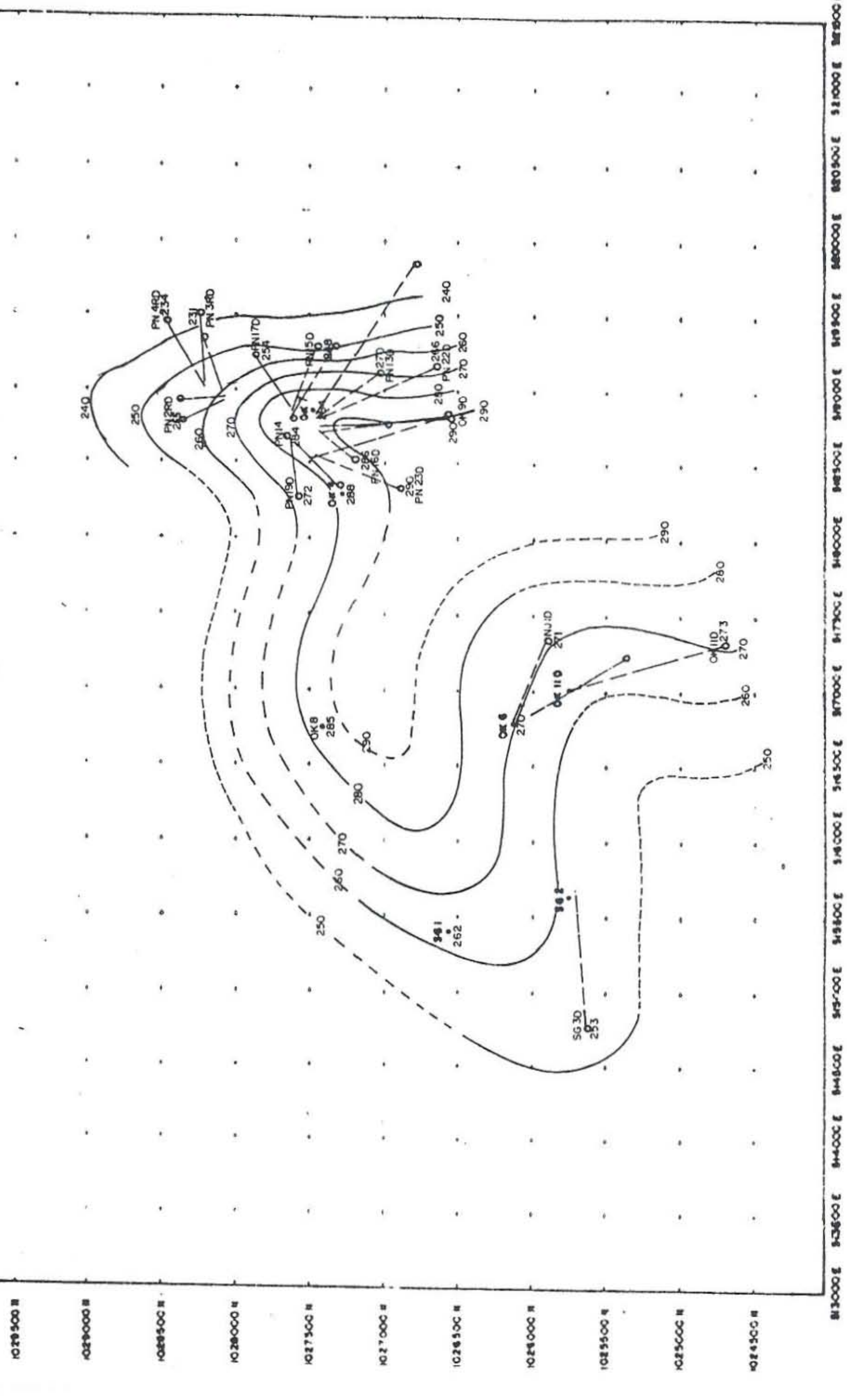

JHD-HSI 9000-DCC
83-09-1199

Fig. 7 Isothermal contours at -1600 m AMSL

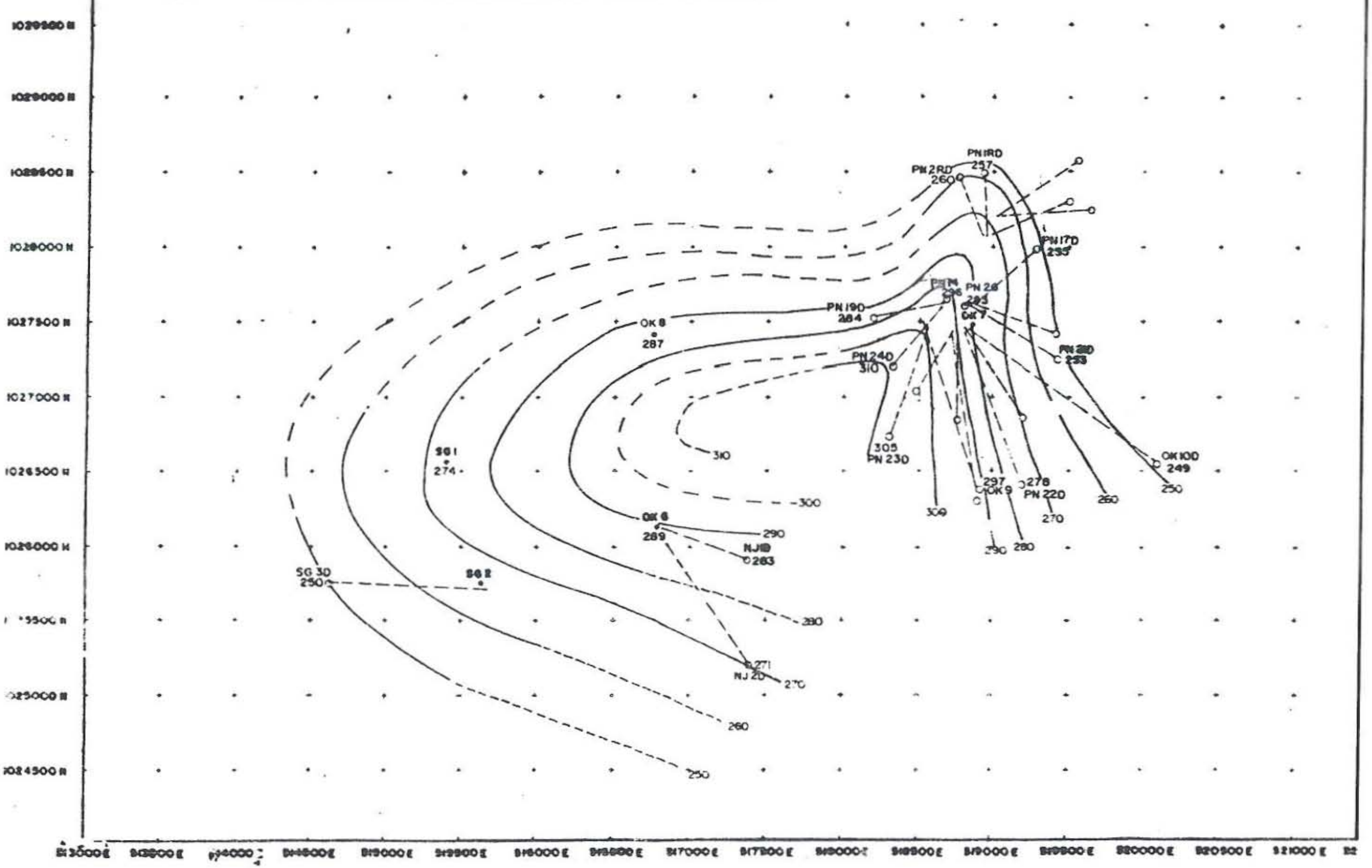

testing suggest that the field has two significant aquifers at depth, aptly referred to as the upper and lower production zones.

2.2 Drilling and production history

Exploration drilling started in 1976 and was concentrated within the 20 ohm-m resistivity anomaly trending E-W along the 9 km long main axis of the Okoy valley. Two shallow wells (N1 and N2) drilled in the easternmost part of the anomaly showed temperature reversals at depth, with N1, drilled west of N2, indicating a relatively higher temperature, implying that the wells had intersected a flow path that originated upstream. With this basis, N3 was drilled farther west. This well showed a temperature of 238°C at 600 m depth, which was higher than those measured at N1 and N2. The well was flowed and a geofluid of 39.5 kg/s was extracted. With this encouraging result, drilling was continued NE and SW of N3 with the objective of defining the extent of the geothermal anomaly. The northeastern wells (Okoy 1 and Okoy 3) showed non-favourable results, whereas, the southwestern wells (Okoy 2, 4, and 5) had good but varying results. Okoy 2 was flowed succesfully yielding 25 kg/s of geofluid at an inflow temperature of 250°C at 950 m. Okoy 4, though it exhibited a high temperature of 299°C at 1980 m, showed low permeability and was flowed for only approximately 24 hours. Okoy 5 is a step-out well in the 50 ohm-m anomaly. After great problems in discharging it, it was successfully flowed by steam injection on the 14th attempt (Catigtig, 1981a). The attempts to flow this well took approximately 6 months after completion of drilling, from December 1978 to May 1979. During this period, the lone drill rig in the area was shipped to the Tongonan geothermal field in Leyte. However, with the successful discharge of Okoy 5 the rig was brought back to the Palinpinon field and drilling was continued SW (Okoy 6) and NE (Okoy 7) of Okoy 5 (Fig. 8). Okoy 7 was successfully flowed by air-compression and Okoy 6 by steam injection. These discharges were carried out in

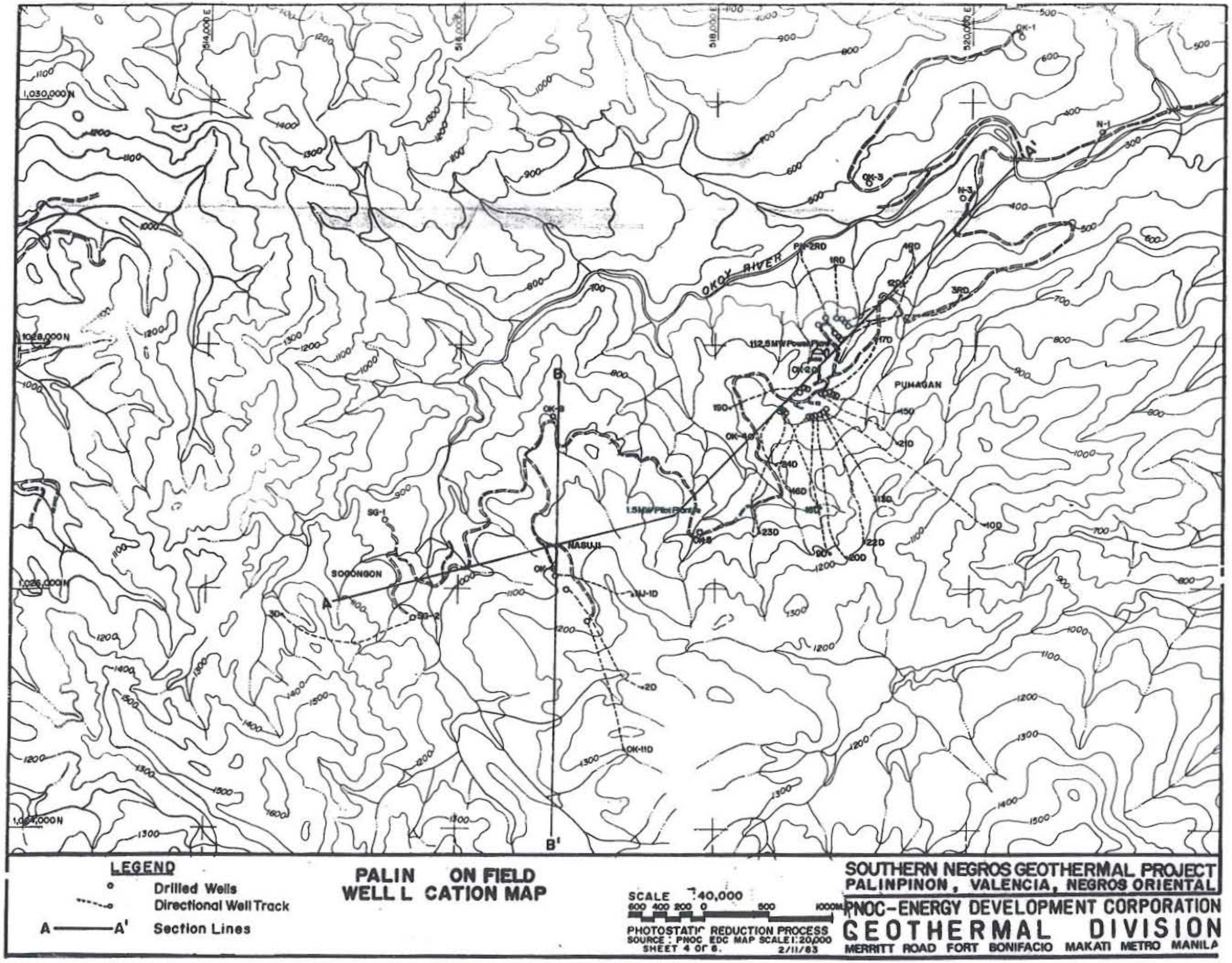

Fig. 8 Plan view of the Southern Negros Geothermal Field

the middle of May 1980. Since then exploration and production drilling has been carried out and a 112.5 MWe installed capacity was committed for 1983 in the Okoy 7 area (Puhagan). An additional 110 MWe was also envisioned in the western part (Okoy 6 area; Nasuji and Sogongon) in the foreseeable future.

Okoy 2, Okoy 5, Okoy 6, and Okoy 7 decided the full scale development of the field. Pertinent data of these wells are as follows;

Well	Elevation (m, AMSL)	Depth (m)	MAXIMUM Temp/Depth (°C/m)	Flow (kg/s)
OK 5	932.2	1975.2	310/1975	32.0
OK 6	1105.4	2770.8	296/2500	82.0
OK 7	756.1	2882.8	319/2600	88.0
OK 2	704.4	1164.4	250/ 950	25.0

2.3 Brief status of geothermal development

The impressive thermal manifestations and encouraging geological, geophysical, and geochemical results, prompted the development of the Palinpinon field ahead of the Baslay-Dauin field. As of July 1983 a total of 45 wells had been drilled. Since October 1980, three wells have been used to supply two pilot units with 1.5 MWe capacity each. These wells are Okoy 5, Okoy 7, and PN 13D, the last of which is directionally drilled. A 112.5 MWe plant is expected to be operational in the Palinpinon I area by 1983, and another 110 MWe plant for the Palinpinon II area in the near future. Fig. 9 shows the location of the wells for the Palinpinon I plant.

The Palinpinon field has been divided into three geographical areas. Farthest to the east is the Puhagan area, where the Palinpinon I plant and production/reinjection

JHD-HSÞ-9000-DCC
83.09.1079-IS

FIG. 9 PRODUCTION / REINJECTION WELLS FR PALINPINON I PLANT

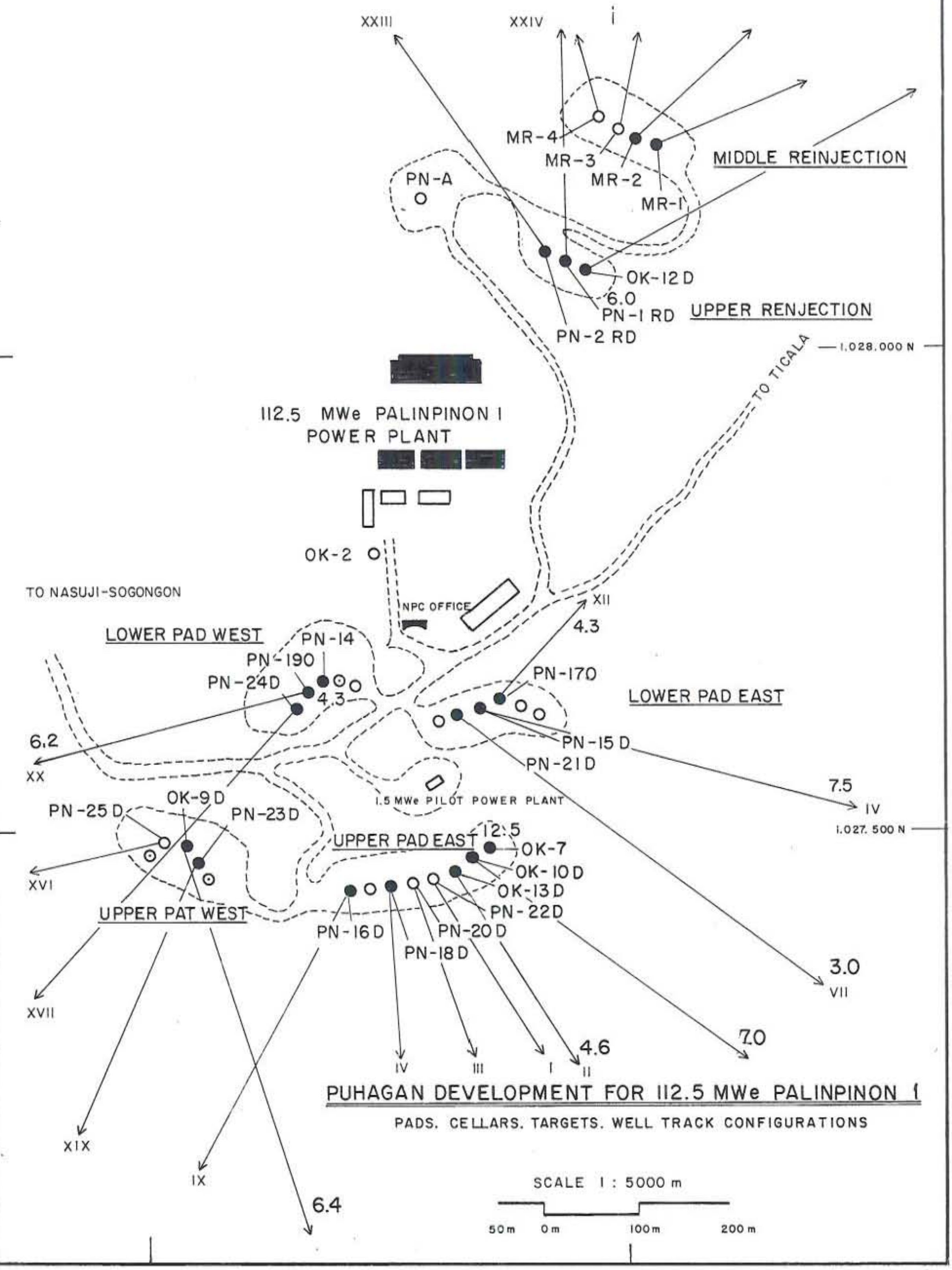

well pads are located, and to the southwest are the Nasuji and Sogongon areas, where the Palinpinon II plant and production/reinjection well pads are to be located.

Due to the steep topography that characterizes the geothermal field, directional drilling has been adopted to reach prospective target areas from pads located near the power station. This method increases drilling cost considerably, but in turn will reduce the costs to be incurred in road construction and site preparation, and installation of fluid collection and transmission systems.

3 PROGRAM APPLICATION

3.1 Introduction

One of the most important parameters used in geothermal reservoir assessment is the downhole pressure data. This can either be measured at static and/or flowing conditions. However, flowing measurements are not always simple, as more often than not, geothermal wells are characterized by high fluid velocities making it impractical to lower a pressure recorder into the well, else it will be thrown out. In common practice, SNGF experience, flowing downhole measurements are conducted with the well discharging at not more than 28 kg/s, measning, the well has to be throttled to maintain a flowrate throughout the test. Thus, flowing downhole measurements are limited to these low flowrates.

This limitation makes simulation of flowing pressure profiles at any discharge condition important. And this can only be done by using two-phase flow models available in the literature (e.g., Hagedorn and Brown, 1965). Some of these models are discussed by Halldorsson (1978).

The ability to predict flowing well pressures and temperatures is of utmost importance in applications such as mentioned below:

1. To establish deliverability curves for a certain well.
2. Determination of the necessary conditions in starting up a well.
3. Determination of the effects of elevation on production.
4. Determination of the effects of casing string diameters on production.
5. Determination of the effects of chemical deposits and/or blockage to production.
6. Determination of the depletion rate of a producing well and aquifer.

These applications are discussed in this paper.

3.2 Fluid mechanics of the flow

Most of the known geothermal fields in the world have a liquid dominated reservoir and produce under-saturated water at the wellface at its early stages of exploitation (Gould, 1974). For the fluid to flow from a producing aquifer to the wellbore, a sufficient pressure differential must exist between them. For a sifficiently low turbulent pressure drop,

$$W = (P.I.) \times (Pa - Pwf) \qquad (1)$$

where; W = mass flowrate at wellface, kg/s; P.I. = productivity index, kg/s-MPa; Pa = aquifer pressure, MPa; Pwf = well pressure, MPa.

From its initial state (undisturbed condition), well pressure is equal to the aquifer pressure at the feed zone. Grant (1981) suggests that this pressure can be measured at the pivot point (pressure Control Point = PCP) of the static pressure profiles during warm-up. However, in wells with a strong downflow, the pressure measured at the PCP may differ from the true aquifer pressure when the well is discharging if the main producing zone is the lower zone, which in most cases is hotter than the downflowing fluid. If the well has only one feed zone then the PCP is most likely to occur adjacent to the feed zone itself, and for multi-zone wells the location of the PCP will be a weighted average between the zones. When production starts, aquifer pressure drops as a result of the fluid extraction. Most of this pressure reduction will be due to turbulence (Fig. 10).

$$(P_a - P_{wf}) = CW^2 \qquad (2)$$

where C = turbulence factor, $MPa/(kg/s)^2$

The turbulence factor, C, can be obtained from the slope of (Pa - Pwf)/W vs. W linear graph (Jacob and Rorabaugh, 1946) for a step drawdown test. However, for self flowing wells with high fluid velocities, Pwf can't be measured at all flowrates. In this paper, a turbulence factor was assumed to calculate for Pwf. If the initial reservoir pressure, Pi, is known, the well can be divided into laminar and turbulent zones (Fig. 11). The total pressure drop from the reservoir to the wellface can be presented as;

$$P_i - P_{wf}) = (dP)_1 + (dP)_t + (dP)_s \qquad (3)$$

where $(dP)_1$ = laminar pressure drop, $(dP)_t$ = turbulent pressure drop, $(dP)_s$ = pressure drop due to skin.

These pressure drops are treated in appendix B.

These pressure drops in the formation, if significantly large compared to the saturation pressure of the inflow temperature, will cause the fluid to flash in the formation itself and hence produce a two-phase column throughout the entire length of the well.

If during the flowing process, the fluid state is still single phase at well entry, a reduction in flowing well pressure occurs until such a time that the fluid eventually flashes developing into a steam-water mixture and experiences temperature and enthalpy drops. The situation will be similar if the fluid flashes in the formation and enters the well as a two-phase mixture (Sanyal and Juprasert, 1977).

Based on an assumption of a steady, homogeneous, one-dimensional fluid flow in a pipe, and using the conservation of mass, momentum, and energy, the following equation is formulated (see appendix A):

$$-(dP/dz) = \rho g + (f/2D)\rho V^2 + \rho V(dV/dz) \qquad (4)$$

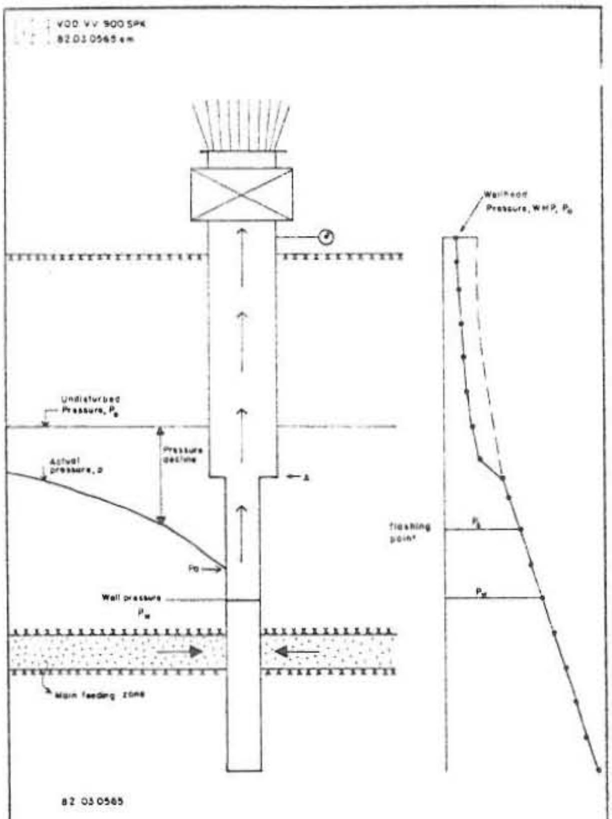

FIG. 10 CONFIGURATION OF A FLOWING WELL
(after Kjaran and Eliasson)

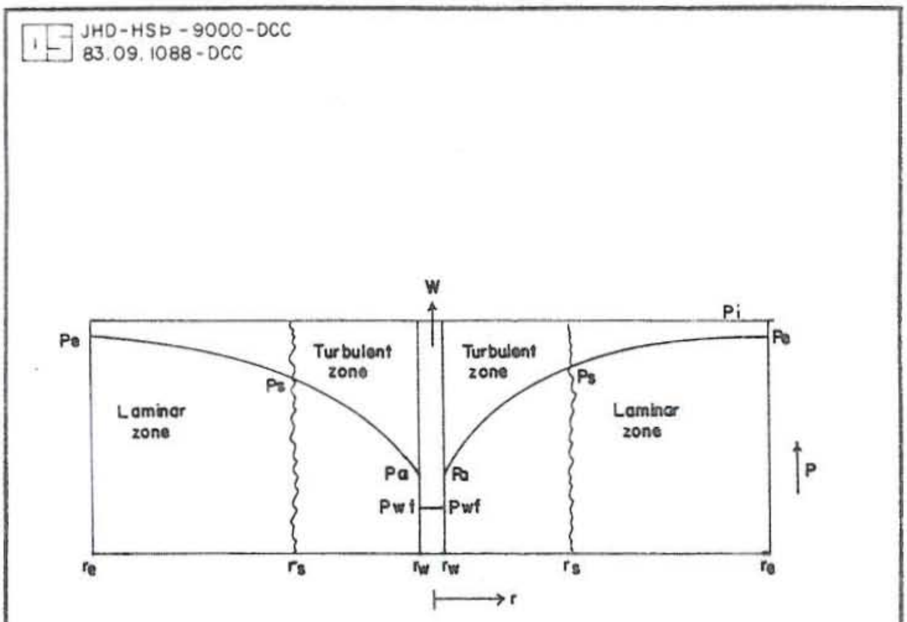

FIG. 11 Pressure configuration in laminar and turbulent zones

From the equation, it can be seen that the total pressure gradient is made up of three individual gradients: potential, friction, and acceleration.

In the single phase section of the flow, the fluid density is substantially constant except for changes in flow area, hence the acceleration term has a negligible effect. Most of the pressure drops then will be caused by potential gradient and friction. At the two-phase section the three gradients should be considered. During the flowing process, the fluid experiences flow regime changes in an upward direction, viz; bubbly, slug, churn, and annular.

BUBBLE FLOW. At the flashing point, vapour bubbles will start to form at nucleation sites within the liquid and at the liquid boundary. These bubbles have substantially the same size at nucleation, but grow at different rates as a consequence of coalescence and/or continuous vaporization arising from continuing pressure reduction. The vapour is the dispersed phase and the liquid the continuous phase.

SLUG FLOW. As pressure reduction continues, large bubbles forme with cross-section that may approximate the cross-section of the pipe itself but are separated at regular intervals by lenghts occupied mainly by liquid.

CHURN FLOW. Further generation of vapour causes reduction in average fluid density and a corresponding increase in fluid velocity occurs. The slug structure becomes unstable and collapses with consequential oscillatory motion. The size, disposition, and movements of the dispersed vapour elements are much less regular than with bubble or slug flow.

ANNULAR FLOW. At this stage of the flowing process, the vapour phase occupies a much larger area than the liquid phase. The vapour then coalesces and forms a continuous phase within the flow leaving the liquid flowing in a form of a thin film occupying the annular space between the vapour phase and the flow pipe. The vapour phase may or may not contain dispersed liquid and the liquid phase may or may not contain residual vapour bubbles. Fig. 12 shows the flow regime patterns, and Fig. 13 shows the flow regime map. The churn flow is the transition regime from slug to annular. In Fig. 13, mist and annular flow is treated as annular, and slug and froth as slug flow in this paper.

For steam-water production wells these flow regimes can coexist in the same pipe. Also, unless the liquid is completely entrained in the steam phase, slip is always occuring between the phases as a result of the differences of their average linear velocities. Evaluation of the fluid properties at the two-phase section depends on the choice of the correlation for the slip, void fraction occupied by the vapour phase, and the two-phase friction correction factor. These correlations are well summarized by Haldorsson (1978).

The Armand and Teacher (1959) correlation to calculate the void fraction, and the Chisholm (1972) correlation to calculate the two-phase multiplier were found to give the best fit. The flow regime map of Griffith and Wallis (1961) was used to determine the flow regimes.

In this report roughness of 1.37E-4 m, 4.57E-5 m, and 3.047E-4 m were used for the liner, production casing, and for depositions respectively. These absolute factors correspond to asphalted cast iron, commercial steel, and concrete in the order presented above.

3.3 General background of the wells considered

To test the validity and predictive capability of the computer program used in this paper, representative downhole flowing temperature and pressure data obtained from wells drilled in specific areas of the Palinpinon geothermal field were used. These wells are; Okoy 5 (Balasbalas), Okoy 6 (Nasuji), Okoy 7 (Puhagan), and SG 1 (Sogongon). The Nasuji, Balasbalas, and Sogongon areas

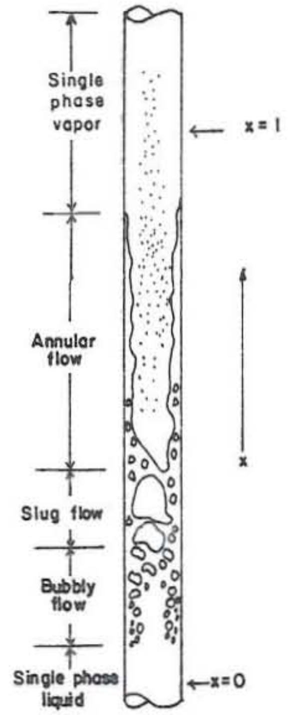

FIG.12 FLOW PATTERNS DURING UPWARD FLOW

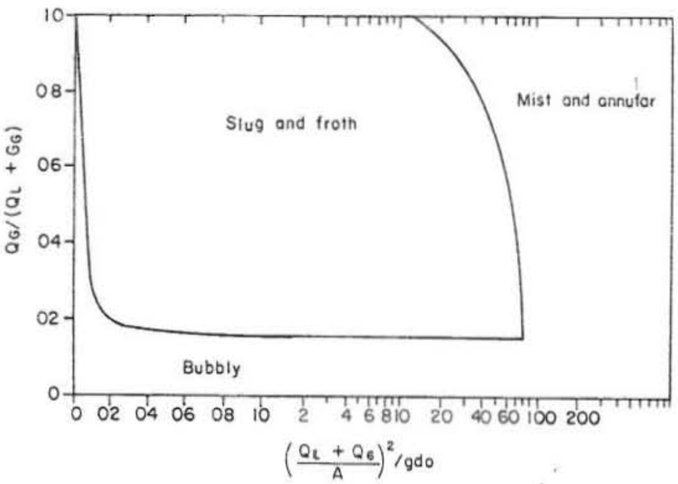

FIG. 13a FLOW REGIME MAP OF GRIFFITH & WALLIS (1961)

belong to the Palinpinon II development scheme, and Puhagan belongs to the Palinpinon I development where, a 112.5 MWe plant is being installed. The program was calibrated against the above mentioned measured data.

3.3.1 Okoy 5

Okoy 5 was drilled in the period 20 Oct. to 3 Dec. 1978 as a step-out well outside the 20 ohm-m resistivity anomaly along the main axis of the Okoy valley. It penetrated through the volcanic Southern Negros Formation (SNF) of late Miocene to Pliocene age, and into the Okoy Sedimentary Formation (OSF). The total drilled depth is 1975 m. Temperature logs conducted on the well indicated loss zones at 1100-1200 m, 1450-1500 m, and at 1700 m. During production, the main feed zone was found to be at 1450-1500 m at a temperature of 264°C. Flow tests showed that the well exhibited an unstable cyclic behaviour at high wellhead pressures due to interaction between the aquifers, but a stable discharge was obtained at low wellhead pressures. A relatively high enthalpy of 1900 J/g average was measured. Flowing pressure profiles indicated that boiling occurs in the aquifer during discharge, although at static conditions the well contains single-phase fluid and has a zero shut-in wellhead pressure. This pre-flashing of the fluid in the formation caused it to become two-phase at the wellface. Geochemical analysis of the discharge fluid confirmed the existence of the three feed zones and the boiling of the fluid in the aquifer during discharge. Okoy 5 was the first well to be discharged by steam injection in the Palinpinon field, after 13 unsuccessful discharge attempts using various stimulation techniques, including the injection of compressed air. The well has a power potential of 8.5 MWe at 0.72 MPag separation pressure and 2.82 kg/s-MWe steam rate. The well has been used to supply steam to a 1.5 MWe non-condensing turbine since October 1980, as a part of the 3 MWe pilot plant inatalled in Southern Negros, with the other unit being connected to Okoy 7. The output characteristics are shown in Fig. 14.

JHD-HSÞ-900-DCC
83.09.1083-DCC

FIG. 14 OKOY 5 OUTPUT CHARACTERISTICS

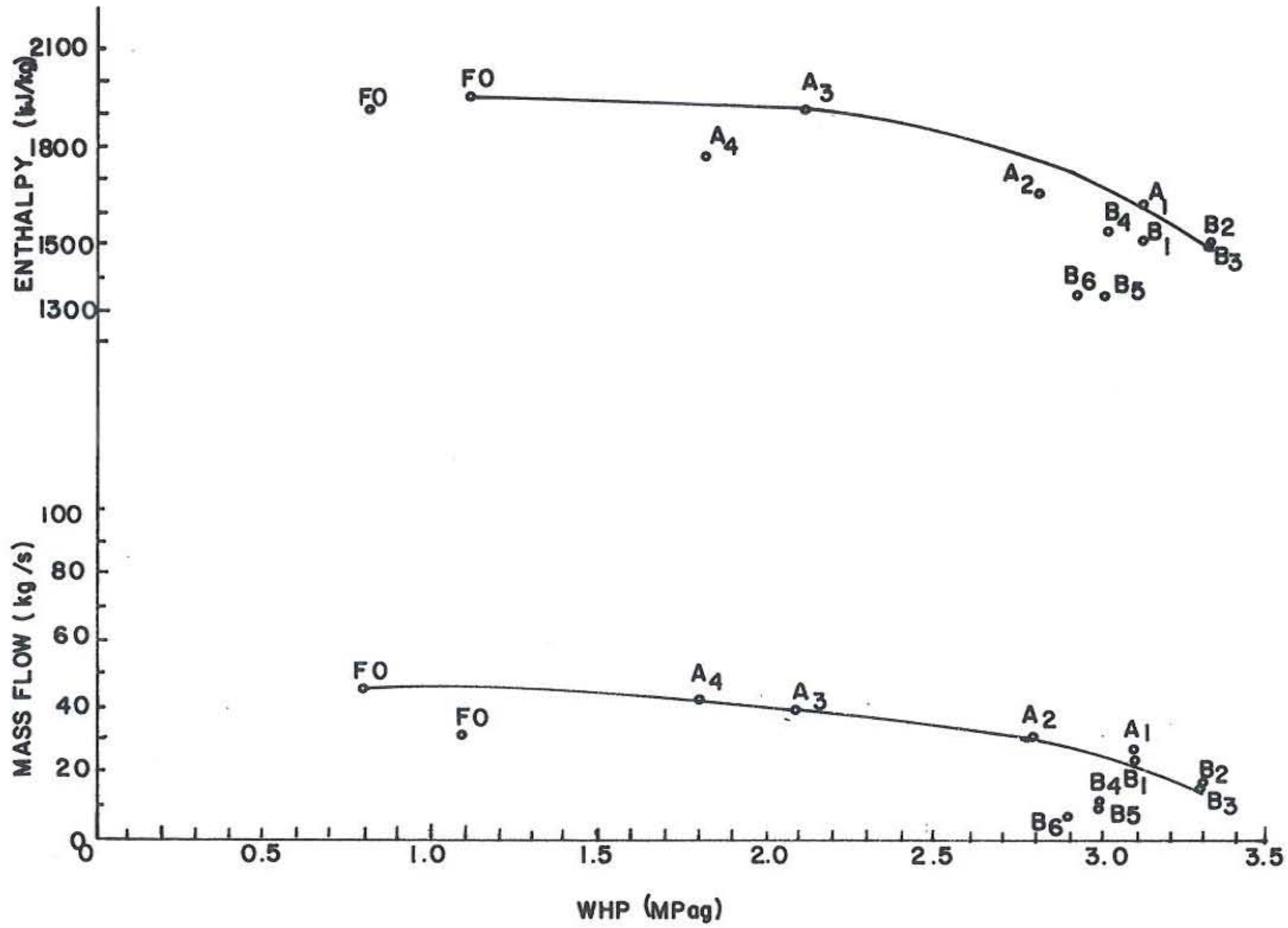

3.3.2 Okoy 6

Okoy 6 was drilled during the period 26 Sept. 1979 to 21 Jan. 1980. This was the first deep well drilled in the Nasuji area, located southwest of Okoy 5. The well penetrated through the SNF and about 1000 m into the underlying quartz diorite intrusion. The OSF was not encountered (see, Fig. 15). The well was drilled to a total depth of 2771 m. From temperature logs conducted during the completion test the loss zones were determined to be at 1340-1500 m and at 2200-2700 m. The upper zone is in the metamorphic zone between the SNF and the diorite intrusion, whereas the lower zone is well within the intrusion itself. At static conditions prior to discharge, a downflow existed between the aquifers. The well was successfully flowed by steam injection technique on the 5th attempt. The stimulation techniques conducted included compressed air injection. Injection tests conducted on the well indicated injectivity index in the range of 63 to over a 100 l/s-MPa, which is higher than measured in Okoy 5 (15 l/s-MPa) and Okoy 7 (59 l/s-MPa). Discharge tests showed that fluid production is mainly derived from a single phase aquifer within the diorite body. At low wellhead pressures, the upper aquifer at 223°C contributes some two-phase inflow as was also confirmed from geochemical studies (Pornuevo et. al., 1981 or Palmasson, 1982). The output characteristics are shown in Fig. 16. The well was rated at 10.1 MWe on the same basis as that of Okoy 5.

3.3.3 Okoy 7

Okoy 7 was drilled from 26 Jan. to 5 Apr. 1980 to a depth of 2883 m. This was the first deep well drilled in the Puhagan area (Palinpinon I), located NE of Okoy 5. The well penetrated through the SNF and OSF and terminated at the metamorphic basement rock (Fig. 15). Loss zones were determined from temperature logs at 1500-1700 m, and

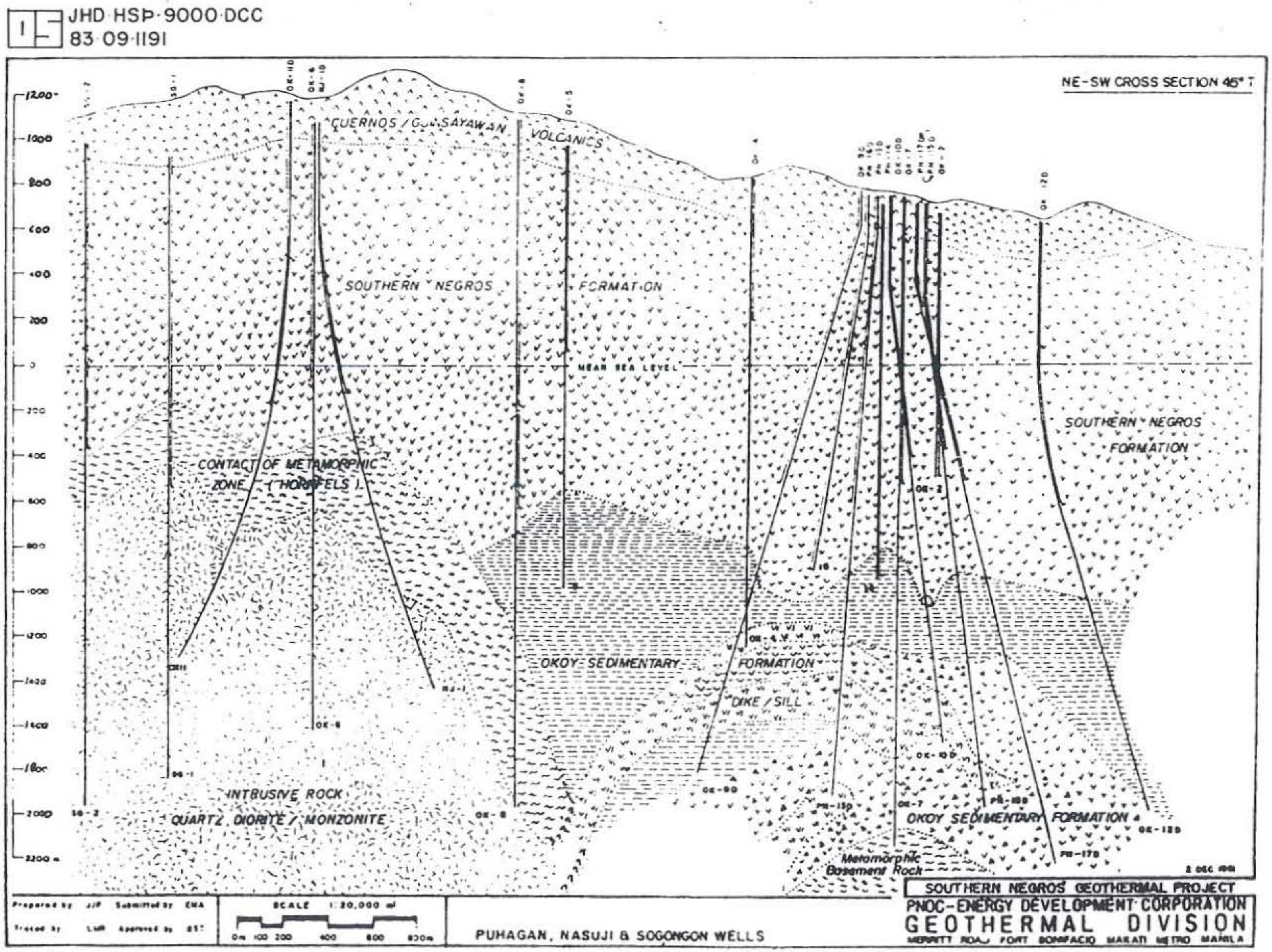

Fig. 15 Vertical section of the Palinpinon Field

JHD-HSI -9000-DCC
83.09. 1080-slá

FIG 16 OKOY 6 WELL OUTPUT CHARACTERISTICS

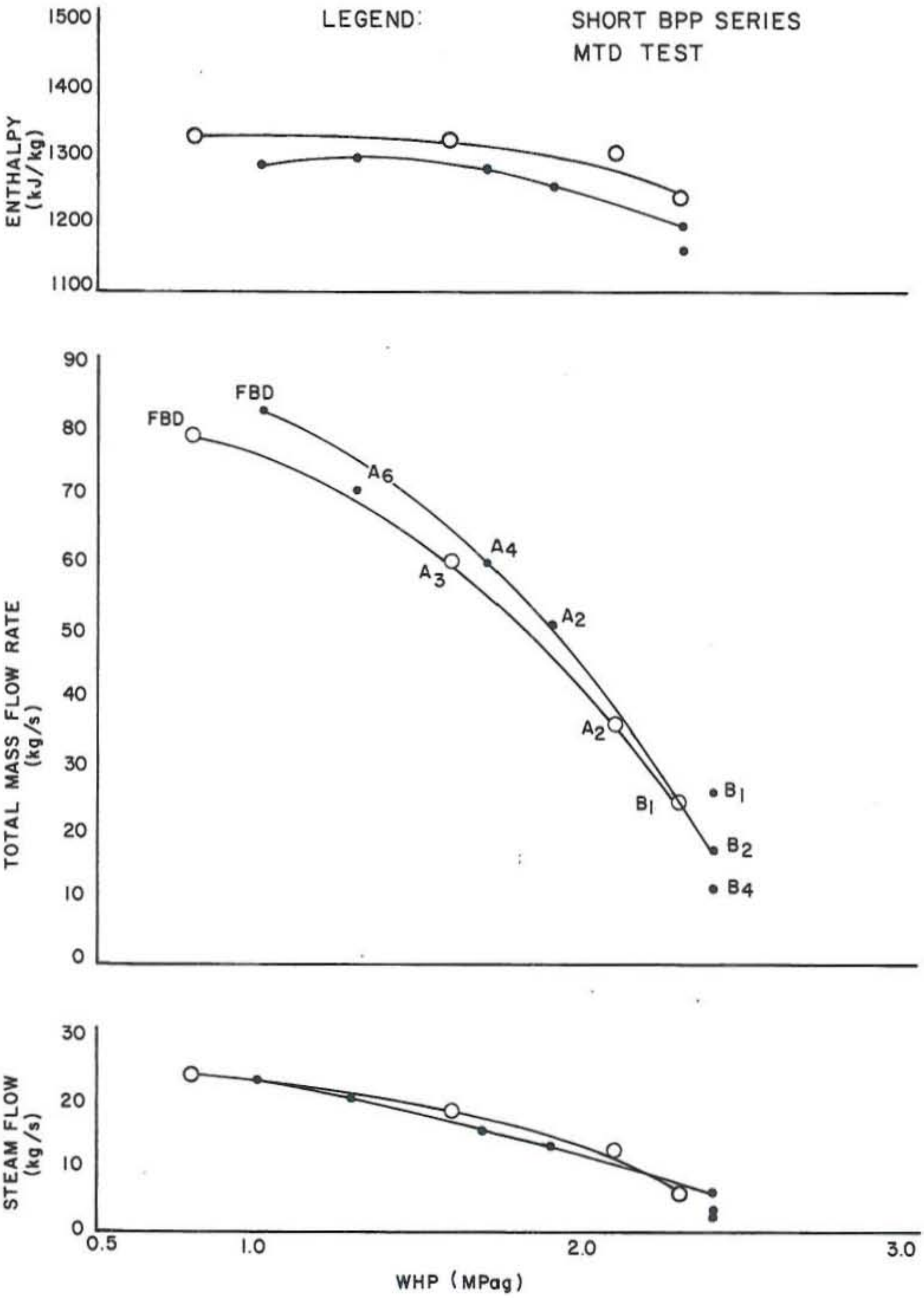

2600-2882 m. At shut-in conditions prior to discharge, a downflow occured between these aquifers. Discharge testing conducted on the well indicated a single-phase inflow at 318°C from the lower zone with a slight contribution of two-phase fluid from the upper zone at 262°C at low wellhead pressures. Pressure transient tests conducted on the well yielded a permeability-thickness product of 2.1-3.8 d-m and an injectivity index of 59 l/s-MPa, suggesting that the well is a good producer. This was confirmed by discharge tests where a maximum flow of 88 kg/s (total) at 1.0 MPa WHP was measured. The well was rated at 10.6 MWe. The output characteristics are shown in Fig. 17. Okoy 7 has been connected to a 1.5 MWe pilot non-condensing turbine since October of 1980 as previously mentioned.

3.3.4 Sogongon 1 (SG 1)

Sogongon 1 was drilled from 29 March to 6 July 1981 to a depth of 2763 m. This was the first deep well drilled in the Sogongon area (Palinpinon II, see Fig. 19), NW of Okoy 6. It penetrated through the SNF and into the contact metamorphic zone at a depth of 1090 m. The diorite intrusion was reached at about 1350 m continuing to well bottom. Temperature logs conducted during completion tests indicated loss zones at 1550-1650 m, 2200-2300 m, and 2550-2650 m. All of these zones are well within the diorite intrusion. The inflow temperature during discharge was measured 276°C at the lowest zone, which was deduced to be the main production zone. A downflow from the uppermost aquifer to the lowest aquifer occured at shut-in static conditions. The well is fed from a single-phase fluid as evidenced by the relatively constant enthalpy of the discharge at varying wellhead pressures. Fig.18 showed the output characteristics of the well. The power potential was estimated at 5.5 MWe based on the same assumption used for Okoy 5.

JHD-HSÞ-9000-DCC
83.09.1089-IS

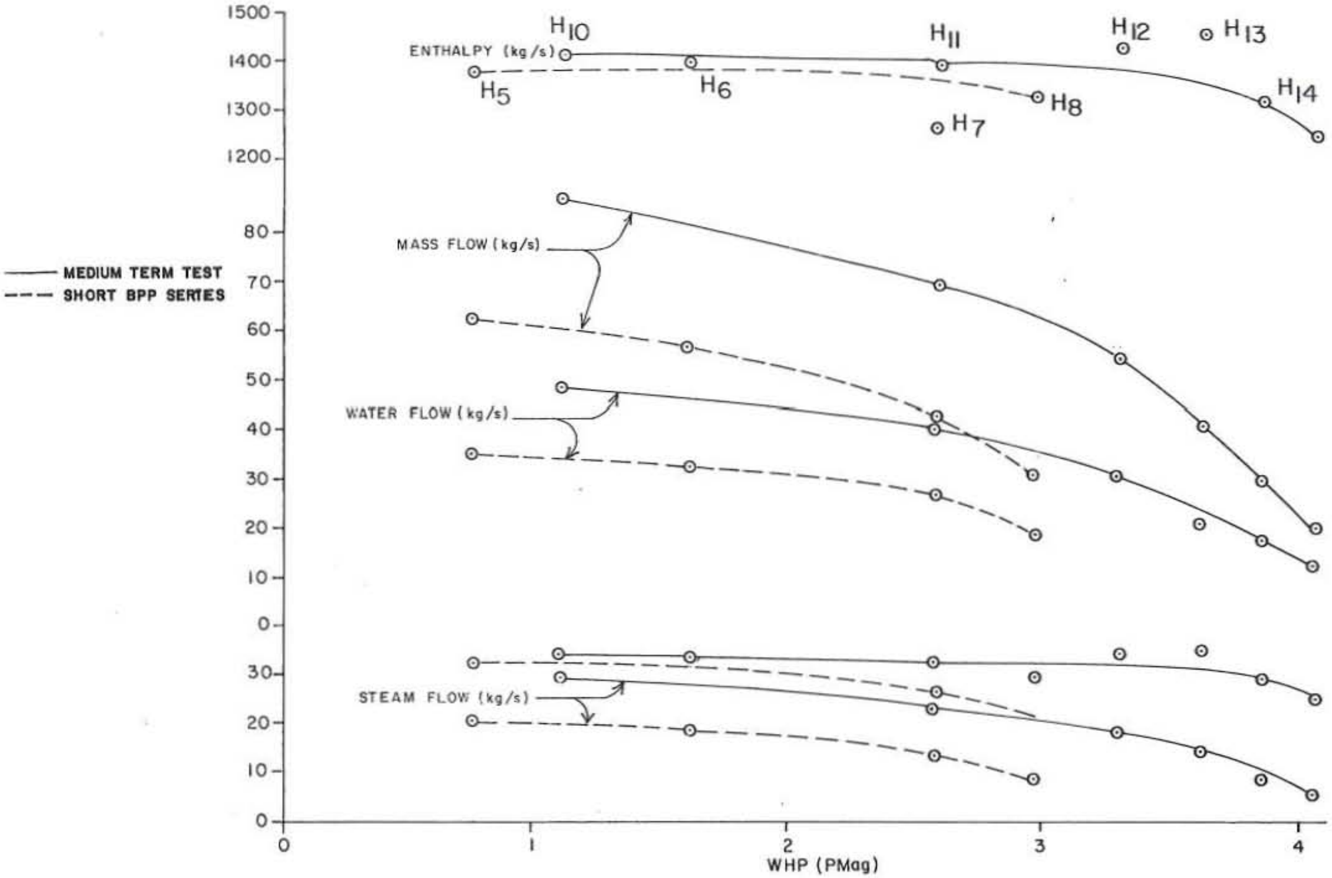

FIG. 17 OKOY 7 WELL OUTPUT CHARACTERISTICS

JHD-HSÞ-9000-DCC
83.09.1081 -DCC

FIG. 18 SOGONGON I OUTPUT CHARACTERISTICS

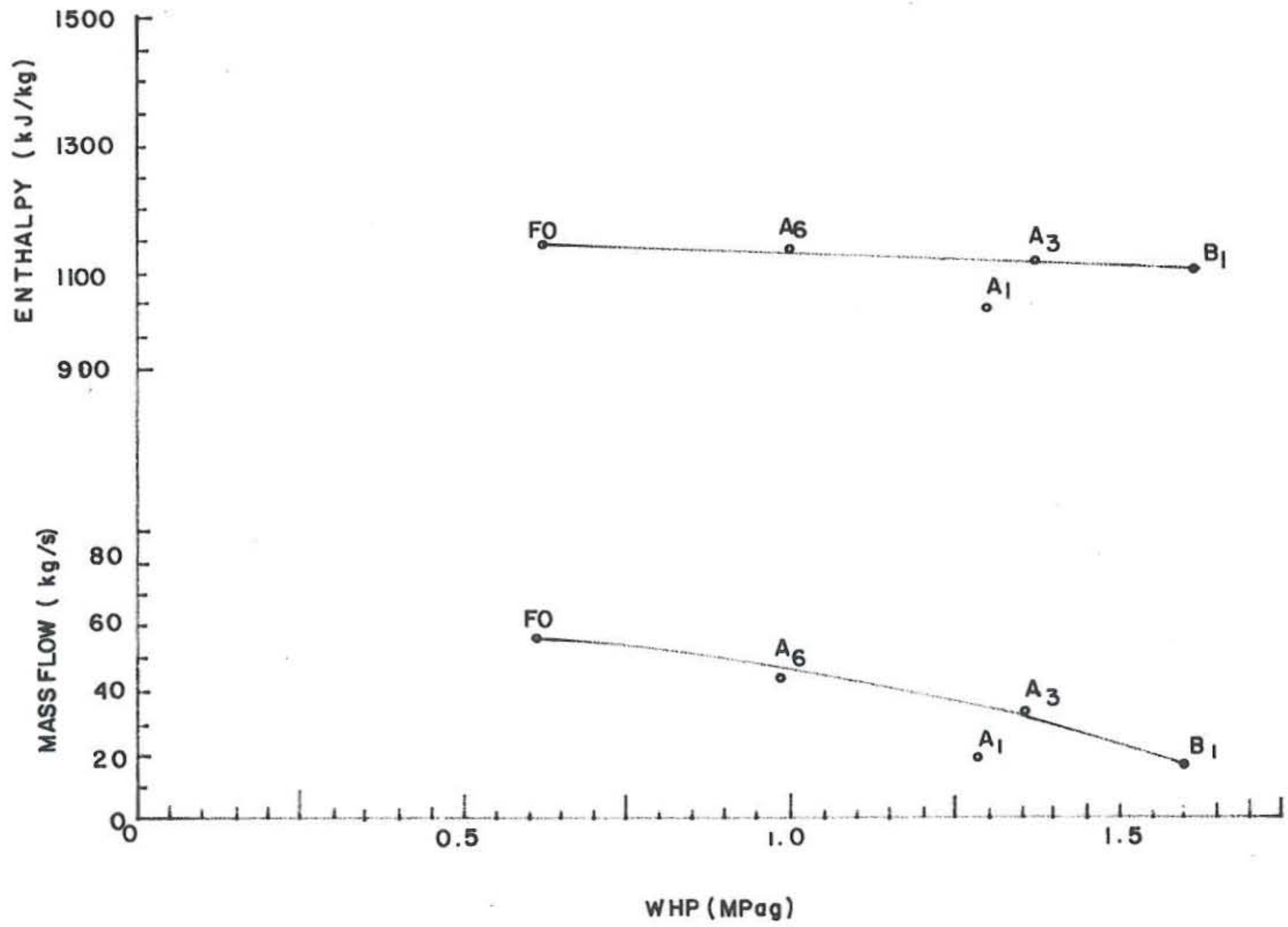

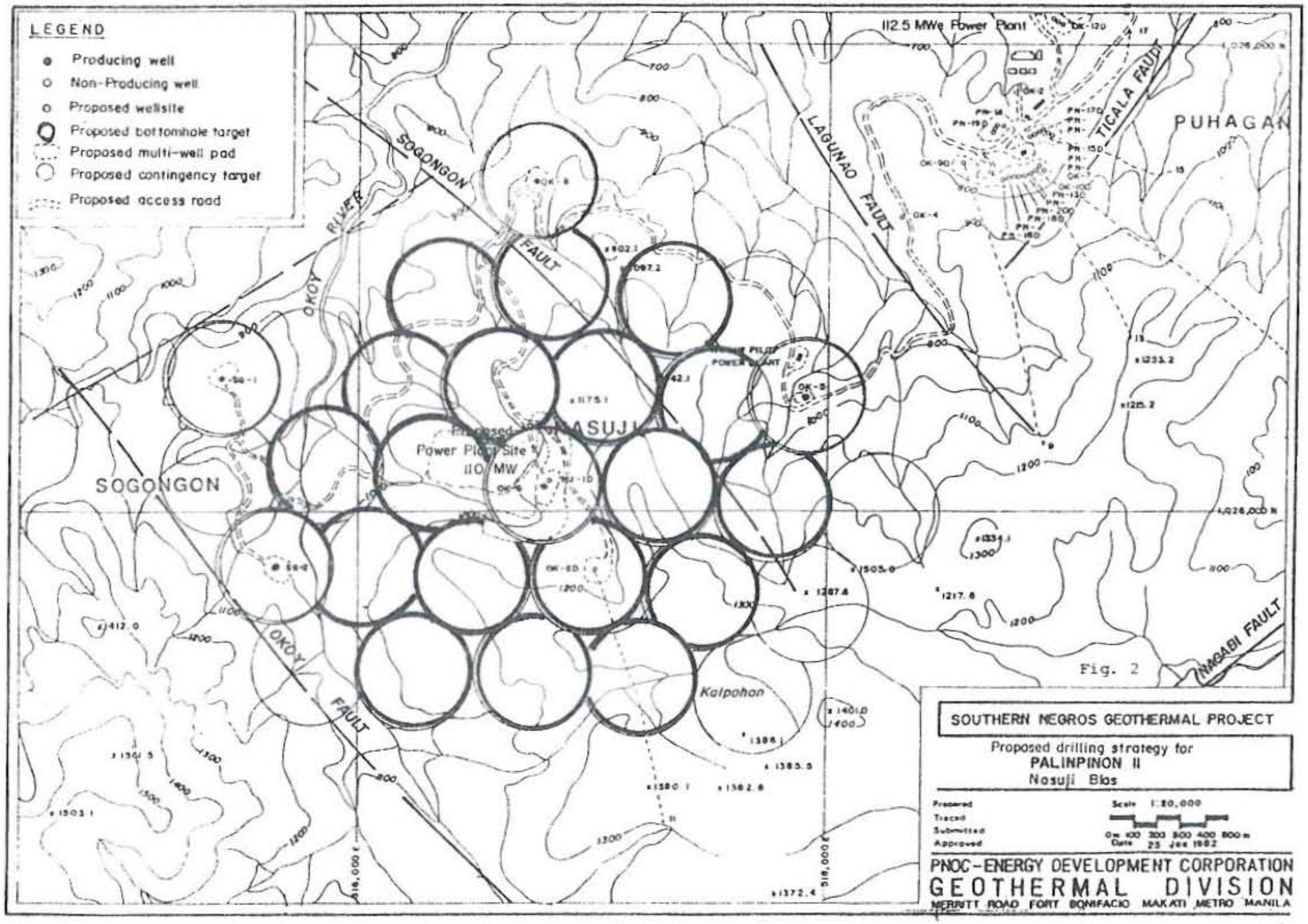

Fig. 19. Palinpinon I and II location sites.

3.4 The computer program

3.4.1 Input parameters

The program listings and output printouts are presented in Appendix D. This program uses the correlation presented by Armand and Teacher (1959), for the void fraction occupied by the vapor phase, and that of Chisholm (1972) for the two-phase multiplier. Effects of salinity and non-condensible gases (see Appendix C) to fluid temperature and pressure, and the presence of multiple feed zones were considered in the calculations. For fluid properties, correlations were made from the steam tables of Keenan et. al., (1978) and are presented in Appendix C. For percentage errors in the correlations, the reader is referred to Appendix E.

The input parameters required for the program are as follows;

Za = depth of main aquifer measured from the wellhead, m.
ZT = reference depth, 0.0 if referred to the wellhead, m.
Za2 = upper production zone measured from the wellhead, m.
N = number of pipe strings (i.e., liner, production casing, lenght of pipe with deposits,etc.).
D(N) = diameter of pipe strings according to N, cm.
Z(N) = lenght of pipe strings according to N, m.
FLAMDA(N) = absolute roughness factor according to N, m.
TC1 = inflow temperature, °C, at the lower zone.
TC2 = inflow temperature, °C, at the upper zone.
FLOW1 = mass flowrate from the lower zone, kg/s.
FLOW2 = mass flowrate from the upper zone, kg/s.
Pa = aquifer pressure, bara.
DZ3 = lenght of section in the calculation for the single-phase section, m.
CCO2,CNACL = correction for non-condensible gases and salinity respectively, ppm.
CTURB = turbulence factor, bar/(kg/s)

The calculation procedure is as follows: 1) Pwf is calculated according to equation (2). 2) With a starting value of DZ1, dP is calculated using Pwf, then the fluid properties are evaluated. 3) The steam quality (x), void fraction (κ, and the two-phase friction factor are calculated using the fluid properties. 4) The potential, acceleration, and friction gradients are then evaluated, see Appendix A. 5) The new value of dP is the sum of the three gradients in step 4. 6) The iterative calculation continues until the difference in the dP in the iteration is less than 0.0025 bars, else calculation goes back to step 1. 7) The next pipe section is then evaluated with Pwf = Pwf - dP, then steps 1 through 6 are repeated. 8) Calculation stops when the wellhead is reached.

If the flowing well pressure (Pwf) at the producing zone is known then the turbulence factor will be zero as input. If the flowing fluid has low non-condensible gases and salinity concentrations the correction parameter will be 0.0 as input.

For the effects of elevation, the aquifer depth will be increased by (new elevation - present elevation), and for wells with two phase inflows, the flowpipe can be extended down, and assuming a single phase inflow at the new depth until the actual inflow temperature and the depth can be duplicated. This is done so as to get the steam quality, void fraction occupied by the vapor phase, and the two-phase multiplier, of the fluid right at well entry. For the output parameters, see Appendix D.

3.5 Program applications

3.5.1 Profile duplication and deliverability curves

3.5.1.1 Okoy 6 KP 29/KT 63

The flowing pressure profile (KP 29, Fig. 20) showed that the upper zone (1340-1500 m) well pressure was built up above the static pressure (KP 23, Fig. 20) indicating no flow from this zone, which suggests that the bulk of the discharge came from a single-phase fluid from the lower aquifer (2200-2700 m) at a temperature of 289°C. This corresponds to a liquid enthalpy of 1284 J/g. The discharge enthalpy as calculated from James (1962) lip pressure method was 1280 J/g, which agrees well with the saturated enthalpy at 289°C indicating that the inflow was single-phase. The calculation done in this paper using the model, indicated a discharge enthalpy of 1266 J/g suggesting some energy loss during the flowing process. These losses can be due to kinetic energy and/or potential energy loss. Grant, et. al.(1982) presented the following tolerances in the James method:

Method	Careful control	Normal
Lip pressure method	h + 20 J/g	h + 50 J/g
	W + 4%	W + 8%
Separator method	h + 10 J/g	h + 30 J/g
	W + 2%	W + 4%

In this calculation, salinity and non-condensible gases were not considered. The calculated flowing pressure profile (Fig. 20) agrees well with KP 29 suggesting that the fluid has low salinity and low concentrations of non-condensible gases. The difficulty in the profile duplication arises when some measurement errors occur. For instance, the measured wellhead pressure (WHP) using a dial pressure gauge (SNGF practice) does not agree with the measured pressure at the wellhead using the Kuster gauge (KP). This phenomenon will be discussed in the case of

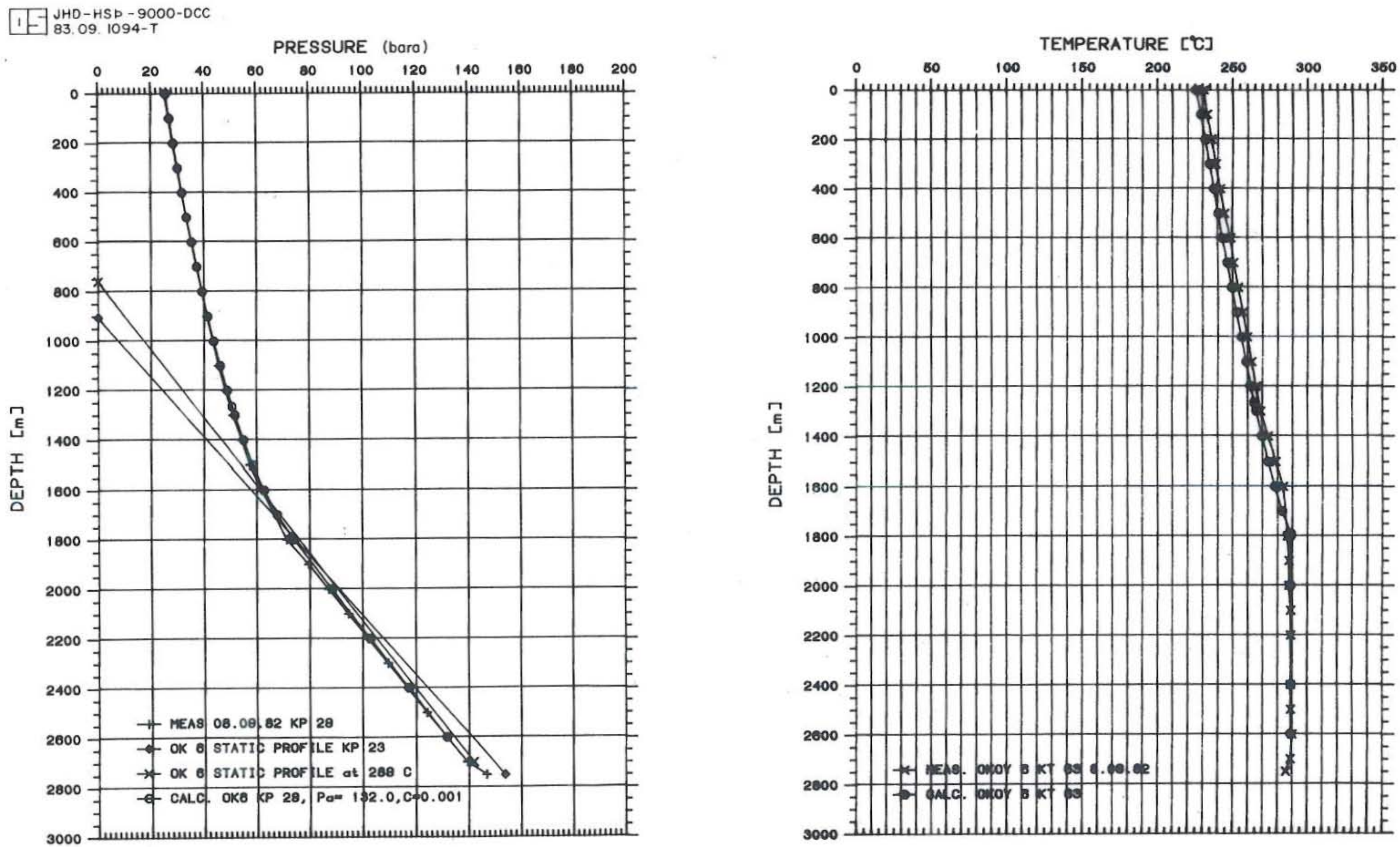

Fig. 20 Okoy 6 measured and calculated flowing profiles

Okoy 7. Checking which of these measurements is erroneous can be done by comparing the saturation temperature corresponding to the measured pressure. The saturation conditions can be used as a check since in a two-phase (steam-water) flow the temperature versus pressure relationship should obey saturation conditions, that is, if as mentioned above, the fluid has low gases and/or salinity concentrations. If otherwise, then corrections should be made on the effect of these impurities. These are presented in Appendix C. The saturation temperature at the wellhead can then be compared to the calculated temperature (using the model described in this paper). This is illustrated in Table 1.

The flowing enthalpy was here calculated considering energy loss due to kinetic effects. The heat loss to the formation was not included as it was found to be very small compared to WH (mass multiplied by enthalpy). At high flow rates, this loss will become even smaller, whereas the kinetic energy loss increases due to a corresponding increase in fluid velocity. If the calculated enthalpy (using this model) is right then the mass flow can be recalculated as;

$$W = \frac{2257(Ww)}{2676 - H} \qquad (5)$$

where; Ww = water flow, kg/s and H = calculated enthalpy, kJ/kg. As a first approximation, the aquifer pressure can be estimated from a plot of pivot point pressure (PCP) versus depth (Fig. 21). However, in wells with strong downflows during the warm-up period, the pressure at the PCP is heavily affected by this, especially if the down-flowing fluid is of relatively low temperature compared to the other zone (lower zone). For Okoy 6, the downflow has a temperature of approximately 223°C compared to 289°C at the lower zone. The effect of this can be seen in the static pressure gradient (KP 23, Fig. 20). The gradient corresponds to a temperature of 223°C, or a fluid density

TABLE 1 Okoy 6 measured and calculated data

Measured WHP = 25.0 bara (Ts = 224 C), Measured Discharge Enthalpy = 1280.0 J/g, Calculated at Pa = 132.0 bara, C = 0.001

	MEASURED		CALCULATED		
DEPTH(m)	P(bara)	TEMP(C)	P(bara)	TEMP(C)	H(J/g)
0.0	25.3	231.0	25.4	225.0	1265.6
100.0	26.9	233.0	26.9	227.9	1266.6
200.0	28.4	236.0	28.4	231.0	1267.6
300.0	30.1	239.0	30.0	234.0	1268.6
400.0	31.8	242.0	31.7	237.0	1269.5
500.0	33.6	245.0	33.4	240.0	1270.5
600.0	35.6	249.0	35.2	243.0	1271.5
700.0	37.5	251.0	37.1	246.0	1272.5
800.0	39.4	254.0	39.2	249.1	1273.5
900.0	41.3	257.0	41.3	252.2	1274.4
1000.0	43.5	260.0	43.5	255.5	1275.4
1100.0	45.6	263.0	45.9	258.8	1276.4
1200.0	48.1	266.0	48.7	262.2	1277.4
1265.0	-	-	50.4	264.5	1278.0
1300.0	51.0	269.0	51.4	265.8	1278.4
1400.0	55.3	274.0	54.7	269.6	1279.3
1500.0	60.3	279.0	58.3	273.7	1280.3
1600.0	64.1	284.0	62.5	278.3	1281.3
1700.0	-	-	67.4	283.4	1282.3
1793.0	-	-	73.3	289.0	1283.8
1800.0	71.4	287.0	73.8	289.0	1284.0
2000.0	87.3	288.0	88.3	289.0	1284.0
2200.0	102.2	289.0	102.8	289.0	1284.0
2400.0	117.0	289.0	117.3	289.0	1284.0
2600.0	131.8	289.0	131.8	289.0	1284.0

NOTE

\- no data available

JHD-HSP-9000-DCC
83.09.1082-DCC

FIG. 21 VERTICAL DEPTH vs. Pressure Control Point PRESSURE OF THE SNGF WELLS

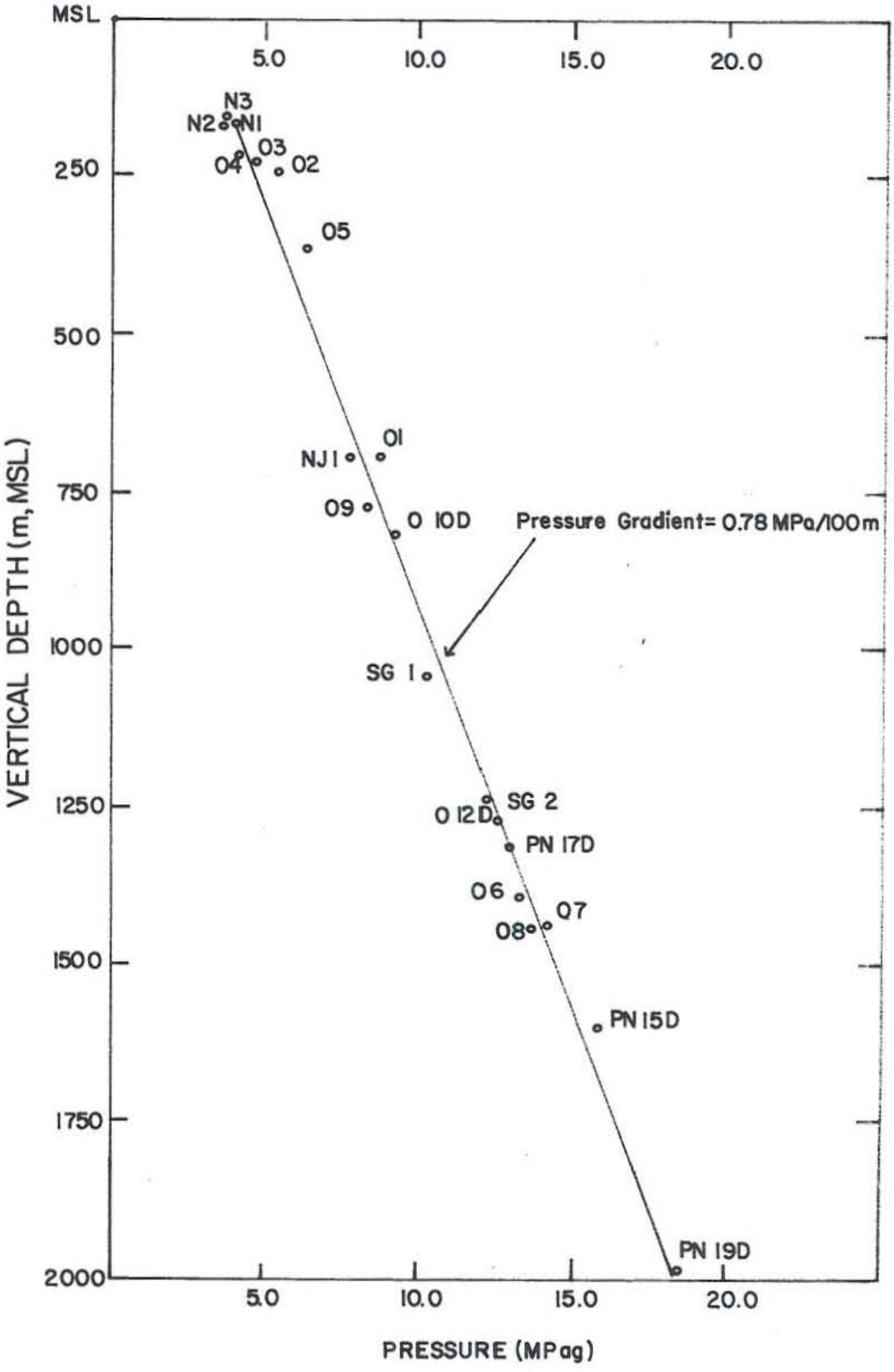

of 836.5 kg/m3. Hence, in this paper trials were made to estimate the aquifer pressure if the main inflow during production is 289°C. It was found out that an aquifer pressure of 132.0 bara gave the best fit. The calculated static profile at 289°C is shown in Fig. 20. This further confirmed that the well has intersected a high permeability zone at 2600 m as shown by the small pressure drawdown (compare static profile at 289°C and KP 29, Fig. 20). Injection tests conducted during well completion gave an injectivity index of 63 to over a 100 l/s-MPa.

3.5.1.2 Okoy 6 delivery curves

Since the measured pressure profile of Okoy 6 was ably duplicated it is most fitting to use the data from this well to further calibrate the predictive capability of the computer program. The measured and calculated data are shown in Tables 2 and 3.

TABLE 2 Okoy 6 measured and calculated output data

Calculation was based on Pa = 132.0 bara, C = 0.001 and inflow temperature, TC = 289°C.

FLOW(kg/s)	MEASURED WHP(bara)	CALCULATED WHP(bara)
14.2	25.0	25.4
26.7	24.9	24.5
51.1	19.9	20.8
60.8	17.9	18.1
71.2	13.9	13.3
75.0	-	10.5
80.0	10.9	choked

TABLE 3 Okoy 6 calculated output data at different aquifer pressures.

Calculation was based on TC = 289°C, C = 0.001

FLOW(kg/s)	Pa = 125.0 WHP(bara)	Pa = 142.0 WHP(bara)
14.2	23.9	127.6
26.7	23.0	26.7
51.1	18.8	23.5
60.8	15.6	21.6
71.2	9.3	17.5
75.0	choked	15.6
86.0	-	choked

TABLE 4 Okoy 6 flowing well pressures at different flow rates.

Calculation was based on Pa = 132.0 bara, turbulence factor, C = 0.001, TC = 289°C.

FLOW(kg/s)	Pwf(bara)	(Pa-Pwf)/W
14.2	131.8	0.01408
26.7	131.3	0.02622
51.1	129.3	0.05284
60.8	128.3	0.06086
71.2	126.9	0.07163

Fig. 22 showed that an aquifer pressure of 132.0 bara gave the best fit. The simulation was done in an attempt to duplicate the wellhead pressure by calibrating with the aquifer pressure and the turbulence factor. The turbulence factor can then be checked by plotting (Pa - Pwf)/W versus W (Jacob and Rorabaugh's (1946) method for step drawdown test).

JHD-HSI - 9000-DCC
83.08.0986-IS

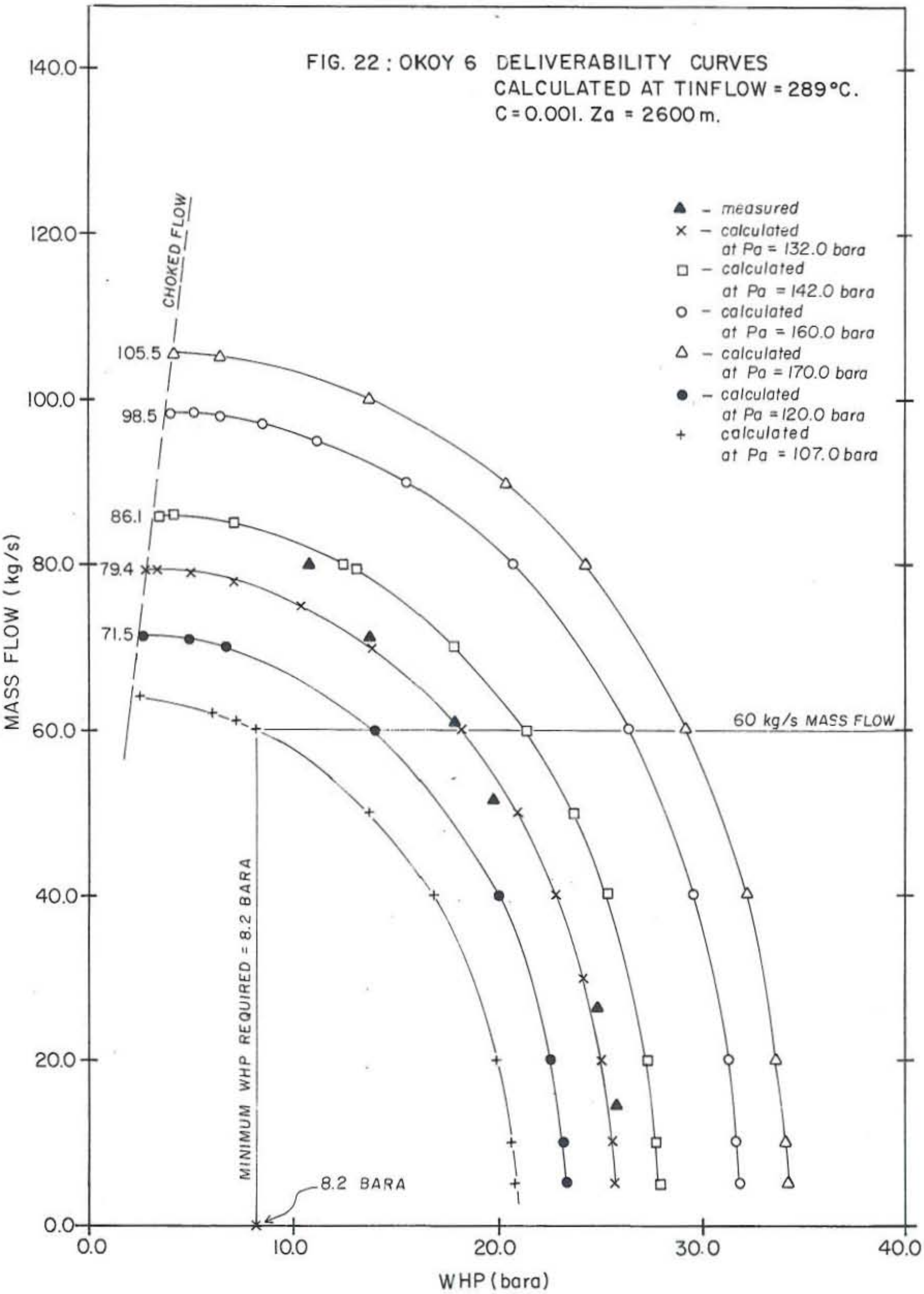

The flowing pressure profiles at different flow rates are shown in Fig. 23. Fig. 24 shows a plot of (Pa-Pwf)/W versus W.

From Fig. 22, it can be seen that choked flow can be attained at 75 kg/s at Pa = 132.0 bara. Generally, choked condition is directly proportional to aquifer pressure. Choked flow is the state at which fluid velocity approaches sonic velocity, in which case the mass flow does not increase when the wellhead pressure is lowered further. Also, from Fig. 22, the maximum discharge pressure can be estimated by extrapolating the curve down to W almost equal to zero. At this stage, liquid and/or vapour velocity is so low that the fluid is not lifted past the wellhead, hence the flow collapses.

If the percentage error in the massflow measurement for the James (1962) approximation will be applied (8%), then the maximum allowable flow for Okoy 6 will be 73.6 kg/s, or say 75.0 kg/s. From the simulation done, it was proven that at 75.0 kg/s of flow the well started to attain choked condition. From Table 2 and Fig. 22, the measured flow at full bore discharge (80 kg/s) deviates from the curve. This can be explained by either of the following: a) additional two-phase inflow from the upper zone at high flow rates (see section 3.3.2), or b) error in measurements as explained above. By ably predicting the delivery curve (if the model is accurate enough), the following aspects of well flow can be determined; choked condition, turbulence pressure drop, maximum discharge pressure, and productivity index, among others. The turbulence pressure drop is discussed in Appendix B. The productivity index can be calculated according to equation (1).

JHD-HSP-9000-DCC
83-09-1190

Fig. 23 Okoy 6 Pressure profiles at different mass flow rates

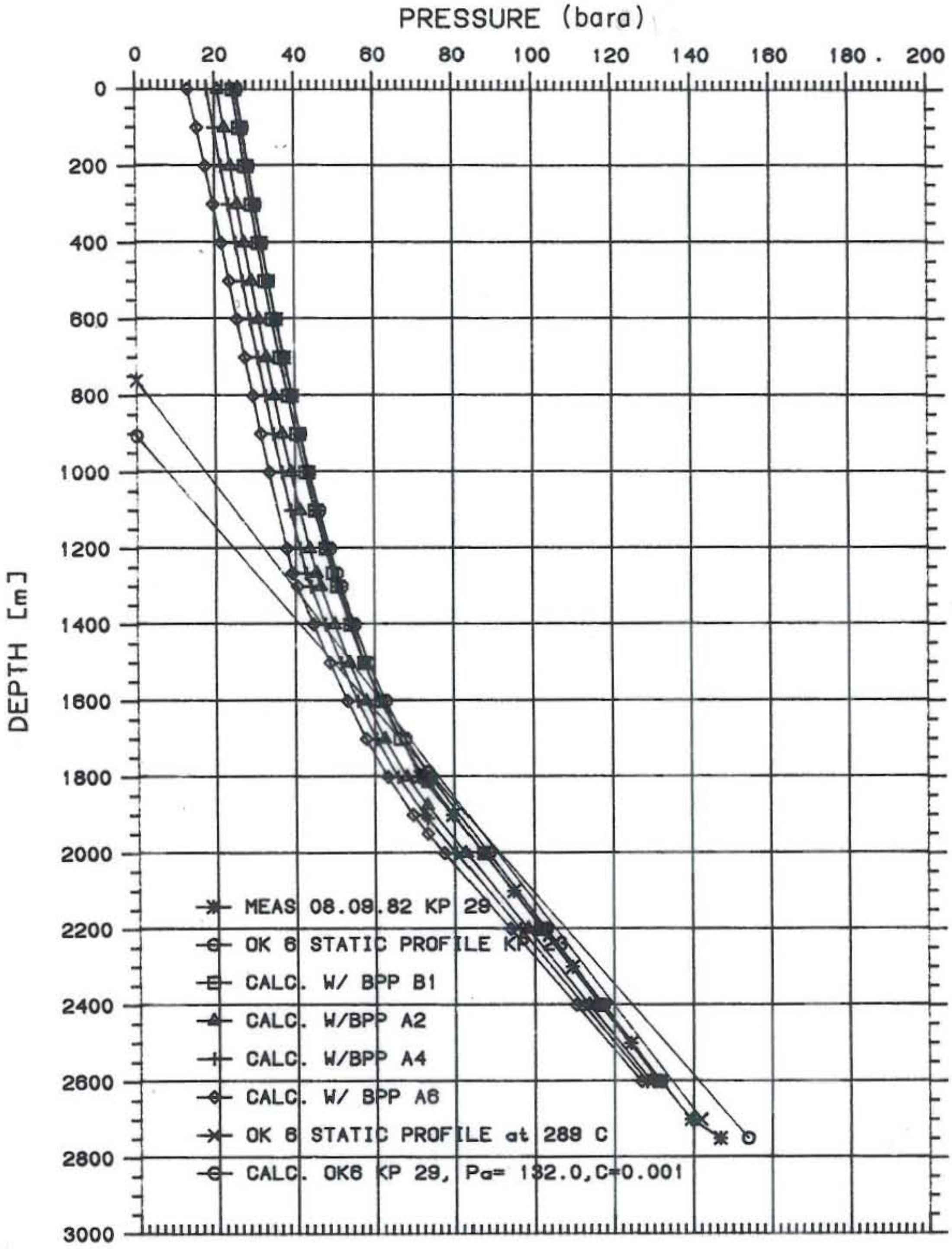

JHD-HSP-9000-DCC
83.08.0987-IS

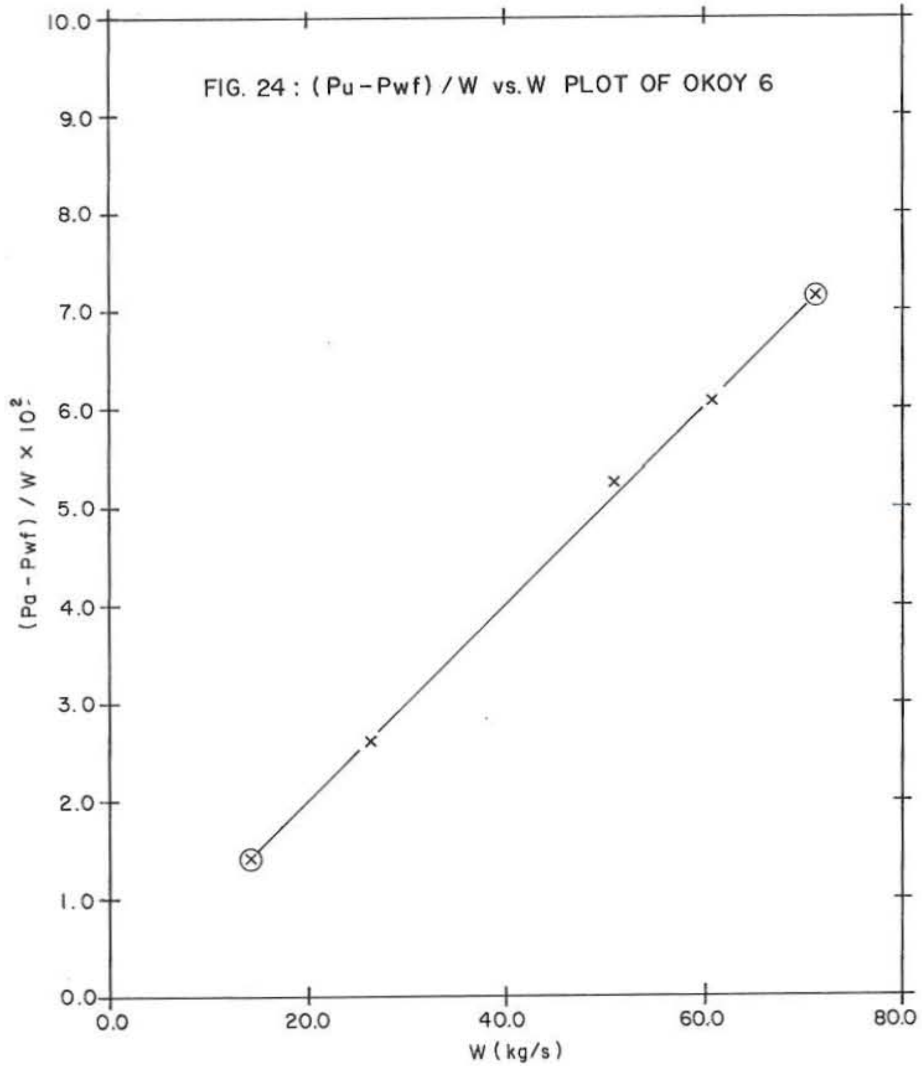

FIG. 24 : (Pu - Pwf) / W vs. W PLOT OF OKOY 6

3.5.1.3 Okoy 7 KP 14/KT 21

Okoy 7 is a well having two significant production zone at 1500-1700 m, and 2600-2882 m. At shut-in conditions, a downflow exists between these aquifers. During heat-up, the static pressure profiles converged at approximately midway between the two zones indicating that these zones have more or less similar permeabilities. At the point of convergence (PCP), formation pressure was deduced to be approximately equal to the pressure measured at this depth. From Fig. 21, the formation pressures in both zones are extrapolated from the straight line drawn for the PCP's of the wells in the Palinpinon field. The injectivity index calculated for this well during cold water injection was 59 l/s-MPa. The flowing pressure profile (KP 14, Fig. 25) indicates that both zones were drawn down below the formation pressures at both depths, suggesting that both zones are feeding.

TABLE 5 Okoy 7 drawdown pressures at the production zones

During measurement of KP 14, WHP = 46.5 bara, and the total flow was, Wt = 13.2 kg/s

PRODUCTION ZONE(m)	Pa(bara)	Pwf(bara)	dP(bar)
(1), 2600	168.0	163.9	4.1
(2), 1700	101.0	100.6	0.4

At the lower zone (1), the flowing well pressure can be expressed as;

$$Pwf1 = Pf1 - W1/I1, \text{ then} \tag{6}$$

$$Wt = W1 + W2 \tag{7}$$

$$W1 = (dP)1 \times I1 \tag{8}$$

$$W2 = (dP)2 \times I2 \tag{9}$$

where; I = injectivity index, l/s-MPa

JHD-HSP-9000-DCC
83.09.1093-T

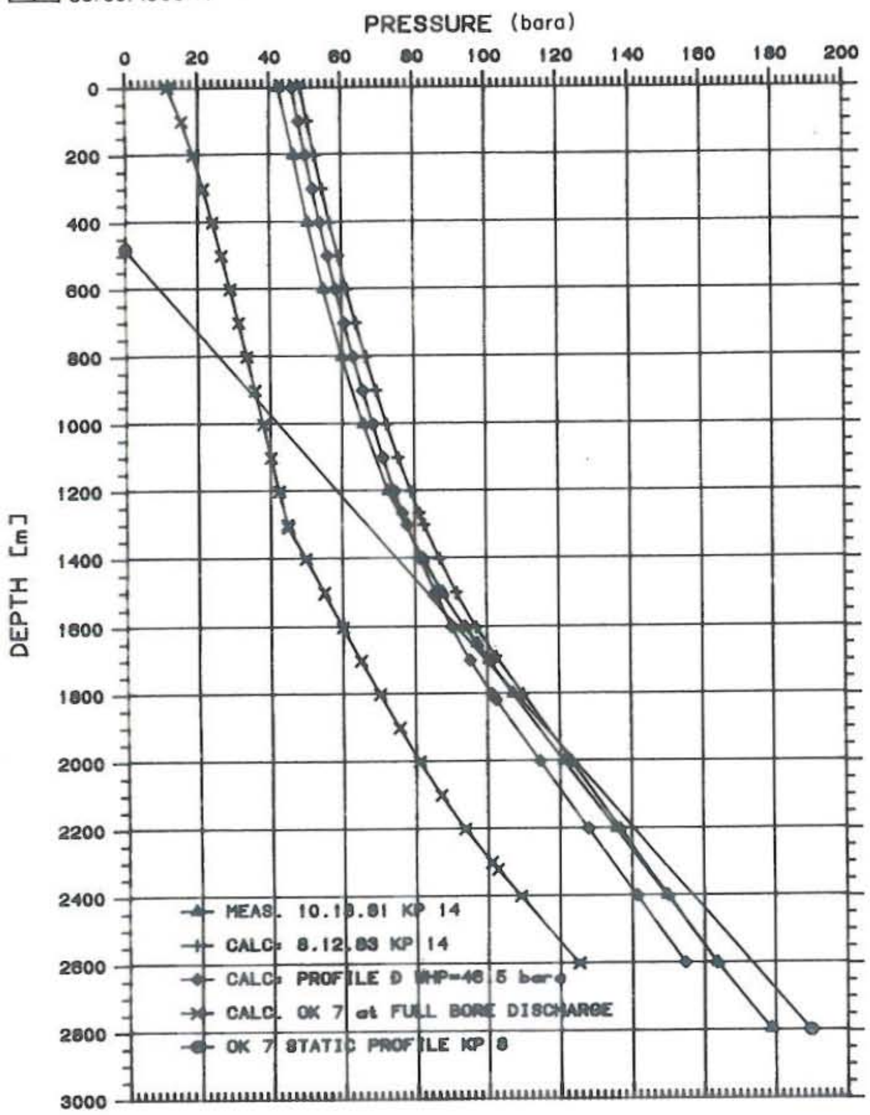

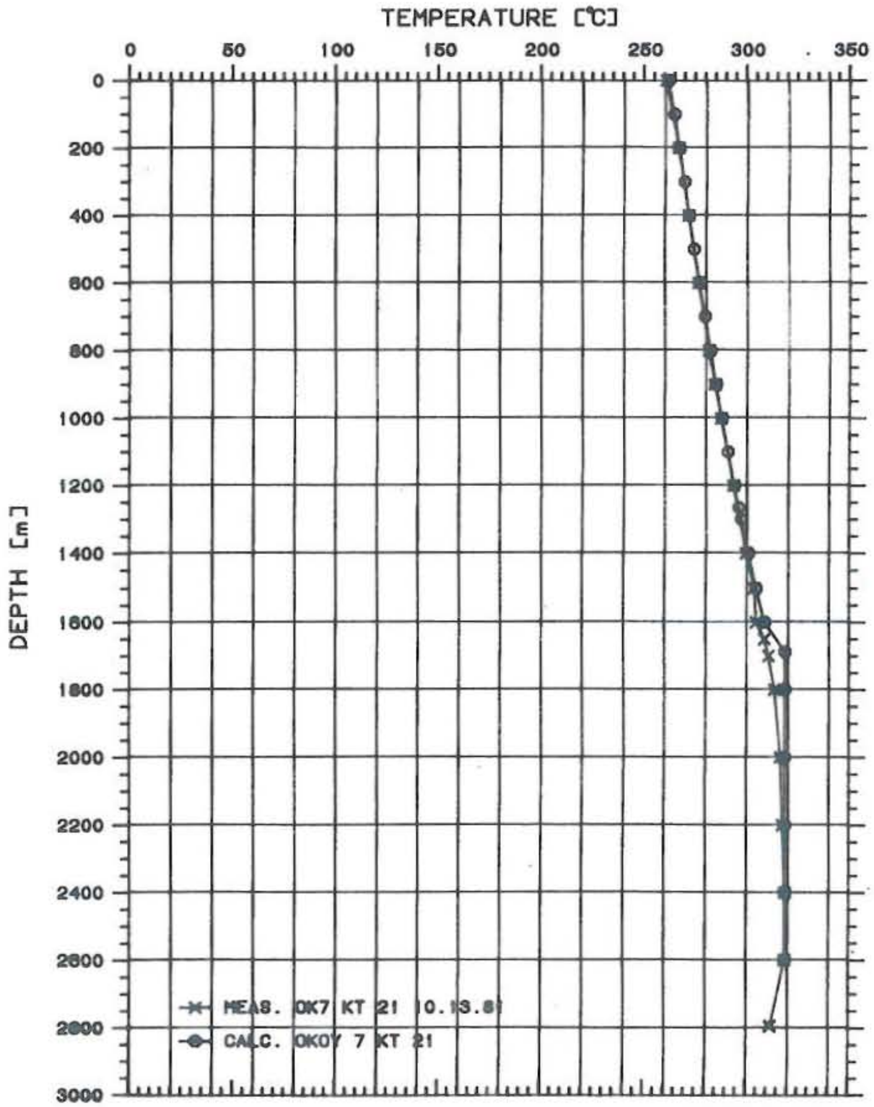

Fig. 25 Okoy 7 measured and calculated flowing profiles

From the location of the PCP, it can be assumed that I1=I2.

Then, (10) W1 = W2(dP1/dP2) From which, W1 = 12.0 kg/s, and W2 = 1.2 kg/s. These values are used in the simulation and the results are shown in Table 6.

As can be seen from the Table 6, the saturation temperature corresponding to the wellhead pressure agrees well with the measured and calculated temperatures at the wellhead, implying that possibly the measured pressure profile has some discrepancies. However, this can also be due to fluid salinity and presence of non-condensible gases. At the wellhead, the measured pressure (KP) was off by 3.8 bara compared to the WHP, and 6.2 bara compared to the calculated pressure.

At 1800-1600 m, from Table 6, a sudden drop in temperature (measured) occured indicating the influence of the 260°C fluid from the upper zone. Applying the maximum error (see section 3.5.1), of 50 J/g for the James lip pressure method, then the maximum discharge enthalpy that can possibly be measured is 1340.0 J/g. The calculated enthalpy from Table 6 is 1402.2 J/g which shows a difference of 62.2 J/g implying that significant heat loss has occured to the formation at this flow rate (13.2 kg/s). At high flowrates this cooling will be minimal due to the increased fluid velocity. A simulation done at full bore discharge indicated a calculated enthalpy of 1395.3 J/g which agrees well with the measured discharge enthalpy (1400 J/g).

To check the effects of salinity and non-condensible gases to the pressure profile, calculation was made taking all non-condensible gases as CO_2 and the chloride concentration for NaCl. The chemical data were taken from Jordan (1982). The presence of dissolved salt lower the saturation pressure at a given temperature. The salt remains in liquid phase, adding to the weight of liquid but does not influence the flashing of the water (Grant, et.al. 1982). The effect of CO_2 causes the solution to flash at higher pressure at a given temperature. These cases are presented

<u>TABLE 6</u> Okoy 7 measured and calculated flowing temperature and pressure.

Measured WHP = 46.5 bara (Ts = 260°C) Measured discharge enthalpy = 1290 kJ/kg. Temperature of the inflow at the upper zone = 260°C, Profile calculated at Pwf=163.9 Mixing temperature = 313°C; CCO2,CNACL = 0.0

	MEASURED		CALCULATED		
DEPTH(m)	P(bara)	TEMP(C)	P(bara)	TEMP(C)	H(J/gm)
0.0	42.7	261.0	48.9	262.7	1402.5
200.0	46.8	267.0	52.9	267.4	1404.4
400.0	50.8	272.0	57.0	272.3	1406.4
600.0	55.1	277.0	61.6	277.4	1408.3
800.0	60.1	282.0	66.8	282.7	1410.3
1000.0	65.9	288.0	72.5	288.3	1412.3
1200.0	72.8	294.0	79.2	294.3	1414.2
1400.0	82.4	300.0	87.1	301.1	1416.2
1600.0	94.0	305.0	97.2	309.0	1418.2
1688.0	-	-	102.7	313.0	1419.0
1800.0	107.3	314.0	110.2	319.0	1452.1
2000.0	121.3	317.0	123.6	319.0	1452.1
2200.0	135.7	318.0	137.0	319.0	1452.1
2400.0	150.0	319.0	150.4	319.0	1452.1
2600.0	163.9	319.0	163.9	319.0	1452.1

in Appendix C. The calculations are presented in Appendix D.2, D.3, D.4, and D.5. Fig. 25 shows the simulated profile at full bore discharge and at a WHP of 46.5 bara.

Proper duplication of the measured profile can be helpful in the determination of the true temperature and pressure profile, the determination of the inflows from a multi-zone well, the determination of the effect of heat transfer to the formation at low flow rates, and the effects of impurities to the pressure profile.

3.5.2 Determination of the necessary conditions for a successful well discharge

Initially, discharging of wells in SNGF was done by compressed air stimulation. That is, by injecting compressed air into the well in an attempt to depress the water column to a depth where the temperature is sufficient enough to support a thermodynamic flow of the fluid. However, it was found out that in wells with very deep water levels, this method failed, especially in the Nasuji/Sogongon area of the SNGF. This was because as the fluid started to flash and flow up the well, much of its energy was lost to the cold column from the flashing point to the wellhead (Algopera, 1980).

To minimize this energy loss external heat from outside source, i.e., a boiler or another discharging well, is required to heat up the cold column (Brodie, 1980). This method requires injection of steam or two-phase fluid into the well thereby heating up and depressing the water column to a condition (temperature) sufficient to support a continuous flow. Unloading the injected fluid would stimulate the well to flow provided the total pressure drop it will encounter during the flowing process can be overcome.

The critical condition that should be attained for the well to sustain flow is the minimum temperature of the water column attained during stimulation, Fig. 26, KT 58 and 48. The saturation pressure should be higher than the total pressure reduction due to elevation change, wall friction, and acceleration. In the calculation, the depth of the occurence of the minimum temperature can be determined from temperature surveys conducted during stimulation or can be assumed as will be shown later. The starting Pwf is the saturation pressure corresponding to the critical (minimum) temperature. The mass flow can be calculated as follows;

$$Wt = Wi + Ww \qquad (11)$$

$$Ww = \frac{Qi}{H2 - H1} \qquad (12)$$

where; Wt = total mass flow rate, kg/s; Ww = mass that can be derived from the water column, kg/s; Wi = mass injected into the well, kg/s; Qi = heat injected into the well, kJ/s; H2 = saturated liquid enthalpy of the fluid at minimum temperature, T2, kJ/kg; H1 = saturated liquid enthalpy corresponding to the temperature of the water prior to stimulation, i.e, at the water level, kJ/kg.

In actual case, however, the mass derived from the depressed water column may be lower than what can be calculated in equation (12), as a portion of the injected heat is used to heat up the cold column. After some time from the start of stimulation, when the cold column has already been heated, Ww can be approximated using equation (12). The starting depth will be the location of T2. The minimum temperature can be known from either of the following: a) Temperature logging during stimulation. b) Monitoring the WHP during stimulation. This can be done by assuming a temperature drop between the temperature of the injected fluid at the wellhead (Ps at WHP), and the minimum temperature. By simulation, the depth of occurence and the minimum temperature can be calculated, i.e, at a

JHD-HSI -9000-DCC
83.09.1078-IS

FIG. 26 OKOY 5 TEMPERATURE AND PRESSURE PROFILES DURING DISCHARGE ATTEMPTS

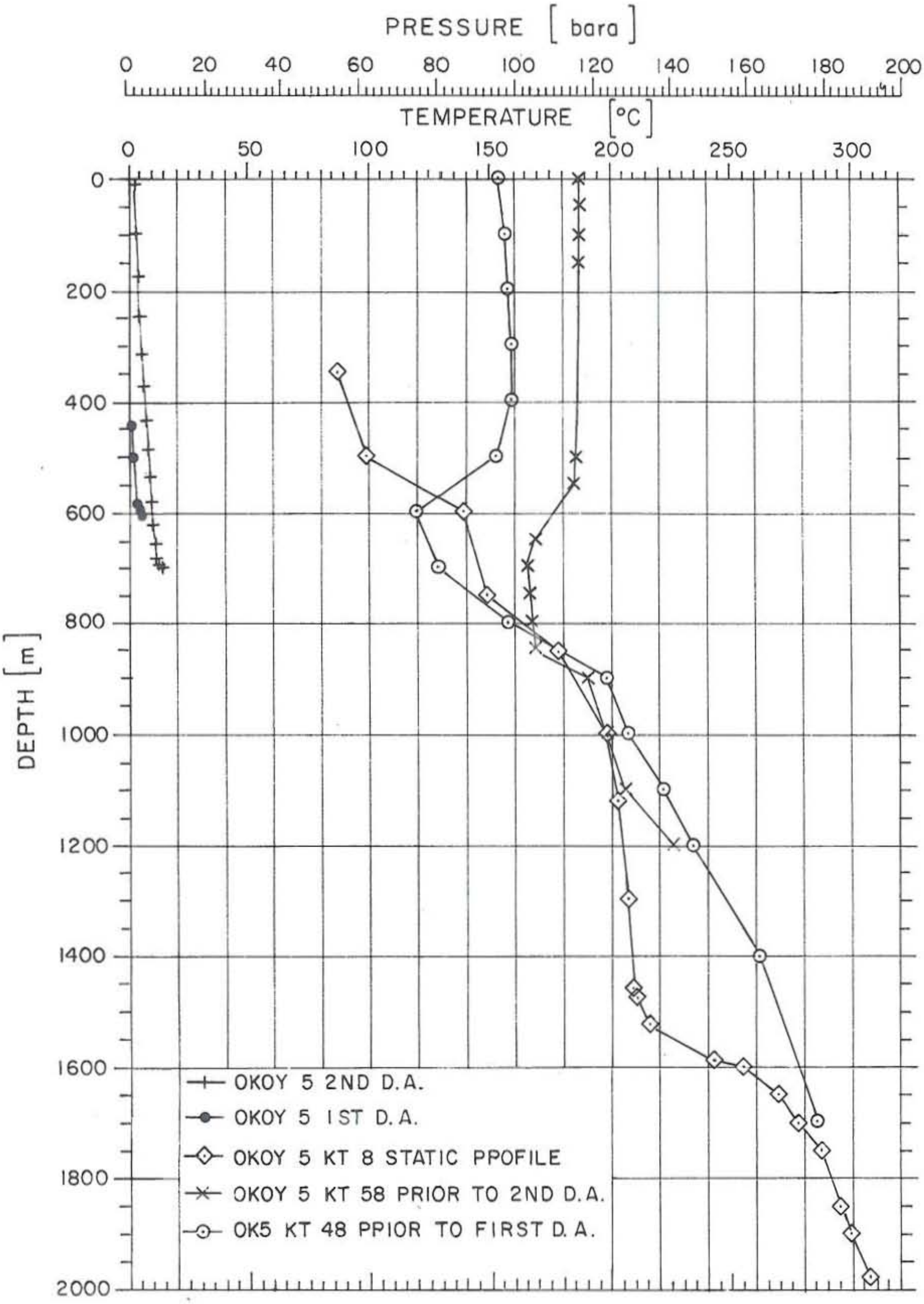

condition where a flowing pressure of slightly greater than atmospheric is attained at the wellhead during the flowing process. The temperature at the wellhead can then be calculated as

$$T_{wh} = T_{min} + dT \tag{13}$$

The wellhead pressure can then be determined as

$$WHP = Ps \text{ at } T_{wh} \tag{14}$$

Stimulation can then be stopped if the required stimulation WHP is reached and the well consequently opened up. For SNGF, dT has been found to be 25°C. Figs. 26 and 27 show the pressure profiles during the discharge attempt for Okoy 5, and the simulated discharge attempt for SG 1 at a minimum temperature of 212°C estimated to occur at 1425 m.

At a minimum temperature of 121°C occuring at 600 m, Okoy 5 failed to discharge, whereas, at a minimum temperature of 167°C occuring at 700 m, a successful discharge was attained (Fig.26).

3.5.3 Effect of elevation on production

For future expansion and assessment of a partially developed field, simulated output curves at different elevations were made for Okoy 6. The object of the simulation is to predict the probable well operating outputs at different elevations. The simulation was based on an assumption that the wells to be drilled at other elevations are to obtain production from the same aquifer intersected by the base well (Okoy 6 in this case), as a first estimate.

From Fig. 28 and Table 7, it can be seen that the well output is inversely proportional to the well elevation. This is due to the additional pressure drop that will occur

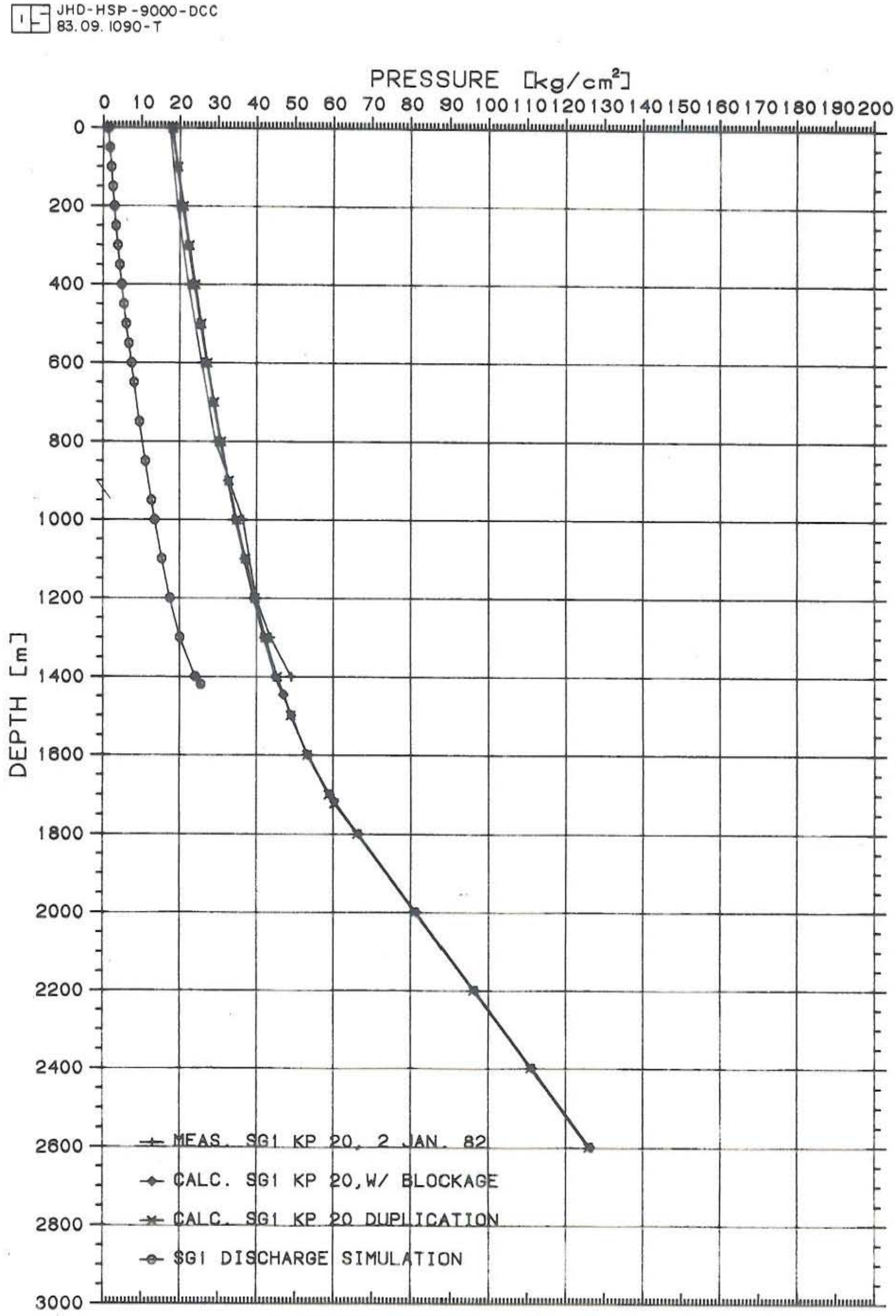

Fig. 27 Sogongon discharge simulation (by steam injection)

JHD - HSÞ - 9000 - DCC
83.08. 0985 - IS

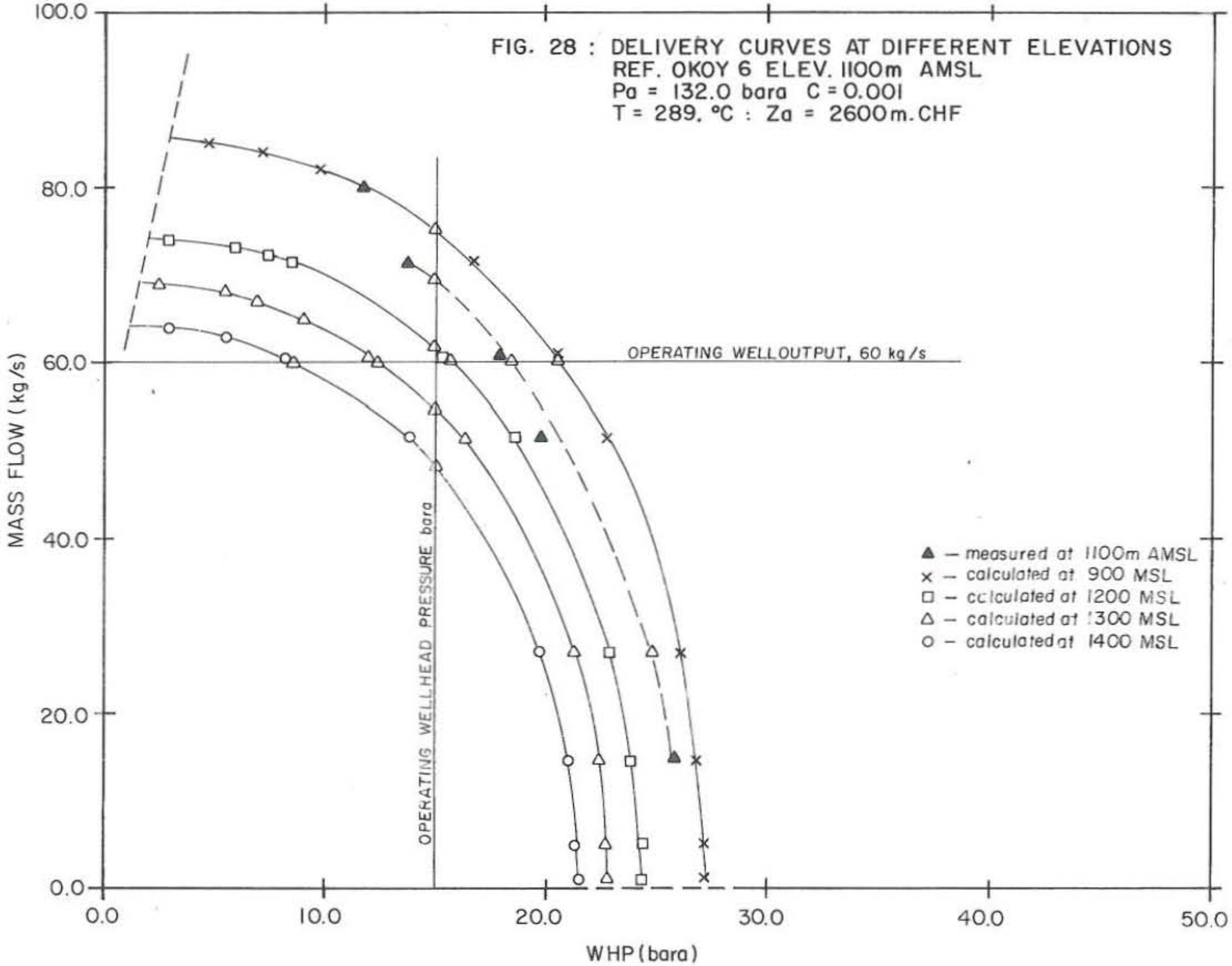

TABLE 7 Okoy 6 output at different elevations.

Calculated at Pa = 132.0 bara, C = 0.001, inflow temp., TC = 289°C, Za = 2600 m + (Elev. - 1100.0)

ELEV.(m)	WHP = 15.0 bara FLOW(kg/s)	W = 60.0 kg/s WHP(bara)
900.0	75.0	20.6
1100.0	69.3	18.5
1200.0	61.5	15.8
1300.0	54.5	12.4
1400.0	48.2	8.6

TABLE 8 Okoy 6 delevirabilities at different flow string diameters.

Calculated at Pa = 132.0 bara, C = 0.001, Inflow temperature, TC = 289.0°C, Za = 2600.0 m

CASING x LINER	WHP = 15.0 bara Mass Flow(kg/s)	W = 45.0 kg/s WHP(bara)	%INCREASE in FLOW
9-5/8" x 7"	65.2	21.4*	-
7-5/8" x 5"	38.1	8.0	-41.6
9-5/8" x 7"	65.7	21.9	0.8
13-3/8" x 9-5/8"	129.0	24.9	97.8
13-3/8" x 7-5/8"	95.5	24.1	46.5
13-3/8" x 7"	78.5	23.2	20.4
13-3/8" x 5"	47.5	17.6	-27.1

* measured data

as a result of the lengthening of the flow pipe. To compensate for this pressure drop the flow string diameters can be enlarged.

3.5.4 Optimization of wellbore design from well deliverability conditions

The WHP versus mass flow rate at different casing/liner sizes for Okoy 6 are plotted in Fig. 29. Generally, it can be seen from the curves that production can be enormously increased by enlarging the flow string diameters. For a given operating well pressure and mass flow the following values are tabulated from Fig. 29.

As can be seen from Table 8, a reduction and/or increase in flow string diameters shows a corresponding decrease and/or increase in flow rate. The significance of this simulation is for optimization of wellbore design in a partially developed field. It is clear from the graph that the mass flow increases significantly if the flow string diameter is enlarged. However, for future expansion, careful consideration should be taken in comparing the benefit of increased flow rates against the higher cost of drilling and completion of larger diameter wells. An increase in production rate would also mean a large pressure drawdown at the producing aquifer, hence increasing the rate of depletion.

3.5.5 Effect of deposition to production and data measurements

Fig. 30 shows the calculated and measured pressure profile for SG 1 when a blockage was encountered during measurements. The simulation was done in an attempt to duplicate the measured pressure profile which was only to 1400 m. It was then assumed that a blockage had occured at 1400 m to 1446 m (top of liner) causing a reduction in the diameter from 22.1 cm to 6.35 cm in the 46 m section of the casing. Fig. 30 shows that if there were no blockage, Pwf = 126.0

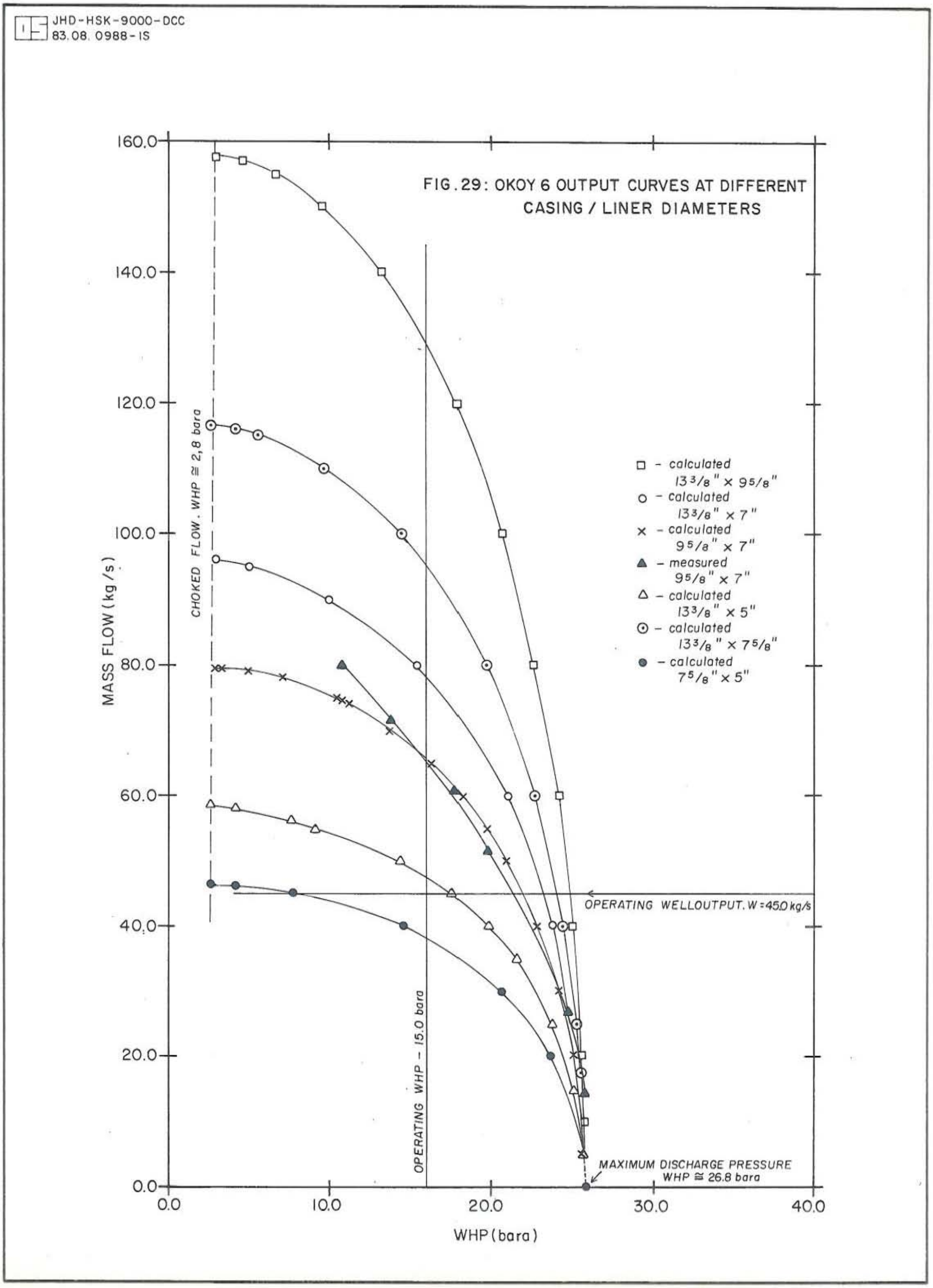
JHD-HSK-9000-DCC
83.08.0988-IS
FIG. 29: OKOY 6 OUTPUT CURVES AT DIFFERENT CASING / LINER DIAMETERS
MASS FLOW (kg/s)
WHP (bara)
CHOKED FLOW. WHP ≅ 2,8 bara
OPERATING WHP - 15.0 bara
OPERATING WELLOUTPUT. W = 45.0 kg/s
MAXIMUM DISCHARGE PRESSURE
WHP ≅ 26.8 bara
□ - calculated 13 3/8" × 9 5/8"
○ - calculated 13 3/8" × 7"
× - calculated 9 5/8" × 7"
▲ - measured 9 5/8" × 7"
△ - calculated 13 3/8" × 5"
⊙ - calculated 13 3/8" × 7 5/8"
● - calculated 7 5/8" × 5"
0.0
10.0
20.0
30.0
40.0
60.0
80.0
100.0
120.0
140.0
160.0

bara at the main zone (2600 m), whereas, with blockage, Pwf = 144.0 bara at that depth. This indicates a difference of 18.0 bara. At 1446 m to 1400 m a sharp reduction occured has occured in pressure as a result of this reduction in diameter.

A proper determination of the reduced diameter is then required to ably predict a near accurate pressure profile. This can be done by either a caliper log or a go-devil survey whichever is applicable.

A pressure survey conducted prior to the occurence of the blockage is tabulated in Table 9.

The effect of calcite deposition on production can be illustrated by well number 4 of the Svartsengi geothermal field in Iceland (SG 4). This well was drilled to a depth of 1024 m. The measured outputs before and after the occurence of the deposition are tabulated in Table 10.

From Table 10, it can be seen that the output has been reduced significantly as a result of the deposition. Choked flow was attained at 85.0 kg/s before the occurence of the deposits, and was attained at a relatively low flow of 52.0 kg/s when calcite had deposited into the well. A caliper log was conducted and the deposition was determined to occur at 340-410 m depth with the highest reduction in flow diameter at approximately 375 m (Fig. 31). To determine the aquifer pressure, simulation was made at different Pa and turbulence factor C, and was calibrated against the measured output curve prior to the deposition (Fig. 32). Pa = 88.0 bara and C = 0.0035 gave the best fit. Flowing pressure profiles were then calculated for the two cases at a flow of 49.0 kg/s using the Pa and C values mentioned above.

The results are plotted in Fig. 33. In the simulation, the average length of the deposits used was between 340-360 m, from which an average diameter of 8.3 cm gave the best fit.

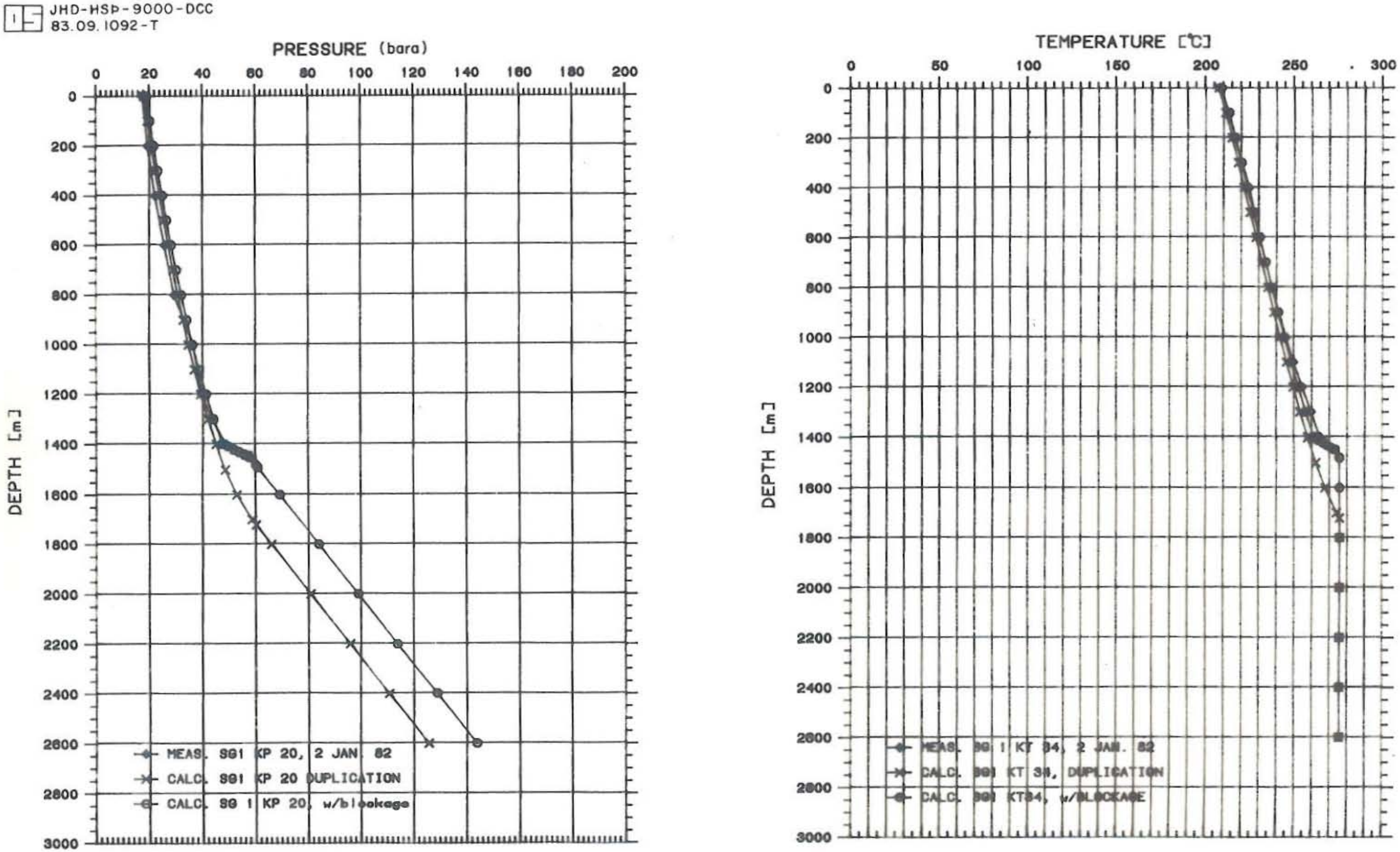

Fig. 30 Sogongon 1 measured and calculated flowing profiles

TABLE 9 SG1 measured and calculated data.

Calculated at TC= 276°C, W = 20.5 kg/s, WHP at KP20 = 18.0 bara, W= 20.5 kg/s, WHP at KP19 = 16.7 bara, W= 20.5 kg/s, Ts at 18.0 bara = 207.0°C, Ts at 16.7 bara = 204.0°C

	KP 20/KT 34		KP 19/KT 32		Calculated	
DEPTH(m)	P(bara)	TEMP(C)	P(bara)	TEMP(C)	P(bara)	TEMP(C)
0.0	17.5	208.0	16.2	212.0	19.0	209.8
200.0	19.5	217.0	18.0	215.0	21.9	217.1
400.0	22.3	225.0	21.0	222.0	25.1	224.1
600.0	25.8	231.0	24.4	230.0	28.4	231.0
800.0	29.4	238.0	28.1	238.0	32.2	237.9
1000.0	33.8	246.0	32.6	245.0	36.5	245.0
1200.0	39.8	255.0	38.6	255.0	41.6	253.0
1400.0	49.1	265.0	49.2	266.0	47.9	261.3
1446.0	-	-	-	-	57.3	272.7
1480.7	-	-	-	-	60.3	276.0
1600.0	-	-	64.7	270.0	69.3	276.0
1800.0	-	-	80.1	271.0	84.2	276.0
2000.0	-	-	95.2	272.0	99.2	276.0
2200.0	-	-	110.2	272.0	114.1	276.0
2400.0	-	-	125.5	275.0	129.1	276.0
2600.0	-	-	140.7	276.0	144.0	276.0
2650.0	-	-	144.6	277.0	-	-

- no data available

From the above data a large temperature and pressure drop has occured at 1400-1446 m.

TABLE 10 SG4 output measurements before and after the deposition.

Before		After	
WHP(bara)	Flow(kg/s)	WHP(bara)	Flow(kg/s)
19.0	33.0	18.9	28.0
17.1	59.0	16.8	39.0
14.0	75.0	13.5	49.0
13.2	80.0	11.2	52.0
11.7	84.0	9.2	51.0
10.6	85.0	8.9	52.0

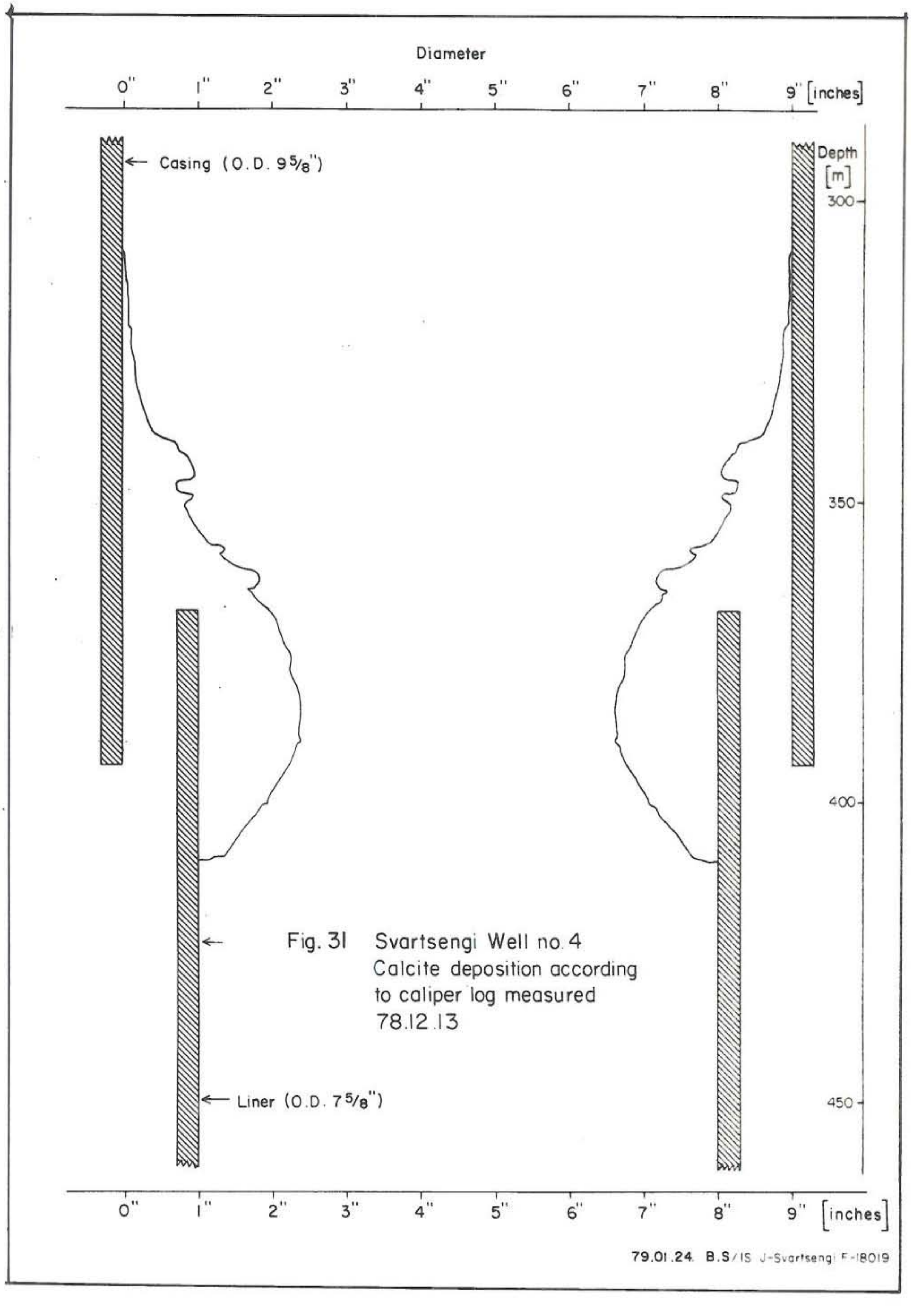

Fig. 31 Svartsengi Well no. 4
Calcite deposition according
to caliper log measured
78.12.13

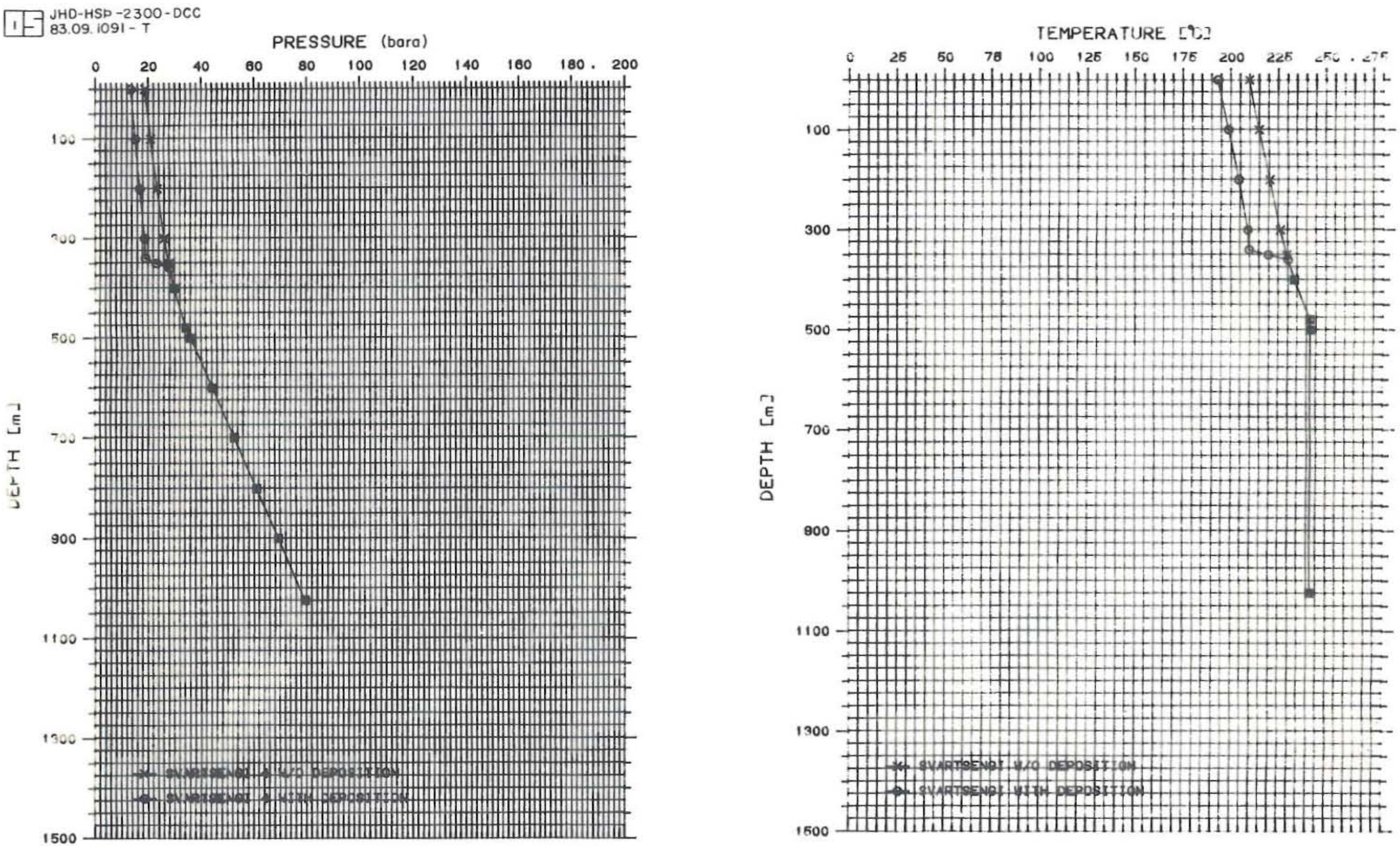

Fig. 32 Svartsengi calculated flowing pressure profiles

JHD-HSP-2300-DCC
83.09.1086-DCC

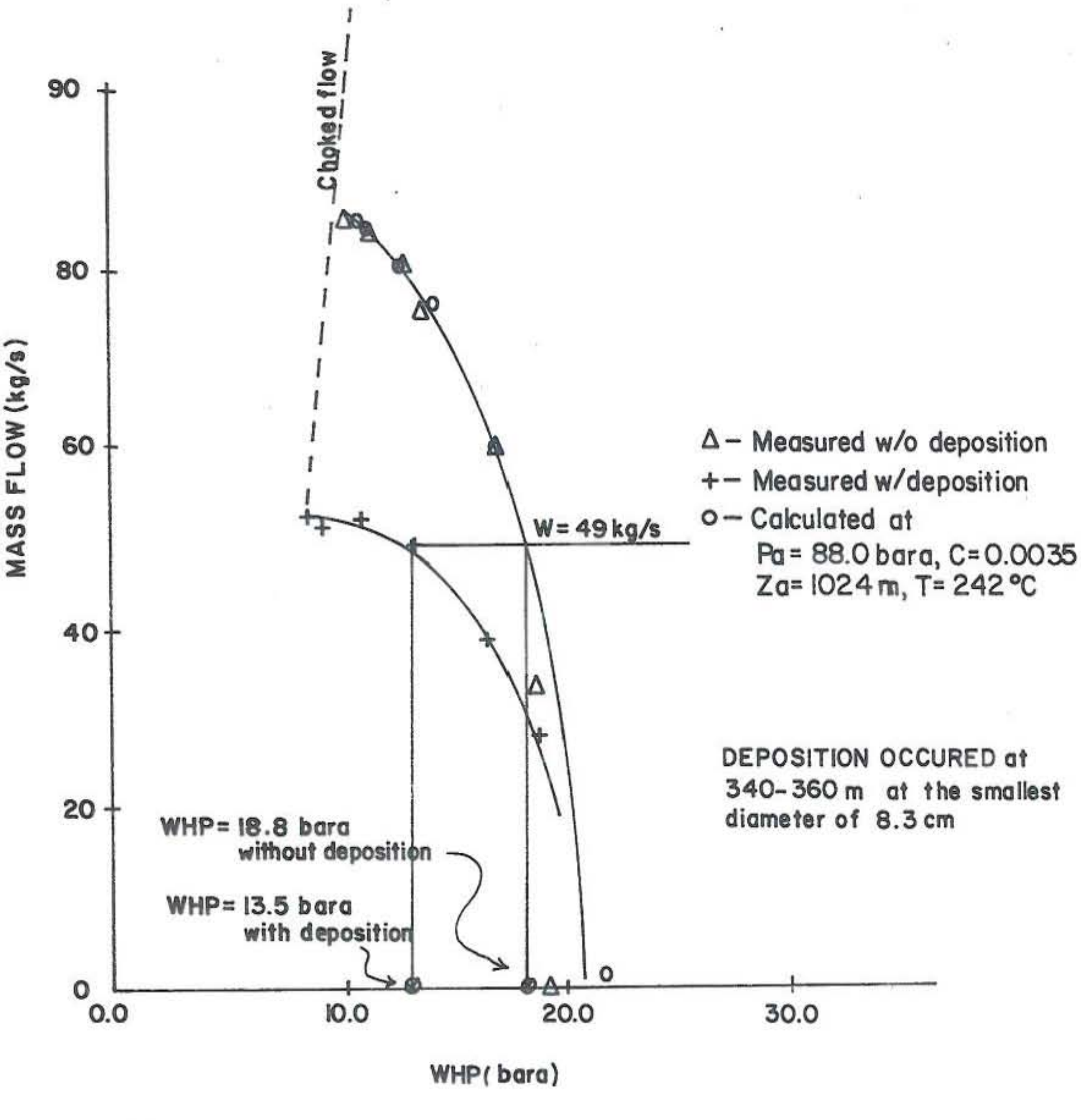

FIG. 33 Svartsengi Well no. 4 Output Characteristics

As shown in Figs. 32 and 33, the reduction in flow diameter caused a drop of 5.3 bara and 16.3 C from 360 m to the wellhead.

This section illustrates that the effects of blockage and calcite depositions on droduction is significant enough to be considered in the assessment and management of a geothermal field. The effect of deposition on production can be monitored by keeping a close watch on the WHP of the well. At a given Pa and C values, a plot of WHP versus deposits diameter can be made at any flow rate from calculations to be made using the computer program used in this paper.

3.5.6 Determination of the depletion rate of a producing aquifer

The general equation for the pressure decline in the reservoir is

$$(Pi - P(r,t)) = \frac{W\mu}{2\pi\rho kh} (P_D(r_D,t_D) + s) \quad (15)$$

where; Pi = initial reservoir pressure, P(r,t) = pressure of the aquifer as a function of r(radius), and t(time), D = subscript for dimensionless quantities, and s = skin factor (let s = 0.0 for the discussions to follow).

$$r_D = r/r_w \quad (16)$$

$$t_D = \frac{kt}{\phi\mu c_t r_w} 2 \quad (17)$$

Using the exponential integral (Ei) solution for an infinite reservoir case, the dimensionless pressure can be approximated as

$$P_D = 0.5\ [-Ei(-u)] \tag{18}$$

$$u = \frac{r_D^2}{4t_D} \tag{19}$$

Defining the storativity and transmissivity parameters as follows,

$$S = \phi\ c_t\ h \tag{20}$$

$$T = kh/\mu, \tag{21}$$

and combining equations (16) and (17), equation (19) will become

$$u = \frac{r^2\ S}{4Tt}$$ and eq. (15) can be rewritten as,

$$dP = \frac{W}{2\pi\rho T}\ (P_D) = Pi - P(r,t)$$

The -Ei(-u) function can be estimated from Fig. 35 (u=x) or for $u < 0.01$, can be calculated using the logarithmic approximation (Matthews and Russell, 1967).

$$-Ei(-u) = -2.303 \log u - 0.5772 \tag{24}$$

For a producing well the depletion rate at any given plant conditions can be estimated as will be shown for Okoy 6. Fig. 34 shows a plot of the massflow versus WHP at different aquifer pressures for Okoy 6. From the plot, a line was drawn for constant flowrate of 60 kg/s. Taking 8.2 bara as the minimum WHP required to allow two-phase fluid from this well to flow to the separator (separation pressure, say 7.2 bars, allowing 1.0 bar for pressure loss in the transmission line), the minimum aquifer pressure required is 107.0 bara at a flow of 60 kg/s. The depletion rate can roughly be estimated, with a plant life of 25 years, as,

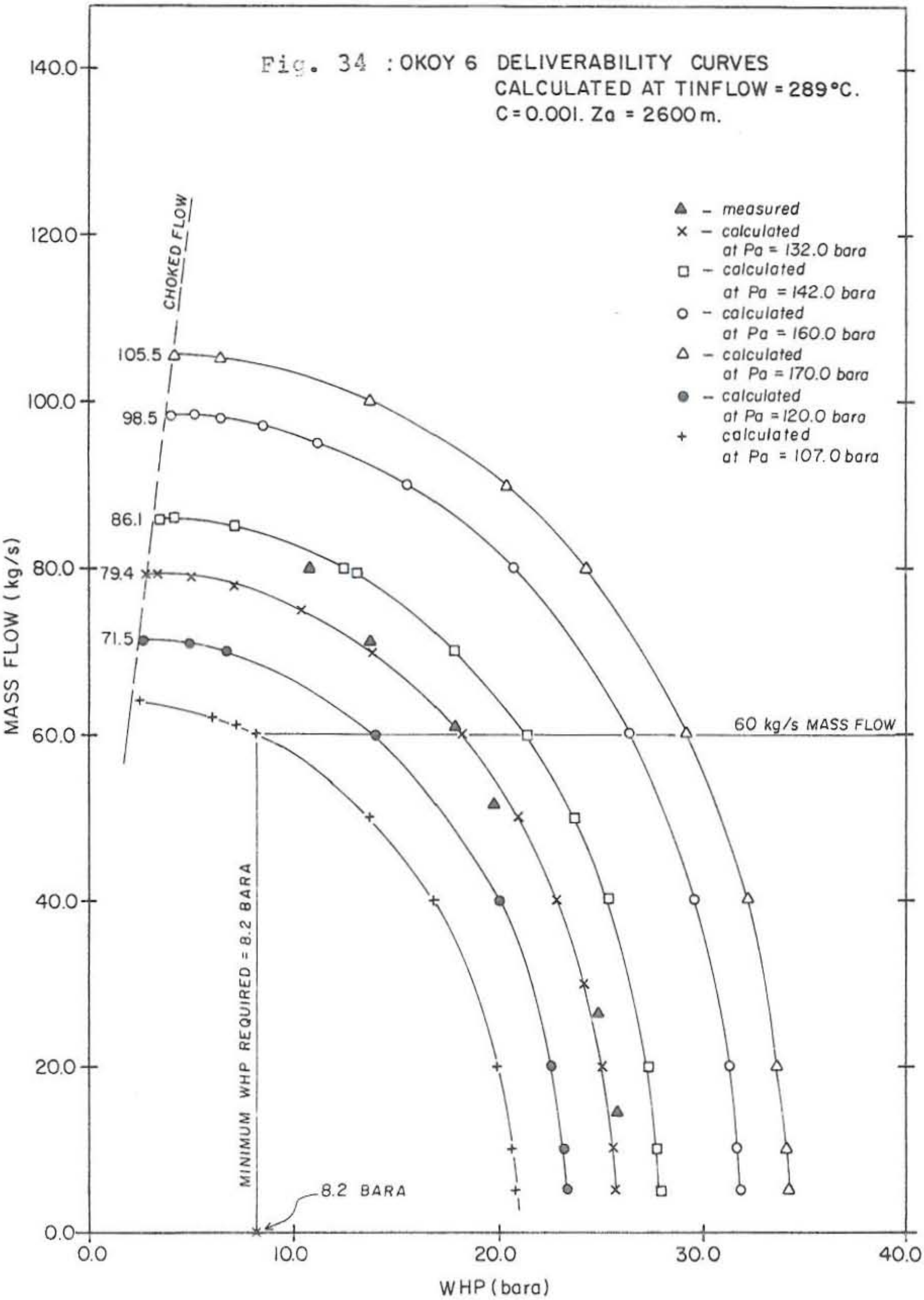
Fig. 34 : OKOY 6 DELIVERABILITY CURVES
CALCULATED AT TINFLOW = 289°C.
C = 0.001. Za = 2600 m.
▲ – measured
× – calculated at Pa = 132.0 bara
□ – calculated at Pa = 142.0 bara
○ – calculated at Pa = 160.0 bara
△ – calculated at Pa = 170.0 bara
● – calculated at Pa = 120.0 bara
+ calculated at Pa = 107.0 bara
CHOKED FLOW
105.5
98.5
86.1
79.4
71.5
60 kg/s MASS FLOW
MINIMUM WHP REQUIRED = 8.2 BARA
8.2 BARA
MASS FLOW (kg/s)
WHP (bara)
0.0
20.0
40.0
60.0
80.0
100.0
120.0
140.0
10.0
30.0

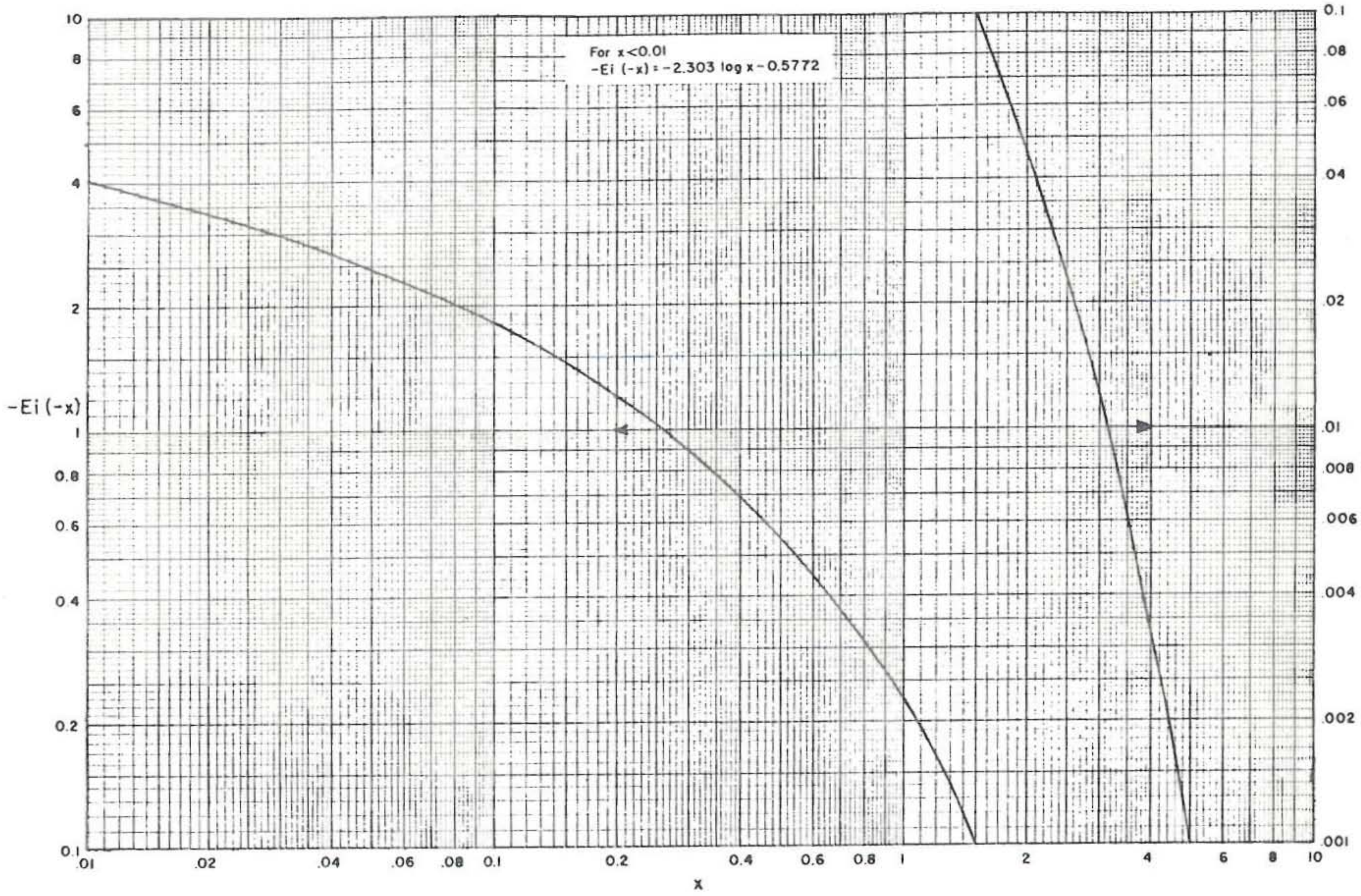

Fig. 35 Exponential Integral (Ei) graph (after, Matthews & Russel, 1967)

depletion rate = (132.0 - 107.0)/25 = 1.0 bar/year

The actual depletion rate will, however, depend on the geometry of the reservoir where the well is located and the nature of the boundaries surrounding it. The actual depletion rate may be lower than what was calculated (dP = 1.0 bar/year). The above depletion rate can, however, be used as a maximum limit at which the well has to be produced. In a reservoir which is being tapped by a number of wells, interference may cause the drawdown to accelerate. Hence, the interference should be kept to a minimum and this depends on the spacing of their production zones. Roughly, this can be estimated from the drainage radius, r. As can be seen from Fig. 11, the pressure propagates slowly as the drainage radius is increased. Hence, the drainage radius can be estimated at which the propagation of P(r,t) is relatively small. This will be illustrated for the Nasuji-Sogongon area considering an infinite system with a circular geometry.

For the Nasuji-Sogongon area, a 110 MWe plant has been planned for the near future. Given the turbine inlet pressure and the turbine steam rate the amount of steam and/or geofluid required for this installation can be estimated. For the Southern Negros project, for example, the wells are rated at a turbine inlet pressure of 7.2 bara and a steam rate of 2.82 kg/s-MWe.

The Nasuji-Sogongon field has a liquid dominated reservoir of approximately 283°C reservoir temperature (based on Okoy 6 and SG 1). The amount of steam and geofluid required for the 110 MWe can be estimated as;

$$Ws = 110 \times 2.82 = 310.2 \text{ kg/s of steam} \qquad (25)$$

$$W = Ws \frac{H_v - H_f}{H - H_f}$$

At 7.2 bara, Hv = 2766.3 kJ/kg, Hf = 701.8 kJ/kg, and at 283°C , H = 1252 kJ/kg. Then,

$$W = 310.2 \frac{2766.1 - 701.8}{1252.0 - 701.8}$$

$$= 1164.0 \text{ kg/s of total mass.}$$

For a well production of 60 kg/s, this requires 20 wells, or roughly 5.5 MWe per well.

Well tests carried out on the wells drilled in the area showed an average transmissivity of, T = 3.8E-8 m3/Pa.s (Torrejos, 1983). Cores cut from SG1 and Okoy 6 at the producing horizon (diorite intrusion) showed an average porosity of 0.04 (Bromly, 1981). Assuming an aquifer thickness of 100 m and a total rock and fluid compressibility of 3.1E-9 per Pascal, the storativity is calculated to be 1.24E-8 m/Pa.

The parameter u can be evaluated using equation (22) as a function of radius and time, S and T being known.

$$u = (0.081579)r^2/t, \text{ let } t = 25 \text{ yrs} = 7.884E8 \text{ secs.}$$

Considering the Nasuji-Sogongon area as a single well with circular drainage and producing at 1164 kg/s, the depletion rate can be calculated as shown in Table 11.

From the Table 11, the highest drawdown will occur when r = 50 m. The average depletion rate per year can be estimated as

$$dP = \frac{477.44}{(25)} = 19.1 \text{ bar,}$$

and for r = 500 m,

$$dP = \frac{326.86}{(25)} = 13.08 \text{ bar},$$

The calculations show that the depletion rate seems too high and unrealistic. This maybe due to the low values of S and T used. For the Svartsengi geothermal field in Iceland, the S and T values were found to be 1.483E-6 m/Pa and 1.483E-6 m3/Pa.s, respectively (Kjaran, 1980). Using these values for the above calculations, for r = 50 and 500 m, and t = 25 years,

$$u = \frac{0.25(50)(50)(1.483E-6)}{(1.483E-6)(7.884E8)} = 7.927E-7$$

$$\begin{aligned} -Ei(-u) &= -2.303 \log (7.927E-7) - 0.5772 \\ &= 13.473 \end{aligned}$$

$$P_D = 6.736$$

$$dP = \frac{1164(6.736)}{2(3.1416)(745)(1E5)(1.483E-6)}$$

$$= 11.29 \text{ bars for 25 years}$$

and dP = 7.43 bars for r = 500 m, also at t = 25 yrs, which are much lower than those tabulated in Table 11.

All calculations done were based on an infinite reservoir case. For bounded reservoirs, the depletion rate is expected to be higher, hence boundary effects should be taken with much caution into the calculations. For the Svartsengi field for instance, Fig. 36 (Regalado, 1981), it was shown that the actual depletion rate was much higher than what was calculated using the Theis method. It is illustrated here that the flowing pressure profile and the depletion rate of the producing well can be predicted using the two-phase flow model. However, for the whole reservoir, accurate predictions can only be made with a thorough study of the pressure history of the field as well as the nature of its boundaries, and this of course will much depend on the accuracy of the measurements made, from which the reservoir parameters such as S and T are estimated.

For accurate calculations of the depletion rate and the well spacing, pressure transient tests should be carried out with utmost care so as to get a good estimate of S and T. Hence the electrical power potential of the field can be estimated from the production data and the pressure history.

TABLE 11 Nasuji-Sogongon area depletion rate.

Calculated at t = 25 yrs, T = 3.8E-8, S = 1.24E-8, W = 1164 kg/s.

r(m)	u	-Ei(-u)	PD	dP(bara)
50.0	2.587E-7	14.59	7.296	477.44
100.0	1.035E-6	13.21	6.605	432.22
200.0	4.139E-6	11.82	5.910	386.74
300.0	9.313E-6	11.01	5.506	360.30
400.0	1.656E-5	10.43	5.215	341.26
500.0	2.587E-5	9.99	4.995	326.86

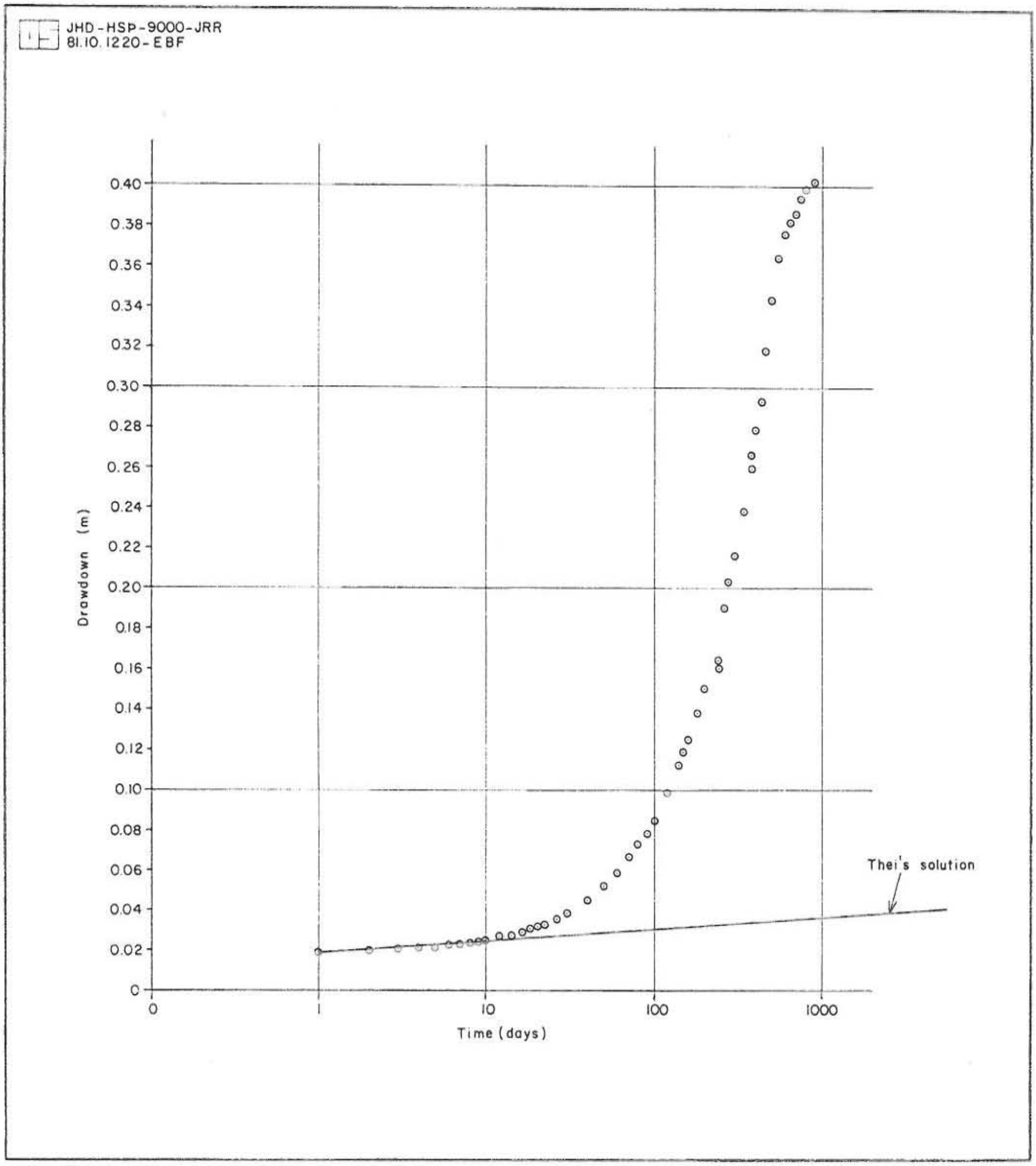

Fig. 36 Svartsengi geothermal field unit response function
(after Regalado, 1981)

4 CONCLUSIONS AND RECOMMENDATIONS

Two-phase flow models can be used as a tool in geothermal well analysis and the geothermal reservoir as a whole. Using the model presented here, information can still be obtained where actual measurements failed. It is recommended that the usage of two-phase flow models be made an integral part in geothermal well evaluation and data interpretation.

From the profile duplications made in the previous sections of this report, the best fit is obtained by using the correlations presented by Armand and Teacher(1959) for the void fraction occupied by the vapour phase, and that of Chisholm(1972) for the two-phase multiplier, hence these correlations are used in all the calculations presented.

For a partially developed field, it is found that by using the model presented here, an estimate can be made of the following aspects pertaining to the well and the reservoir:

1) Profile duplication. Proper duplication of the measured pressure and temperature profiles can be helpful for example in the determination of the true temperature and pressure profiles, in the determination of the inflows for a multizone well, in qualifying the effects of heat transfer to the formation at low flow rates, and in detecting the effects of impurities to pressure and temperature profiles at flowing conditions.

2) Deliverability curves. By ably predicting the deliverability curve, the following aspects of well flow can be determined: choked condition, turbulence pressure drop, maximum discharge pressure, and productivity index, to mention a few.

3) Well start-up. The method of well start-up presented here is the steam or two-phase fluid injection. It is found out that the probability of a successful well

discharge using the above mentioned method depends on the minimum temperature of the water column attained during the stimulation process.

4) Well elevation. Using the two-phase model it is illustrated that for a partially developed field, output of the wells to be drilled at other elevations can be estimated.

5) Wellbore design. For a field with a proven capacity, extraction of the geothermal fluid from the reservoir to the surface largely depends on the wellbore design. The simulations suggest that production can be increased significantly by enlarging the diameter of the wells. However, care should be taken in comparing the benefits of increased production against the higher cost of drilling larger diameter wells, and the rate of depletion of the producing well.

6) Chemical deposition. Chemical deposits within the well will reduce the effective flow diameter, hence the flow rate will decrease. By simulation, the reduction in flow rate and the size of the deposition can be estimated, hence a decision can be made as to the size of deposits that can be tolerated to accumulate, and the time that well cleaning is required.

7) Depletion rate. Using the model, the depletion rate of a producing well can be estimated. Hence given an expected plant life, a decision can be made as to how much flow is needed for a well to last within the entire life of the plant. For the reservoir, a thorough investigation is required on the pressure history of the field, and pressure transient tests should be carried out with utmost care so as to get a good estimate of the reservoir parameters (S and T), hence a reliable prediction of the depletion rate.

As enumerated above, boreflow simulation can aid significantly in decision making on various aspects of reservoir and plant management.

ACKNOWLEDGEMENTS

The author is greatly indebted to the following whose help made the completion of this paper possible: The personnel and staff of Orkustofnun and the United Nations University - in the use of the computer and other facilities, and valuable communications related to this paper with some of the staff. The staff of Vatnaskil Ltd., consulting engineers, especially Jonas Eliasson, and Snorri Pall Kjaran, who acted as my supervisors for this work, and Gisli Karel Haldorsson who allowed me to use his original computer program and modify it. Personnel and staff of PNOC-EDC - who provided me with the required data.

I also wish to extend my gratitude to Dr. Ingvar Birgir Fridleifsson, the director of the UNU Geothermal Training Programme, and the management of PNOC-EDC Geothermal Division who made my training under the UNU Fellowship possible, hence the writing of this report.

Special acknowledgements are also due to Dr. Ingvar Birgir Fridleifsson, Snorri Pall Kjaran, and Jonas Eliasson for critical reading of this report.

And lastly thanks are due to Sigurjon Asbjornsson for his assistance in all the neccessary arrangements, making our stay in Iceland fruitful.

REFERENCES

Algopera, W.N. (1980): Discharging of Wells by Steam Injection at SNGF. Diploma thesis, Geothermal Institute, Auckland, New Zealand.

Armand, A.A., G.G. Teacher(1959): Investigation of the Resistance During the Movement of Steam-water Mixtures in a Heated Boiler Pipe at High Pressures. Atomic Energy Research Establishment, Hartwell, Berkshire.

Bagamasbad, N.G. (1979): Geology of Well Okoy 5 in SNGF. UNU Geothermal Training Programme, Reykjavik, Iceland Report 1979-2, 50 pp.

Brodie, A.J. (1980): Personal Communications.

Brodie, A.J., et. al. (1981): Well Discharge Stimulation Techniques in Hot-water Dominated Fields. KRTA, 583.

Bromley, C.J. (1981): Core Density Measurements - Southern Negros Wells. Unpublished report, 1-2.

Catacutan,A.V. (1982):Okoy Field Field Pressures. PNOC-EDC Internal Report, 8.

Catigtig, D.C. (1982): Boreflow Simulation Using HP 41CV. PNOC-EDC Internal Report, 90 pp.

Catigtig, D.C. (1981a): Okoy 5 Well Analysis Report. PNOC-EDC Internal Report, 12-13.

Catigtig, D.C. (1981b): Okoy 7 Well Analysis Report. PNOC-EDC Internal Report, 10-12.

Chisholm, D. (1972): Pressure Gradients due to Friction during the Flow of Evaporating Two-phase Mixtures in Smooth Tubes and Channels. Int. Jou. Heat and Mass Transfer, vol. 16, 347-358.

DiPippo, R. (1980): Geothermal Energy as a Source of Electricity. U.S. Dept. of Energy, 175-176, 189-191, 201-202.

Elizagaque, R.F. and B.S. Tolentino (1982): Geothermal Development in the Philippines. Geothermal Resources Council Bulletin, 5-7.

Grant, M.A., I.G. Donaldson, and P.F. Bixley. (1982): Geothermal Reservoir Engineering, Academic Press, 129, 319-324.

Grant, M.A. (1981): Some Notes on the Wells and Reservoir of the Okoy Field, DSIR, 6 pp.

Griffith, P. and G.B. Wallis (1961): Two-phase Slug Flow. Jou. Heat Transfer, Trans., AIME, 307-320.

Gould, T.L. (1974): Vertical two-phase Steam-water flow in Geothermal Wells. SPE-AIME, Intercomp, 5 pp.

Haldorsson, G.K. (1978): Pressure Drop in Geothermal Blowing Wells Rekjavik, Iceland, chap. 5, app. II and III.

Jacob, C.E.(1946): Radial flow in a Leaky Artesian Aquifer. Transaction American Geophysical Union, vol. 27, 198-205.

James, Russel (1962): Steam Water Critical Flow Through Pipes. Inst. of Mech. Engr's. Proc., vol. 176, no. 26, 741.

Jordan, O.T. (1982): Implications of Solution Mineral Equilibria on the Exploitation of the Southern Negros Geothermal Field. UNU Geothermal Training Programme, Reykjavik, Iceland, Report 1982-7, 67 pp.

Kjaran, S.P. and J.E. Eliasson. (1983): Personal Communications.

Kjaran, S.P. and J.E. Eliasson. (1983): Geothermal Reservoir Engineering Lecture Notes. UNU Geothermal Training Programme, Reykjavik, Iceland, Report 1983-2 238 pp.

Keenan, and Keyes, et.al. (1978): Steam Tables. 153 pp.

Martinelli, R.C. and D.B. Nelson (1948): Prediction of Pressure Drop During Forced Circulation Boiling of Water. ASME Trans., 70, 695-702.

Matthews, C.S. and D.G. Russel. (1967): Pressure Build-up and Flow Test in Wells. SPE-AIME, 163.

Michaelides, E.E. (1981): Thermodynamic Properties of Geothermal Fluids. GRC 5, 361-364.

Michels, D.E. (1981): CO2 and Carbonate Chemistry Applied to Geothermal Engineering. Rep LBL-11509(GREMP-15), Lawrence Berkely Laboratory, Berkely, California.

Palmason , G. (1982): Philippines. UN Report No. 24, 17-22.

Pornuevo, J.B., O.T. Jordan, and D.C. Catigtig (1981): Okoy 6 Comprehensive Report. PNOC-EDC Internal Report, 8-10.

Regalado, J.R.(1981): A study of the Response to Exploitation of the Svartsengi Geothermal Field, SW Iceland. UNU Geothermal Training Programme, Reykjavik, Iceland Report 1981-7, 111 pp.

Sanyal, S.K. and S. Juprasert (1977): Numerical Simulator for Flow in Geothermal Wellbores. Geothermal Resources Council, vol. 1, 159.

Sigurdsson, Omar (1983): Personal Communications.

Sutton, F.M. (1976): Pressure-temperature Curve for a Two-phase Mixture of Water and Carbon Dioxide. N.Z.J. Sci. 19, 297-301.

Torrejos, A.T. (1983): Updated Measurements and Data Interpretations of SNGF. PNOC-EDC Internal Report, 1-2.

Torrejos, A.T. (1983): Updated Okoy Field temperature Contours. PNOC-EDC Internal Report, 18-21.

APPENDIX A: DERIVATION OF THE PRESSURE DROP EQUATIONS

A.1 Homogeneous model

For notations, refer to Fig. A.1

This derivation was based on an assumption of a steady homogeneous one-dimensional fluid flow in a pipe, and using the conservation equations for mass, energy, and momentum.

The mass continuity equation is

$$\text{(A1.1)} \qquad W = \rho VA$$

The energy equation is

$$\text{(A1.2)} \qquad dE = WdH + W\,d(V^2/2) + Wgdz - dQ$$

In most cases, Q is very much smaller compared to WH; i.e., the well operation is substantially adiabatic. At this stage, for an adiabatic process, Q = 0. For a self-flowing well, there is no energy input, hence E = 0. The energy equation will then reduce to

$$\text{(A1.3)} \qquad 0 = WdH + Wd(V^2/2) + Wgdz$$

$$\text{(A1.4)} \qquad 0 = dH + d(V^2/2) + gdz$$

Integrating eq. (A1.4) at any two points in the well in an upward direction, the following equation can be derived

$$\text{(A1.5)} \qquad H_2 = H_1 - 0.5(V_2^2 - V_1^2) - g(Z_2 - Z_1)$$

$$\text{(A1.6)} \qquad H_1 = x_1(H_{v1}) + (1-x_1)H_{f1}$$

$$\text{(A1.7)} \qquad H_2 = x_2(H_{v2}) + (1-x_2)H_{f2}$$

$$\text{(A1.8)} \qquad x_2 = \frac{H_1 - 0.5(V_2^2 - V_1^2) - g(Z_2 - Z_1) - H_{f2}}{H_{v2} - H_{f2}}$$

where x = mass fraction of steam; H = enthalpy, kJ/kg; V = fluid velocity, m/s; W = mass flow, kg/s; = density, kg/m ; v,f = subscripts for steam and liquid, respectively; and g = acceleration due to gravity, 9.81 m/s .

The momentum equation is

$$\text{(A1.9)} \qquad P = \rho V dV + dF/A + \rho g dz + P + dP$$

$$\text{(A1.10)} \qquad -dP = \rho V dV + dF/A + \rho g dz$$

where dF/A is the frictional pressure drop defined by Darcy-Weisbach as;

$$\text{(A1.11)} \qquad (dP)fric = dF/A = \rho f V^2 \, dz/2D$$

$$\text{(A1.12)} \qquad f = f(Re)$$

$$\text{(A1.13)} \qquad Re = \rho V D/\mu$$

From the modified Colebrook's equation,

$$\text{(A1.14)} \qquad f = \{[-2\log(\varepsilon/D + (7/Re)^{0.9})]^2\}^{-1}$$

where ε = the absolute roughness factor of the flow pipe.

The acceleration pressure drop is

$$\text{(A1.15)} \qquad (dP)acc = \rho V dV$$

If the mass flux will be defined as G = W/A and using eq. (A1.1), (A1.16) $$V = G/\rho$$

Then, eq. (A1.15) can be expressed as

(A1.17) $$(dP)acc = GdV$$

The potential pressure drop is

(A1.18) $$(dP)pot = \rho gdz$$

Then the total pressure drop is

(A1.19) $$-(dP)t = (dP)fric + (dP)acc + (dP)pot$$

A.2 Single-phase region

In the single phase section of the well, the fluid density is substantially constant and this corresponds to the saturated liquid density at the inflow temperature. Then $V1 = V2$, $(dP)acc = 0$.

(A1.20) $$-(dP)t = (dP)fric + (dP)pot$$

$$= (\rho fV^2dz)/2D + \rho gdz$$

dz = incremental pipe lenght, m.

(A1.21) $$H_2 = H_1 = H_{f1} = H_{f2}$$

where H is the saturated liquid enthalpy corresponding to the inflow temperature.

A.3 Determining the flash level

Refer to Fig. A.2. From eq. (A1.20),

$$-(dP)t = (dP)fric + (dP)pot.$$

Throughout the lenght (Za - Z*),

(A1.22) $$-(dP)t = (Pwf - Ps), \text{ then}$$

(A1.23) $$(Pwf-Ps) = \frac{\rho f V^2 (Za-Z^*)}{2D} + \rho g(Za-Z^*)$$

(A1.24) $$Z^* = Za - \frac{(Pwf - Ps)}{\rho g + \dfrac{\rho f V^2}{2D}}$$

$$Z^* = Za - \frac{(Pwf - Ps)}{\rho g + \dfrac{G^2 f}{2\rho D}}$$

If the aquifer pressure is known, Pa

(A1.25) $$Pa = Pwf + CW^2$$

where CW^2 is the pressure drop due to turbulence.

Then, eq. (A1.24) will become,

(A1.26) $$Z^* = Za - \frac{(Pa - CW^2 - Ps)}{\rho g + \dfrac{G^2 f}{2\rho D}}$$

JHD-HSÞ-9000-DCC
83.09.1084-DCC

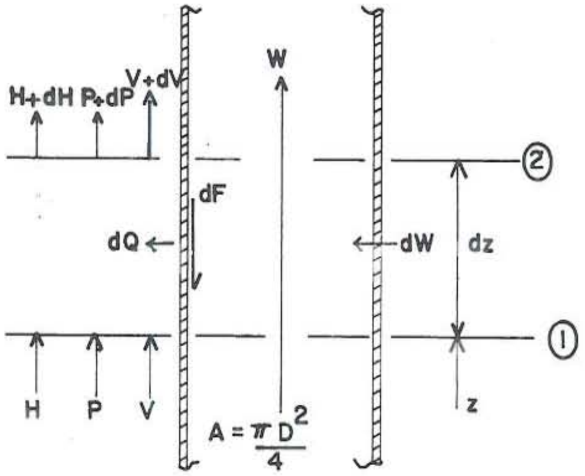

FIG. A.1 COMPONENTS OF FLUID FLOW IN A PIPE

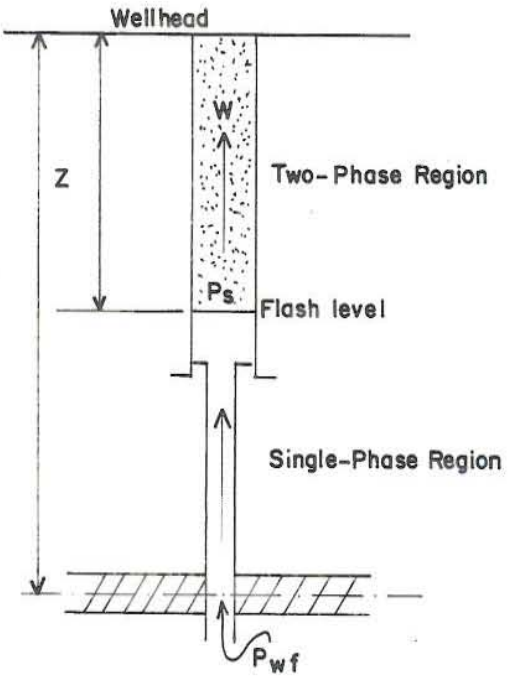

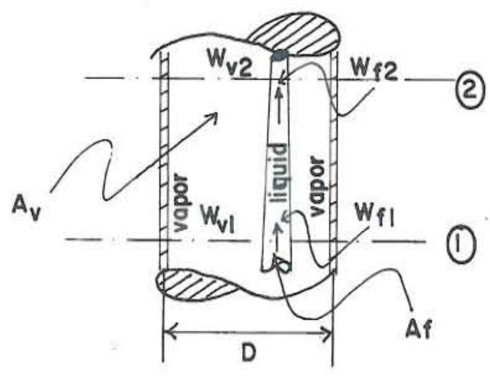

FIG. A.3 PHASE SEPARATION DURING FLOW

FIG. A.2 FLASHING LEVEL IN THE WELL

A.4 Two-phase region

As the flowing process continues, flowing well pressure continuosly drops until it will reach the saturation pressure corresponding to the inflow temperature, at which stage the fluid will then start to flash. In this section of the well, the fluid undergoes flow regime changes, i.e., bubble, slug, churn, and annular in an upward direction. These regimes are discussed in Section 3.1.

In any of these flow regimes, the liquid and the vapour phases flow separately and travel at different velocities. The vapour phase travels faster than the liquid phase resulting into a slippage between the phases. Hence, corrections should be made on the homogeneous pressure drop equation, eq. (A1.20). These are the slip, void fraction occupied by the vapor phase and the liquid phase, and the two-phase friction factor. The void fraction occupied by the vapour phase is defined as;

(A1.27) $\alpha = A_v/A,$

where Av is the cross-sectional area occupied by the vapor phase, and A is the cross-sectional area of the flow pipe.

The void fraction occupied by the liquid phase is defined as

(A1.28) $(1 - \alpha) = A_f/A,$

where Af is the cross-sectional area occupied by the liquid phase.

The slip factor or the velocity ratio is defined as

(A1.29) $$K = \frac{V_v}{V_f}$$

where V_v and V_f are the vapour and the liquid phases velocities respectively.

From the continuity equation, eq. (A1.1),

$$(A1.30) \qquad V_v = \frac{xW}{\rho_v A_v}$$

where x is the mass fraction of the vapor in the flow.

$$= G \frac{x}{\alpha \rho_v}$$

$$(A1.31) \qquad Vf = \frac{(1-x)W}{\rho_f A_f} = G \frac{(1-x)}{(1-\alpha)\rho f}, \quad \text{then}$$

$$(A1.32) \qquad K = \frac{x\rho_f(1-\alpha)}{(1-x)\alpha\rho_v}$$

in the two-phase section, the individual pressure drops can then be written as

$$(A1.33) \qquad (dP)pot = [\alpha\rho_v + (1-\alpha)\rho f]gdz$$

$$(A1.34) \qquad (dP)acc = G\ dV$$

$$= G^2\ d\left[\frac{x^2}{\rho_v} + \frac{(1-x)^2}{(1-\alpha)\rho f} \right]$$

$$(A1.35) \qquad (dP)fric = \frac{fV2[\alpha\rho_v + (1-\alpha)\ \rho f]}{2D}\, dz$$

The friction factor is evaluated using eqs. (A1.12), (A1.13), and (A1.14) using the two-phase correction factor discussed below.

However, this incurs the difficulty in defining the satisfactory definition of a two-phase viscosity, and it is usual to devise an expression which recognizes the mass proportions of both the saturated liquid and saturated vapour (DiPippo, 1980).

Martinelli and Nelson (1948) introduces an empirical relation to calculate the friction pressure gradient;

$$\text{(A1.36)} \quad \phi^2{}_{v \text{ or } f} = \frac{(dP/dz)ftp}{(dP/dz)v \text{ or } f}$$

where; (dP/dz)ftp = the two-phase frictional pressure gradient.

(dP/dz)v or f = the frictional pressure gradient if only vapor or liquid is flowing in a pipe.

$$\text{(A1.37)} \quad (dP)fric_{tp} = (dP)fric_f \cdot \phi^2$$

In this paper, the correction factor used is for liquid, hence the friction factor is evaluated using the single phase (liquid) properties.

The Armand and Teacher (1959) correlation for α is,

$$\text{(A1.38)} \quad = \frac{0.833 + 0.05 \log(P)}{1 + \frac{(1-x)\rho v}{x\rho f}}$$

The Chisholm (1972) correlation for ϕ_f^2 is,

$$\text{(A1.39)} \quad \phi_f^2 = 1 + (CX^{-1}) + (X^{-2})$$

$$X = \frac{(1-x)^2 \rho_v}{x\rho f}$$

$$C = 1 + \frac{xv_v}{xv_v + (1-x)v_f} - \alpha$$

P is in bars, v is the specific volume, and x is the mass fraction of steam.

For further discussion of these correlations, the reader is referred to Haldorsson (1978).

APPENDIX B. FLOW MEASUREMENTS AND TURBULENT PRESSURE DROPS

B.1. Flow measurements

James (1962) showed that by means of a lip pressure tapping at the end of a pipe discharging geothermal fluid critically to the atmosphere, a fairly accurate estimate of the mass flow rate can be made provided the stagnation enthalpy of the fluid is known.

Over a critical pressure range of 97 to 440 kPa, and a stagnation enthalpy of 535 to 2791 kJ/kg, the following empirical equation was formulated by James (1962) with a claimed accuracy of _ 3% .

$$(B.1) \qquad \frac{G\ H^{1.102}}{P^{0.96}} = 22106$$

where G is the mass flux, W/A, $kg/m^2.s$; H is the enthalpy, kJ/kg; P is the critical lip pressure, kPa.

For reference, see Figs B.1 and B.2.

$$(B.2) \qquad W = \frac{22106\ P^{0.96}}{H^{1.102}} \cdot \frac{(\pi)D^2}{4}$$

where D is the discharge pipe diameter, m.

From Fig. B.1, the mass and heat balance equations are as follows;

$$(B.3) \qquad W = W_f + W_v$$

where; W_f = water flow and W_v = steam flow, kg/s.

$$(B.4) \qquad WH = W_f H_f + W_v H_v$$

From equations (B.3) and (B.4),

$$(B.5) \qquad W = \frac{W_f(H_f - H_v)}{H - H_v}$$

Equating equations (C.2) and (C.5), and rearranging,

$$(B.6) \qquad \frac{4}{(\pi)} \cdot \frac{W_f}{D^2 P^{0.96}} = \frac{(H_v - H)}{(H_v - H_f)} \cdot \frac{22106}{H^{1.102}}$$

Defining the James Factor as, $JF = \dfrac{W_f}{D^2\ P^{0.96}}$

and taking the steam and water enthalpies at atmospheric pressure (1.0 ata),

$$H_v = 2676 \text{ kJ/kg}, \quad H_f = 419 \text{ kJ/kg}$$

Then equation (B.5) will become,

$$(C.7) \quad W = \frac{2257\ W_f}{2676 - H}$$

From which Wf can be measured (weir method), using a weir plate at the water collecting device (silencer weir box). For a trapezoidal ceppoletti weir for example, (see fig B.2),

$$(B.8) \quad W_f = h^{1.5} \cdot L \cdot 0.0562$$

where h is the water height (mm), and L is the length of weir (m).

Evaluating equation (B.6) and using the definition of the JF, the enthalpy can be solved as

$$(B.9) \quad 1.273\ JF\ H^{1.102} + 9.79\ H - 26210 = 0$$

JHD-HSÞ-9000-DCC
83.09.1088-DCC

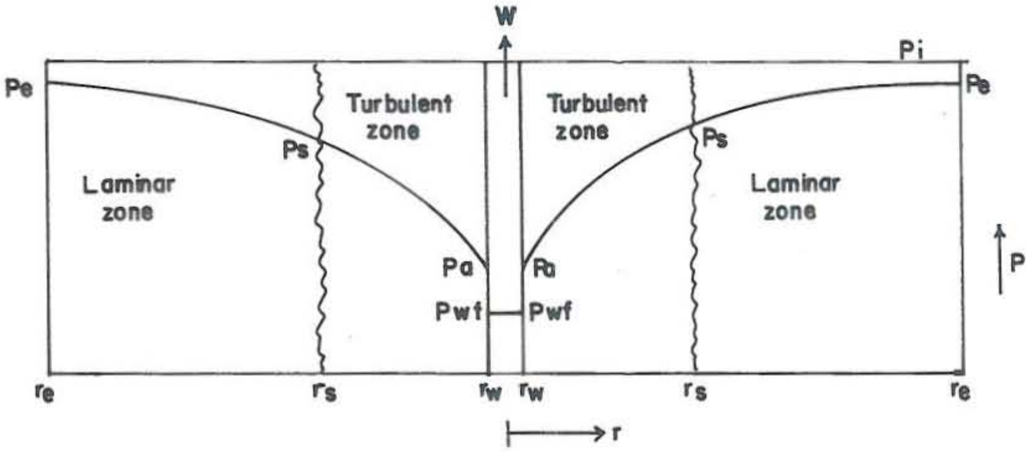

FIG. 11 Pressure configuration in laminar and turbulent zones

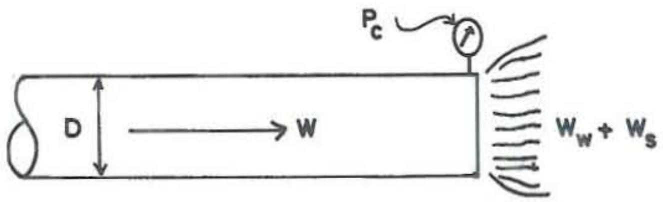

Fig. B.1 Fluid Discharge to the Atmosphere.

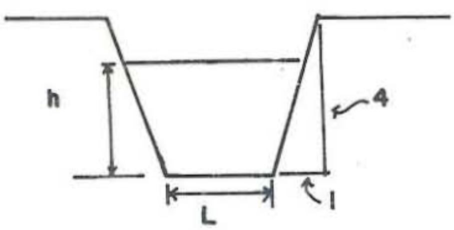

Fig. B.2 Water Flow Measurements Configuration.

B.2 Pressure drop due to turbulence

Refer to Figs. 10 and 11 in section 3.2.

For the laminar zone, considering a steady state case,

$$(B.10) \qquad P_e - P_s = \frac{W}{2\pi\rho T} \cdot \ln \frac{r_e}{r_s}$$

where T = kh/

For the turbulent zone,

$$(B.11) \qquad \frac{\partial P}{\partial r} = \mu a V + \mu b V2$$

Using the continuity equation,

$$(B.12) \qquad V = \frac{W}{2\pi\rho r h}$$

$$(B.13) \qquad V = \frac{W2}{4\pi 2\rho 2h2r2}$$

Defining a = 1/k, equation (B.11) will then become,

$$(B.14) \qquad \frac{\partial P}{\partial r} = \frac{W}{2\pi\rho T r} + \frac{\mu b W2}{4\pi 2\rho 2h2r2}$$

Integrating from Pwf to Ps, and r_w to r_s,

$$(B.15) \qquad Ps - Pwf = \frac{W}{2\pi\rho T} \cdot \ln\frac{r_s}{r_w} + \frac{\mu W^2 b}{4\pi^2\rho^2h^2}\left(\frac{1}{r_w} - \frac{1}{r_s}\right)$$

Adding equations (C.10) and (C.15), and if rs >> rw,

$$(B.16) \quad Pe - Pwf = \frac{W}{2\pi\rho T} \cdot \ln\frac{r_e}{r_w} + \frac{W^2\mu b}{4\pi^2\rho^2h^2rw}$$

Defining, $B = \dfrac{1}{2\pi\rho T} \cdot \ln \dfrac{r_e}{r_w}$, and $C = \mu b/(4\pi^2\rho^2h^2r_w)$

Equation (B.17) will reduce to,

$$(B.17) \quad Pe - Pwf = B\ W + C\ W^2$$

From which C can be determined from a linear plot of (Pe-Pwf)/W versus W for eq. (B.17), B is the intercept and C is the slope.

APPENDIX C: EFFECTS OF SALINITY and CO2 TO FLUID PROPERTIES

C.1 Salinity effects (NaCl)

A Geothermal fluid with a significant amount of salts boils at a higher temperature and lower pressure than pure water. The geothermal fluids are solutions of chloride, sulfate, and carbonate salts in water. Not all of these salts however, are present in every geothermal field. NaCl is the most abundant and is commonly present.

The equations presented here, unless specified, are those suggested by Michaelides (1981) which was based on " the equivalent NaCl content". The "equivalent NaCl content" is the content of NaCl in solution that will bring the same effect on the properties as the amount of all salts combined considering that the major constituent of the salts in the geothermal fluid is NaCl. The saturation temperature of a salt solution is higher than the saturation temperature of pure water by an amount, (Michaelides, 1981) of

$$(C.1) \quad dT = \frac{1.8\ R\ (T + 273)}{L} \quad \frac{m}{55.56}, \ ^{\circ}C$$

where R = universal gas constant, 0.461519 kJ/kg.°K; T = saturation temperature of pure water, °C; L = latent heat of the solution, kJ/kg; m = molality of the solution, moles of salt per kg of water.

The enthalpy of the solution is

$$(C.2) \quad H_n(T,m) = x_1 H_1 + x_2 H_2 + m.dH, \ kJ/kg$$

where x_1 = mass fraction of water, 1000/(1000 + 58.44 m)

x_2 = mass fraction of salt, 58.44/(1000 + 58.44 m)

H_1, H_2 = enthalpies of water and salt respectively at T

(C.3) $$dH = \frac{4.184}{(1000 + 58.44)} \sum_{i=0}^{3} \sum_{j=0}^{2} a_{ij} T^i m^j \text{ , kJ/kg}$$

where; $a_{00} = 9633.66$, $a_{01} = -4080.0$, $a_{02} = 286.49$

$a_{10} = 166.58$, $a_{11} = 68.577$, $a_{12} = -4.6856$

$a_{20} = -.90963$, $a_{21} = -.36524$, $a_{22} = 0.0249667$

$a_{31} = 1.7965E-3$, $a_{32} = 7.1924E-4$, $a_{33} = 4.9E-5$

(C.4) $$H_1(T) = 0.12453E{-4}\ T^3 - 0.4517E{-2}\ T^2 + 4.81155\ T - 29.578, \text{ kJ/kg}$$

(C.5) $$H_2(T) = (-0.83624E{-3}\ T^3 + 0.16792\ T^2 - 25.9293\ T)\cdot 0.0716 \text{ , kJ/kg } T \text{ in } {}^\circ C.$$

For correlations of viscosity, density, and entropy, the reader is referred to Michaelides (1981).

The vapor pressure at saturation temperature, T is lowered by an amount

(C.6) $$dP = \frac{1.8\ R\ (T+273)}{v_v - v_f} \cdot \frac{m}{55.56} \text{ , kPa}$$

The flashing pressure of a salt solution is;

$$P_s' = P_s(T) - dP$$

For numerical calculations, correlations are made from Keenan, et. al.(1978), to calculate for properties of pure water.

Equations (C.7) to (C.12) are from Catigtig(1982), unless specified.

(C.7) $P(T) = 10^{Y}$, MPa.

$$\text{where;} \quad Y = \frac{-4.8628E-4 + X}{2(9.9586E-6)}$$

$$X = \sqrt{4.8628E-4^{2} - 4(9.9586E-6)(t - 2.20781E-3)}$$

$$t = \frac{1.0}{(T + 273)} \qquad T \text{ in } {}^{\circ}C.$$

(C.8) $T(P) = [2.20781E-3 - 4.8628E-4 \log P - 9.9586E-6 (\log P)^{2}]^{-1}$, °K, P in MPa.

(C.9) $v_{v}(T) = (1.81E-8\ T^{3} - 4.06E-6\ T^{2} + 1.05E-3\ T + 0.96)E-3$, m^{3}/kg, T in C.

(C.10) $\mu_{f}(T) = 21.31E-6 \times 10^{b}$, kg/ms

where; $b = \left(274.13/(T+144.27)\right)$, T in °C, (Sigurdsson,1983).

(C.11) $\mu_{v}(T) = 495.8E-15\ T^{3} - 256.3E-12\ T^{2} + 76.42E-9\ T + 6.622E-6$, kg/ms

(C.12) $\sigma(T) = 4.33E-10\ T^{3} - 3.55E-7\ T^{2} - 13.57E-5\ T + 0.075565$, N/m, T in °C.

Equations (C.13) to (C.15) are from A.J. Brodie(1980).

(C.13) $v_{v}(T,P) = [54.94(P/T)^{2} + 2.212(P/T) - 8.93E-6]\ E-3$, m^{3}/kg
P in MPa, T in °K.

(C.14) $H_f(T) = 44.85E-9\ T^4 - 72.848E-6\ T3 + 45.601E-3\ T^2 - 8.726\ T + 241.75$, kJ/kg

(C.15) $H_v(T) = -5.96E-12\ T^6 + 16.969E-9\ T^5 - 20.11E-6\ T^4 + 12.6734E-3\ T3 - 4.4781\ T^2 + 842.947\ T - 63599.7$, kJ/kg. T in °K.

Results of these correlations are presented in Appendix E for 70 < T, °C < 330.0.

C.2 Effects of non-condensible gases (CO_2)

When the fluid starts to boil, vapour is produced. All the salts present in the geothermal fluids are non-volatile and hence the produced vapour is free of salts. The vapour phase though, contains non-condensible gases such as, CO_2, NH_3, H_2S ,and N_2.

In this discussion however, all non-condensible gases will be treated as CO_2 as this is the most abundant gas.

For the liquid phase, Sutton(1976) gives the formula

(C.16) $n_c = \alpha(T)\ Pc(0)$

where n_c = concentration of CO_2 in water

$Pc(0)$ = partial pressure of CO_2 at first boiling

(C.17) $(T) = [5.4 - 3.5(\frac{T}{100}) + 1.2(\frac{T}{100})2]\ E-9,\ Pa^{-1}$
T in C.

Michels (1981), gives the formula

(C.18) $$\frac{P_c}{Pc(0)} = 1 + [\frac{44 v_v x}{R(T+273)}]^{-1}$$

where x = mass fraction of steam; Pc = partial pressure of CO_2 at T; R = 8.314 kJ/kgmole K

The pressure at the two-phase region is

(C.19) Pwf = Ptp + Pc
Ptp = partial pressure of the steam-water mixture.

The pressure of the two-phase (steam-water) mixture only at any point in the well is

(C.20) Ptp = Pwf - Pc

APPENDIX D. PROGRAM LISTINGS AND OUTPUT PRINTOUTS

D.1 Program Listings

```
C       U07SN6
C       MAIN PROGRAM TO CALL U07SN5
        COMMON X,V,B,HSTAR,VS,VL,VG,HL,HG,G
        DIMENSION ZZ(10),DD(10),FLAM(10)
        REAL*8 FIELD,NAME,DATE
        G=980.67
        WRITE (6,4)
4       FORMAT(' ENTER NAME OF FIELD,WELL NAME,DATE')
        READ (5,5)FIELD
5       FORMAT(A8)
        READ (5,6)NAME
6       FORMAT(A8)
        READ (5,7)DATE
7       FORMAT(A8)
        TYPE 8, FIELD,NAME,DATE
8       FORMAT('1 NAME OF FIELD:',2x,A8/,'  WELL NAME:',2x,A8/,
     1  '  DATE CALC:' ,2x,A8//)
        call assign(1,'pipe.dat')
10      READ(1,701,END=20)ITYPE,DZ1,TYPEZ,ZA,ZT,ZA2
        READ(1,702) N,(ZZ(I),DD(I),FLAM(I),I=1,N)
        READ(1,703)TC1,TC2
        READ(1,704)PAA,FLOW1,FLOW2
        READ(1,705)DZ3,CCO2,CNACL
        READ(1,706)CTURB
15      CONTINUE
        TURBUL=CTURB*FLOW1**2
        PA=PAA-TURBUL
        TYPE 803,PAA,TURBUL,PA
803     FORMAT(' SINGLE-PHASE(WATER) SECTION:'/
     2  ' Pa =',-6PF8.3,'  bars'/,' (dP)turb =',-6PF8.3,'  bars'/,
     3  ' Pwf =',-6pf8.3,'  bars'/)
706     FORMAT(F8.3)
        CALL U07SN5(ZA,ZA2,ZT,N,ZZ,DD,FLAM,PA,FLOW1,FLOW2,
     4  PT,ITYPE,TYPEZ,DZ1,DZ3,CCO2,CNACL,TC1,TC2)
        TYPE 801,PT
        READ(1,910,END=20) J,FLAM(J),JI,FLAM(JI),FLOW
        GO TO 15
20      STOP
701     FORMAT(I2,-2P5F8.0)
702     FORMAT(I2,(-2PF8.0,0PF8.2,0PF9.7))
703     FORMAT(0P2F9.2,1PF8.3)
704     FORMAT(-6PF8.0,-3P2F10.2)
801     FORMAT(' ',-6PF10.2)
705     FORMAT(-2PF8.0,0P2F8.1)
910     FORMAT(I2,F8.0,I2,F8.0,-3PF8.0)
        END
```

```
      SUBROUTINE U07SN5(ZA,ZA2,ZT,IN,ZZ,DD,FLAM,PA,FLOW1,FLOW2,
     5 PT,ITYPE,TYPEZ,DZ2,DZ3,CCO2,CNACL,TC1,TC2)
      COMMON X,V,B,HSTAR,VS,VL,VG,HL,HG,G
      REAL*8 FLKIND,BUBB,SLUG,ANNU
      DATA IBLANK,ISTAR/' ','*'/
      DATA BUBB,SLUG,ANNU/' BUBBLY ','  SLUG  ',' ANNULAR'/
C     VSTAR,B AND G ARE OBTAINED FROM COMMON
C     VSTAR IS THE SPECIFIC VOLUME OF THE WATER AT THE FLASHING
C     POINT. IT MAY BE DIFFERENT FROM THE STEAM TABLE VALUE
C     ONLY THE HYDROSTATIC TERM IS INCLUDED BELOW THE
C     FLASHING POINT
      DIMENSION ZZ(1),DD(1),FLAM(1)
C     THESE ARRAYS GIVE THE PIPE CHARACTERISTICS AS A FUNCTION
C     OF DISTANCE ORDERED FROM THE WELL HEAD DOWN TO THE
C     WELL BOTTOM. DISTANCES DOWNWARDS ARE POSITIVE
      LOGICAL LTYPE
      LTYPE=(ITYPE.NE.0)
C     INITIALIZATION
      FRIC=0.
      POT=0.
      III=IBLANK
      DZ1=DZ2
      NINT=0
      N=IN
      PTC=SQRT(4.8628E-4**2-4*9.9586E-6*(1./(TC1+273.)
     6 -2.20781E-3))
      P=10**((PTC-4.8628E-4)/(2*9.9586E-6))
      IF (ZA2.EQ.0.0)TS=TC1
      TS=(FLOW1*TC1+FLOW2*TC2)/(FLOW1+FLOW2)
      ATS=(5.4-3.5*(TC1/100.)+1.2*(TC1/100.)**2)*1E-9
      PCO=CCO2*1E-5/ATS
      STP=SQRT(4.8628E-4**2-4*9.9586E-6*
     7 (1./(TS+273.)-2.20781E-3))
      PS=10**((-4.8628E-4+STP)/(2*9.9586E-6))*1E7
      VS=1.81E-8*(TS)**3-4.06E-6*(TS)**2
     8 +1.05E-3*(TS)+.96
      VGS=((PS*1E-7/TS)**2*54.94+(PS*1E-7/TS)*2.212-8.93E-6)
     9 **-1
      CN=CNACL/58500.
      HL=(44.85E-9*(TC1+273.)**4-72.848E-6*(TC1+273.)**3
     1 + 45.601E-3*(TC1+273.)**2-8.726*(TC1+273.)+241.75)*1E7
      HG=(-5.96E-12*(TC+273.)**6+16.969E-9*(TC1+273.)**5
     2 -20.109E-6*(TC1+273.)**4+12.6734E-3*(TC1+273.)**3
     3 -4.4781*(TC1+273.)**2+842.947*(TC1+273.)-63599.7)*1E7
      VL=1.81E-8*TC1**3-4.06E-6*TC1**2+1.05E-3*TC1+.96
      VG=((P/(TC1+273.))**2*54.94+(P/(TC1+273.))*2.212-8.93E-6)
     4 **-1
      DPS=(14.9652*(TC1+273.)/((VG-VL)*1E-3)*(CN/55.56))*1E4
      PSTAR=PS-DPS+PCO
      ZSTAR=U07VA1(ZA,ZA2,PA,ZZ,DD,FLAM,FLOW1,FLOW2,DZ3,CNACL,
     5 IN,TC1,TS,PSTAR,VS,VL,VGS,DPS)
      FLOW=FLOW1+FLOW2
      Z=ZSTAR
```

```
      P=PSTAR
      PP=PSTAR
      IF(PSTAR.GE.PS)P=PS
      P3=ALOG10(P*1E-7)
      T=(2.20781E-3-4.8628E-4*P3-9.9586E-6*P3**2)**-1-273.
      VSTAR=1.81E-8*T**3-4.06E-6*T**2+1.05E-3*T+0.96
      HSTAR=(44.85E-9*(T+273.)**4-72.848E-6*(T+273.)**3
     6 +45.601E-3*(T+273.)**2-8.726*(T+273.)+241.75)*1E7
      HL=HSTAR
      Q=HSTAR-ZSTAR*G
      VISF=(30.904+12538.2/T+1934503.1/T**2-6.694E7/T**3)*1E-5
      PACC=0.0025
      TEMPZ=AINT(Z/TYPEZ+1.)*TYPEZ
      DZ=-(Z-AINT((Z-1.)/DZ1)*DZ1)
      IF(Z.GT.ZZ(N)) TYPE 610,PA,DD(N)
   10 IF(N.LE.1) GO TO 20
      IF(Z.GT.ZZ (N-1)) GO TO 20
      N=N-1
      GO TO 10
   20 D=DD(N)
      FLAMDA=FLAM(N)
      FLOWA=FLOW/(D*D*0.78539816)
      FLOWA2=FLOWA*FLOWA
      Reyn=4*FLOW/(VISF*3.1416*D)
      Ffact=((-2*ALOG10(FLAMDA/(3.7*D*1E-2)+(7/Reyn)**.9))**2)**-1
      B=0.5*Ffact*FLOWA2/D
      U=Q+G*ZSTAR
      EKIN=0.5*FLOWA2*VL*VL
      PFLUX=FLOWA2*VSTAR
      VBAR1=VL
      VBAR2=VL
      VBAR3=VL
      VBAR4=VL
      VEFF=VL
      F=G/VS
      X=0
      ALPHA=0.
      IF(.NOT.LTYPE) GO TO 30
      TYPE 620,FLOW,PA,HSTAR,PSTAR
      TYPE 630
      TYPE 670
C     START THE INTEGRATION LOOP
C     MODIFY THE PIPE CHARACTERISTICS
   30 IF(N.LE.1) GO TO 40
      IF(Z.GT.ZZ(N-1)) GO TO 40
      N=N-1
      IGO=1
      GO TO 300
   35 FLOWAO=FLOWA
      FLAMDA=FLAM(N)
      D=DD(N)
      P8=ALOG10(P*1E-7)
```

```
      T=(2.20781E-3-4.8628E-4*P8-9.9586E-6*P2**2)**-1-273.
      VISF=(30.904+12538.2/T+1934503.1/T**2-6.694E7/T**3)*1E-5
      Reyn=4*FLOW/(VISF*3.1416*D)
      Ffact=((-2*ALOG10(FLAMDA/(3.7*D*1E-2)+(7/Reyn)**.9))**2)**-1

      FLOWA2=FLOWA*FLOWA
      B=0.5*Ffact*FLOWA2/D
      DZ=0.
      PFLUXO=PFLUX*FLOWA/FLOWAO
      GO TO 70
   40 FLOWAO=FLOWA
      IGO=2
      IF(-DZ.EQ.0.) GO TO 300
      IF(Z.GT.TEMPZ) GO TO 45
      GO TO 300
   45 PFLUXO=PFLUX
C     DETERMINE THE Z-INCREMENT DZ
   50 DZ=-(Z-AINT((Z-1.)/DZ1)*DZ1)
      IF(N.LE.1) GO TO 65
      IF(Z+DZ.GT.ZZ(N-1)) GO TO 70
      DZ=-(Z-ZZ(N-1))
   65 IF(Z+DZ.GT.ZT) GO TO 70
      DZ=-(Z-ZT)
C     CALCULATE ONE INTEGRATION STEP USING AN EXPLICIT
C     SOLUTION METHOD
   70 U=Q+(Z+DZ)*G
      DP=F*DZ+FMOM*DZ
      IF(DZ.EQ.0) DP=(X**2*VG/ALPHA+
     7(1-X)**2*VG/(1-ALPHA))*(FLOWAO**2-FLOWA**2)
      NINT=0
      DX=X
      XLAST=X
      DDP=DP
      ISTOP=0
      FOLD=F
  210 NINT=NINT+1
      PPDP=P+DP
      IF(PPDP.GE.0.3119E6) GO TO 211
      DZ1=DZ1/2.
      IF( DZ1.LT.10.) GO TO 90
      X=XLAST
      GO TO 50
  211 P4=ALOG10(PPDP*1E-7)
      TP=(2.20781E-3-4.8628E-4*P4-9.9586E-6*P4**2)**-1
      HL=(44.85E-9*TP**4-72.848E-6*TP**3+45.601E-3*TP**2
     8-8.726*TP+241.75)*1E7
      HG=(-5.96E-12*TP**6+16.969E-9*TP**5-20.109E-6*TP**4
     9+12.6734E-3*TP**3-4.4781*TP**2+842.947*TP-63599.7)*1E7
      VL=1.81E-8*(TP-273.)**3-4.06E-6*(TP-273.)**2+1.05E-3*(TP-273.)
     1+.96
      P5=PPDP*1E-7
      VG=((P5/TP)**2*54.94+(P5/TP)*2.212-8.93E-6)**-1
```

```
      IF(DP.EQ.0.0) GO TO 230
      IF(ISTOP.EQ.1.AND.ABS(DDP/DP).LE.PACC) GO TO 230
      EKIN=0.5*FLOWA2*VBAR4*VBAR4
      X=(U-EKIN-HL)/(HG-HL)
      IF(X.GT.0.) GO TO 214
      ALPHA=0.
      VBAR1=VL
      VBAR2=VL
      VBAR3=VL
      VBAR4=VL
      GO TO 216
214   AT=(5.4-3.5*(T/100.)+1.2*(T/100.)**2)*1E-9
      RATIO= (1+(44*VG*1E-3*X)/(AT*8.314E3*(T+273.)))**-1
      PC = PCO*RATIO
      PPDP=PPDP-PC
      ALPHA=U07TP5(PPDP,X,VL,VG,FLOWA,D,ALPHA)
      C1=ALPHA
      C2=1.-ALPHA
      B1=X/C1
      B2=(1.-X)/C2
      VBAR1=1./(C1/VG+C2/VL)
      C1=C1*B1
      C2=C2*B2
      VBAR2=C1*VG+C2*VL
      CC1=C1*B1
      CC2=C2*B2
      VBAR3=CC1*VG+CC2*VL
      CC1=CC1*B1
      CC2=CC2*B2
      VBAR4=SQRT(CC1*VG*VG+CC2*VL*VL)
      VEFF =U07TP4(X,ALPHA,PPDP,VL,VG,FLOWA,D)
      IF (PPDP.GT.PSTAR) POT=0.0
216   POT=C/VBAR1
      FRIC=B*VEFF
      F=POT+FRIC
      PFLUX=FLOWA2*VBAR3
      DPMOM=PFLUXO-PFLUX
      DPOLD=DP
      DP=(F+FOLD)*0.5*DZ+DPMOM
      DDPOLD=DDP
      DDP=DP-DPOLD
      IF(DDP.NE.0.0) GO TO 217
      ISTOP=1
      GO TO 220
217   IF(NINT/2*2.NE.NINT) GO TO 210
      IF(ABS((DDPOLD-DDP)/P).GT.1E-8) GO TO 218
      COR=3*DDP
      GO TO 219
218   COR=-DDP*DDP/(DDP-DDPOLD)
      DP=DP+COR
219   IF(ABS(COR/DDP).LT.1.) ISTOP=1
      DDPOLD=DDP
```

```
      DDP=COR
220   GO TO 210
230   P=P+DP
      PP=PP+DP
      IF(DZ.NE.0) FMOM=DPMOM/DZ
      IF(DZ.EQ.0) FMOM=FMOM*FLOWA/FLOWAO
      Z=Z+DZ
      X=(U-EKIN-HL)/(HG-HL)
      IF(Z.GT.ZT) GO TO 30
C     INTEGRATION COMPLETED
 90   IF(DZ1.GE..1) GO TO 100
      PCRIT=(HSTAR**1.102*FLOWA)**1.04167*3.029E-8
      TYPE 660,PCRIT
      GO TO 110
100   IGO=3
      GO TO 300
110   PT=P
      RETURN
300   IF(.NOT.LTYPE) GO TO 360
      VGOVL=VG/VL
      IF(X.GT.1.) GO TO 306
      XO1MX=X/(1.-X)
      AO1MA=ALPHA/(1.-ALPHA)
      IF(X.GT.0.) GO TO 302
      S=1.
      GO TO 304
302   S=XO1MX/AO1MA*VGOVL
304   QX=AO1MA/(AO1MA+VGOVL)
      BETA=XO1MX/(XO1MX+1./VGOVL)
      GO TO 308
306   S=VGOVL
      QX=1.
      BETA=1.
308   CONTINUE
      R1=VBAR1/VBAR2
      R3=VBAR3/VBAR2
      R4=VBAR4/VBAR2
      REFF=VEFF/VBAR2
      HBAR=X*HG+(1.-X)*HL
      FR=FLOWA2/G/D*VBAR2*VBAR2
      IF(BETA.LT.0.15) GO TO 320
      IF(BETA.LT.0.55) GO TO 310
      IF(BETA.LT.(-0.0085*FR+0.9962)) GO TO 330
      GO TO 340
310   IF(BETA.LT.(-FR*.02+1.85)) GO TO 330
      GO TO 340
320   FLKIND=BUBB
      GO TO 350
330   FLKIND=SLUG
      GO TO 350
340   FLKIND=ANNU
350   CONTINUE
```

```
      IF(Z.GT.ZA) III=ISTAR
      P6=ALOG10(P*1E-7)
      T=(2.20781E-3-4.8628E-4*P6-9.9586E-6*P6**2)**-1-273.
      DPPOT=POT*DZ
      DPFRIC=FRIC*DZ
      TYPE 650,Z,PP,T,D,X,
     2 DP,DPPOT,DPMOM,DPFRIC,
     3 HBAR,FLOW,Ffact,S,ALPHA,FLKIND
      IF(Z.LE.TEMPZ) TEMPZ=TEMPZ-TYPEZ
  360 GO TO (35,45,110                                   ),IGO
C     FORMAT STATEMENTS
  610 FORMAT(' WHEN THE AQUIFER PRESSURE IS ',-6PF6.3,
     4 '  BARS, FLASHING OCCURS OUTSIDE THE WELL '/
     5 ' THE PIPE IS EXTENDED WITH A DIAMETER OF',0PF6.3,'   cm.')
  620 FORMAT(//'  TWO-PHASE SECTION'/
     6 '       Wt =',-3PF10.2,' kg/s'/'    Pwf =',
     7 -6PF7.2,' bars'/
     8 '        H =',-7PF9.1, ' J/gm'/' PFLASH =',
     9 -6PF7.2,' bars')
  630 FORMAT(' ')
  650 FORMAT(' ',T5,-2PF8.3,-6PF8.3,0PF7.1,0P2F8.3,-6P4F9.4,
     1 -7PF8.1,-3PF6.1,0PF8.4,0P2F7.3,1X,A8)
  660 FORMAT(' JAMES'' CRITICAL PRESSURE=',-6PF7.2,' BARS')
  670 FORMAT(' ','  DEPTH(m)  P(bar) TEMP(C)
     2 D(cm)   DRNS     DPT     DPPOT    DPACC
     3   DPFRIC  H(J/g) W(kg/s)  Ff
     4  SLIP   VOID    TYPE'/)
      END

      FUNCTION U07VA1(ZA,ZA2,PA,ZZ,DD,FLAM,FLOW1,FLOW2,DZ3,
     5 CNACL,IN,TC1,TS,PSTAR,VS,VL,VGS,DPS)
      DIMENSION ZZ(1),DD(1),FLAM(1)
      HROL=1.0/VL
      TYPE 1005
 1005 FORMAT(T5,'DEPTH(m)',T19,'P(BAR)',T32,'Vel(f)',T43,'Ffactor
     6 ',T55,'D(cm)',T68,'DPWAT.',T80,'DPPOT',T91,'DPFRIC',T100,
     7 'FLOW(kg/s)',T111,'TEMP(C)',T122,'PFLASH'/)
      N=IN
      P=PA
      Z=ZA
      DZ=Z-AINT(Z/DZ3)*DZ3
      FLOW=FLOW1
 1010 IF(N.LE.1) GO TO 1020
      IF(Z.GT.ZZ(N-1)) GO TO 1020
      N=N-1
      GO TO 1010
 1020 D=DD(N)
      FLAMDA=FLAM(N)
      VISF=(30.904+12538.2/TC1+1934503.1/TC1**2-6.6941E7/TC1**3)
     8 *1E-5
      VVATN=FLOW1/HROL/(D*D*0.78539816)
      Retp=HROL*VVATN*D/VISF
```

```
      Ffact=((-2*alog10(FLAMDA/(3.7*D*1E-2)+(7/Retp)**.9))**2)**-1
      DPPOT=-(HROL*981*DZ)
      DPFRIC=-(Ffact*HROL*VVATN**2/2/D*DZ)
      DPVATN=DPPOT+DPFRIC
1030  P=P+DPVATN
      Z=Z-DZ
      IF (Z.GE.ZA2) GO TO 1035
      FLOW=FLOW1+FLOW2
      TC1=TS
      HROL=1./VS
1035  IF(P.LE.PSTAR) GO TO 1050
      TYPE 1040,Z,P,VVATN,Ffact,D,DPVATN,DPPOT,DPFRIC,FLOW,TC1,
     9 PSTAR
1040  FORMAT(-2PF12.3,-6PF12.3,-2PF12.3,0PF12.3,0PF12.3,-6P3F12.3,
     9 -3PF10.2,0PF9.1,-6PF12.3)
      DZ=DZ3
      GO TO 1010
1050  P=P-DPVATN
      Z=Z+DZ
      DPVATN=ABS(DPVATN)
      DZSTAR=(P-PSTAR)/DPVATN*DZ
      ZSTAR=Z-DZSTAR
      U07VA1=ZSTAR
      RETURN
      END

      FUNCTION U07TP4(X,ALPHA,P,VL,VG,FLOWA,D)
      X2=((1-X)/X)**2*VL/VG
      X1=SQRT(X2)
      C=1+X*VG/(X*VG+(1-X)*VL)-ALPHA
      F2=1+C/X1+1/X2
      U07TP4=F2*VL*(1-X)**2
      RETURN
      END

      FUNCTION U07TP5(P,X,VL,VG,FLOWA,D,ALPHA)
      FR=(FLOWA*VL)**2/D/981
      ALPHA1=(0.833+0.05*ALOG10(P*1.0E-6))/
     1 (1+(1-X)/X*VL/VG)
      BETA=X*VG/(X*VG+(1.-X)*VL)
      ALPHA2=BETA-0.71*BETA*SQRT(1.-BETA)*
     2 FR**(-0.045)*(1.-P/2.212E8)
      ALPHA=AMAX1(ALPHA1,ALPHA2)
      U07TP5=ALPHA
      RETURN
      END
```

D.2 Okoy 7 with CO_2 and NaCl = 0.0 ppm.

NAME OF FIELD: PUHAGAN, PALINPINON I
WELL NAME: OKOY 7
DATE CALC: AUG. 20, 1983
REF SURVEY: KP 14/KT 21, OCT. 13, 1981

SINGLE-PHASE(WATER) SECTION:

Pa = 163.900 bars
(dP)turb = 0.000 bars
Pwf = 163.900 bars

DEPTH(m)	P(BAR)	Vel(f)	Ffactor	D(cm)	DPWAT.	DPPOT	DPFRIC	FLOW(kg/s)	TEMP(C)	PFLASH
2600.000	163.900	0.884	0.019	15.940	0.000	0.000	0.000	12.00	319.0	103.205
2500.000	157.191	0.884	0.019	15.940	-6.709	-6.676	-0.032	12.00	319.0	103.205
2400.000	150.483	0.884	0.019	15.940	-6.709	-6.676	-0.032	12.00	319.0	103.205
2300.000	143.774	0.884	0.019	15.940	-6.709	-6.676	-0.032	12.00	319.0	103.205
2200.000	137.066	0.884	0.019	15.940	-6.709	-6.676	-0.032	12.00	319.0	103.205
2100.000	130.357	0.884	0.019	15.940	-6.709	-6.676	-0.032	12.00	319.0	103.205
2000.000	123.648	0.884	0.019	15.940	-6.709	-6.676	-0.032	12.00	319.0	103.205
1900.000	116.940	0.884	0.019	15.940	-6.709	-6.676	-0.032	12.00	319.0	103.205
1800.000	110.231	0.884	0.019	15.940	-6.709	-6.676	-0.032	12.00	319.0	103.205
1700.000	103.523	0.884	0.019	15.940	-6.709	-6.676	-0.032	12.00	319.0	103.205

TWO-PHASE SECTION

Wt = 13.20 kg/s
Pwf = 163.90 bars
H = 1420.7 J/gm
PFLASH = 103.21 bars

DEPTH(m)	P(bar)	TEMP(C)	D(cm)	DRNS	DPT	DPPOT	DPACC	DPFRIC	H(J/g)	W(kg/s)	Ff	SLIP	VOID	TYPE
1695.267	103.205	313.6	15.940	0.000	0.0000	0.0000	0.0000	0.0000	1420.7	13.2	0.0193	1.000	0.000	BUBBLY
1600.000	97.238	309.2	15.940	0.017	-0.5830	-0.5744	-0.0001	-0.0039	1419.8	13.2	0.0193	1.089	0.175	SLUG
1500.000	91.850	305.0	15.940	0.032	-0.5065	-0.4991	-0.0001	-0.0040	1418.8	13.2	0.0193	1.109	0.300	SLUG
1400.000	87.108	301.1	15.940	0.045	-0.4500	-0.4433	-0.0001	-0.0041	1417.8	13.2	0.0193	1.130	0.392	SLUG
1308.000	83.182	297.8	15.940	0.056	-0.0816	-0.0806	0.0000	-0.0009	1416.9	13.2	0.0193	1.150	0.456	SLUG
1308.000	83.185	297.8	22.100	0.056	0.0027	0.0000	0.0027	0.0000	1416.9	13.2	0.0150	1.150	0.456	SLUG
1300.000	82.863	297.5	22.100	0.057	-0.3217	-0.3200	0.0000	-0.0005	1416.9	13.2	0.0150	1.152	0.461	SLUG
1200.000	79.035	294.2	22.100	0.067	-0.3676	-0.3653	0.0000	-0.0007	1415.9	13.2	0.0150	1.175	0.516	SLUG
1100.000	75.522	291.0	22.100	0.076	-0.3388	-0.3368	0.0000	-0.0007	1414.9	13.2	0.0150	1.200	0.561	SLUG
1000.000	72.271	287.9	22.100	0.085	-0.3146	-0.3127	0.0000	-0.0007	1413.9	13.2	0.0150	1.225	0.598	SLUG
900.000	69.241	285.0	22.100	0.093	-0.2939	-0.2922	0.0000	-0.0008	1412.9	13.2	0.0150	1.253	0.629	SLUG
800.000	66.403	282.2	22.100	0.101	-0.2760	-0.2744	0.0000	-0.0008	1412.0	13.2	0.0150	1.282	0.655	SLUG
700.000	63.730	279.4	22.100	0.108	-0.2604	-0.2588	0.0000	-0.0008	1411.0	13.2	0.0150	1.313	0.678	SLUG
600.000	61.203	276.7	22.100	0.115	-0.2466	-0.2451	0.0000	-0.0009	1410.0	13.2	0.0150	1.347	0.698	SLUG
500.000	58.805	274.1	22.100	0.121	-0.2344	-0.2329	0.0000	-0.0009	1409.0	13.2	0.0150	1.382	0.716	SLUG
400.000	56.522	271.5	22.100	0.127	-0.2234	-0.2220	0.0000	-0.0009	1408.0	13.2	0.0150	1.420	0.732	SLUG
300.000	54.343	269.0	22.100	0.133	-0.2136	-0.2121	0.0000	-0.0010	1407.0	13.2	0.0150	1.460	0.745	SLUG
200.000	52.256	266.5	22.100	0.139	-0.2047	-0.2033	0.0000	-0.0010	1406.1	13.2	0.0150	1.503	0.758	SLUG
100.000	50.254	264.1	22.100	0.145	-0.1967	-0.1952	0.0000	-0.0011	1405.1	13.2	0.0150	1.550	0.769	SLUG
0.000	48.328	261.6	22.100	0.150	-0.1893	-0.1878	0.0000	-0.0011	1404.1	13.2	0.0150	1.599	0.779	SLUG

D.3 Okoy 7 considering the effects of CO_2 and NaCl.

CO_2 = 11879.0 ppm, NaCl = 3786.5 ppm.

NAME OF FIELD: PUHAGAN, PALINPINON II
WELL NAME: OKOY 7
DATE CALC: 9/17/83
REF SURVEY: KP 14/KT 21

SINGLE-PHASE(WATER) SECTION:

Pa = 163.900 bars
(dP)turb = 0.000 bars
Pwf = 163.900 bars

DEPTH(m)	P(BAR)	Vel(f)	Ffactor	D(cm)	DPWAT.	DPPOT	DPFRIC	FLOW(kg/s)	TEMP(C)	PFLASH
2600.000	163.900	0.884	0.019	15.940	0.000	0.000	0.000	12.00	319.0	114.770
2500.000	157.191	0.884	0.019	15.940	-6.709	-6.676	-0.032	12.00	319.0	114.770
2400.000	150.483	0.884	0.019	15.940	-6.709	-6.676	-0.032	12.00	319.0	114.770
2300.000	143.774	0.884	0.019	15.940	-6.709	-6.676	-0.032	12.00	319.0	114.770
2200.000	137.066	0.884	0.019	15.940	-6.709	-6.676	-0.032	12.00	319.0	114.770
2100.000	130.357	0.884	0.019	15.940	-6.709	-6.676	-0.032	12.00	319.0	114.770
2000.000	123.648	0.884	0.019	15.940	-6.709	-6.676	-0.032	12.00	319.0	114.770
1900.000	116.940	0.884	0.019	15.940	-6.709	-6.676	-0.032	12.00	319.0	114.770

TWO-PHASE SECTION

Wt = 13.20 kg/s
Pwf = 163.90 bars
H = 1420.7 J/gm
PFLASH = 114.77 bars

DEPTH(m)	P(bar)	TEMP(C)	D(cm)	DRNS	DPT	DPPOT	DPACC	DPFRIC	H(J/g)	W(kg/s)	Ff	SLIP	VOID	TYPE
1867.663	114.770	313.6	15.940	0.000	0.0000	0.0000	0.0000	0.0000	1420.7	13.2	0.0193	1.000	0.000	BUBBLY
1800.000	110.435	310.4	15.940	0.012	-0.6095	-0.6005	-0.0001	-0.0039	1420.1	13.2	0.0193	1.088	0.131	BUBBLY
1700.000	104.825	306.1	15.940	0.028	-0.5256	-0.5180	-0.0001	-0.0040	1419.1	13.2	0.0193	1.108	0.269	SLUG
1600.000	99.920	302.1	15.940	0.042	-0.4645	-0.4577	-0.0001	-0.0041	1418.1	13.2	0.0193	1.128	0.368	SLUG
1500.000	95.541	298.5	15.940	0.054	-0.4177	-0.4113	-0.0001	-0.0043	1417.1	13.2	0.0193	1.150	0.443	SLUG
1400.000	91.575	295.0	15.940	0.064	-0.3805	-0.3743	-0.0001	-0.0044	1416.1	13.2	0.0193	1.173	0.502	SLUG
1308.000	88.223	292.0	15.940	0.073	-0.0702	-0.0692	0.0000	-0.0009	1415.2	13.2	0.0193	1.195	0.546	SLUG
1308.000	88.226	292.0	22.100	0.073	0.0031	0.0000	0.0031	0.0000	1415.2	13.2	0.0150	1.195	0.546	SLUG
1300.000	87.949	291.8	22.100	0.074	-0.2766	-0.2752	0.0000	-0.0006	1415.2	13.2	0.0150	1.197	0.549	SLUG
1200.000	84.631	288.7	22.100	0.083	-0.3208	-0.3189	0.0000	-0.0007	1414.2	13.2	0.0150	1.223	0.588	SLUG
1100.000	81.545	285.7	22.100	0.091	-0.2993	-0.2975	0.0000	-0.0008	1413.2	13.2	0.0150	1.250	0.621	SLUG
1000.000	78.656	282.9	22.100	0.099	-0.2807	-0.2790	0.0000	-0.0008	1412.2	13.2	0.0150	1.279	0.648	SLUG
900.000	75.940	280.1	22.100	0.106	-0.2645	-0.2629	0.0000	-0.0008	1411.2	13.2	0.0150	1.310	0.672	SLUG
800.000	73.375	277.4	22.100	0.113	-0.2503	-0.2487	0.0000	-0.0009	1410.3	13.2	0.0150	1.342	0.693	SLUG
700.000	70.943	274.7	22.100	0.120	-0.2377	-0.2361	0.0000	-0.0009	1409.3	13.2	0.0150	1.377	0.711	SLUG
600.000	68.629	272.2	22.100	0.126	-0.2264	-0.2249	0.0000	-0.0009	1408.3	13.2	0.0150	1.415	0.727	SLUG
500.000	66.422	269.6	22.100	0.132	-0.2163	-0.2148	0.0000	-0.0010	1407.3	13.2	0.0150	1.455	0.742	SLUG
400.000	64.310	267.1	22.100	0.138	-0.2071	-0.2057	0.0000	-0.0010	1406.3	13.2	0.0150	1.497	0.755	SLUG
300.000	62.285	264.6	22.100	0.144	-0.1989	-0.1974	0.0000	-0.0011	1405.4	13.2	0.0150	1.543	0.766	SLUG
200.000	60.338	262.2	22.100	0.149	-0.1914	-0.1898	0.0000	-0.0011	1404.4	13.2	0.0150	1.592	0.776	SLUG
100.000	58.463	259.8	22.100	0.154	-0.1845	-0.1829	0.0000	-0.0012	1403.4	13.2	0.0150	1.645	0.786	SLUG
0.000	56.653	257.4	22.100	0.160	-0.1782	-0.1766	0.0000	-0.0012	1402.4	13.2	0.0150	1.702	0.794	SLUG

D.4 Okoy 7 with salinity (K,Na,Ca,Cl) = 6405.4 ppm, CO2 = 0.0 ppm.

NAME OF FIELD: PUHAGAN, PALINPINON II
WELL NAME: OKOY 7
DATE CALC: 9/17/83
REF SURVEY: KP 14/ KT 21

SINGLE-PHASE(WATER) SECTION:
Pa = 163.900 bars
(dP)turb = 0.000 bars
Pwf = 163.900 bars

DEPTH(m)	P(BAR)	Vel(f)	Ffactor	D(cm)	DPWAT.	DPPOT	DPFRIC	FLOW(kg/s)	TEMP(C)	PFLASH
2600.000	163.900	0.884	0.019	15.940	0.000	0.000	0.000	12.00	319.0	91.597
2500.000	157.191	0.884	0.019	15.940	-6.709	-6.676	-0.032	12.00	319.0	91.597
2400.000	150.483	0.884	0.019	15.940	-6.709	-6.676	-0.032	12.00	319.0	91.597
2300.000	143.774	0.884	0.019	15.940	-6.709	-6.676	-0.032	12.00	319.0	91.597
2200.000	137.066	0.884	0.019	15.940	-6.709	-6.676	-0.032	12.00	319.0	91.597
2100.000	130.357	0.884	0.019	15.940	-6.709	-6.676	-0.032	12.00	319.0	91.597
2000.000	123.648	0.884	0.019	15.940	-6.709	-6.676	-0.032	12.00	319.0	91.597
1900.000	116.940	0.884	0.019	15.940	-6.709	-6.676	-0.032	12.00	319.0	91.597
1800.000	110.231	0.884	0.019	15.940	-6.709	-6.676	-0.032	12.00	319.0	91.597
1700.000	103.523	0.884	0.019	15.940	-6.709	-6.676	-0.032	12.00	319.0	91.597
1600.000	96.814	0.884	0.019	15.940	-6.709	-6.676	-0.032	13.20	313.6	91.597

TWO-PHASE SECTION
Wt = 13.20 kg/s
Pwf = 163.90 bars
H = 1370.1 J/gm
PFLASH = 91.60 bars

DEPTH(m)	P(bar)	TEMP(C)	D(cm)	DRNS	DPT	DPPOT	DPACC	DPFRIC	H(J/g)	W(kg/s)	Ff	SLIP	VOID	TYPE
1523.331	91.597	304.7	15.940	0.000	0.0000	0.0000	0.0000	0.0000	1370.1	13.2	0.0193	1.000	0.000	BUBBLY
1500.000	90.017	303.5	15.940	0.005	-0.6680	-0.6566	-0.0001	-0.0038	1369.9	13.2	0.0193	1.080	0.060	BUBBLY
1400.000	84.034	298.5	15.940	0.022	-0.5498	-0.5411	-0.0001	-0.0039	1368.9	13.2	0.0193	1.104	0.247	SLUG
1308.000	79.365	294.4	15.940	0.035	-0.0949	-0.0939	0.0000	-0.0008	1368.0	13.2	0.0193	1.127	0.360	SLUG
1308.000	79.367	294.4	22.100	0.035	0.0023	0.0000	0.0023	0.0000	1368.0	13.2	0.0150	1.127	0.360	SLUG
1300.000	78.993	294.1	22.100	0.036	-0.3742	-0.3716	0.0000	-0.0005	1367.9	13.2	0.0150	1.129	0.368	SLUG
1200.000	74.628	290.1	22.100	0.049	-0.4127	-0.4096	0.0000	-0.0006	1366.9	13.2	0.0150	1.155	0.454	SLUG
1100.000	70.744	286.5	22.100	0.060	-0.3703	-0.3677	0.0000	-0.0007	1365.9	13.2	0.0150	1.183	0.518	SLUG
1000.000	67.231	283.0	22.100	0.069	-0.3367	-0.3345	0.0000	-0.0007	1365.0	13.2	0.0150	1.213	0.569	SLUG
900.000	64.019	279.7	22.100	0.079	-0.3094	-0.3074	0.0000	-0.0007	1364.0	13.2	0.0150	1.244	0.609	SLUG
800.000	61.054	276.6	22.100	0.087	-0.2866	-0.2848	0.0000	-0.0008	1363.0	13.2	0.0150	1.278	0.642	SLUG
700.000	58.296	273.6	22.100	0.095	-0.2674	-0.2657	0.0000	-0.0008	1362.0	13.2	0.0150	1.314	0.670	SLUG
600.000	55.715	270.6	22.100	0.102	-0.2509	-0.2492	0.0000	-0.0008	1361.0	13.2	0.0150	1.352	0.694	SLUG
500.000	53.286	267.8	22.100	0.109	-0.2365	-0.2350	0.0000	-0.0009	1360.1	13.2	0.0150	1.393	0.714	SLUG
400.000	50.991	265.0	22.100	0.116	-0.2240	-0.2224	0.0000	-0.0009	1359.1	13.2	0.0150	1.438	0.732	SLUG
300.000	48.813	262.3	22.100	0.122	-0.2129	-0.2114	0.0000	-0.0010	1358.1	13.2	0.0150	1.485	0.747	SLUG
200.000	46.739	259.6	22.100	0.128	-0.2031	-0.2015	0.0000	-0.0010	1357.1	13.2	0.0150	1.536	0.761	SLUG
100.000	44.758	256.9	22.100	0.134	-0.1942	-0.1927	0.0000	-0.0011	1356.1	13.2	0.0150	1.592	0.773	SLUG
0.000	42.860	254.3	22.100	0.140	-0.1863	-0.1848	0.0000	-0.0011	1355.2	13.2	0.0150	1.652	0.784	SLUG

D.5 Okoy 7 with CO2 = 11879.0 ppm, salinity (Na,Cl) = 8949.0 ppm.

NAME OF FIELD: PUHAGAN, PALINPINON II
WELL NAME: OKOY 7
DATE CALC: SEPT. 17, 1983
REF SURVEY: KP 14/KT 21

SINGLE-PHASE(WATER) SECTION:
Pa = 163.900 bars
(dP)turb = 0.000 bars
Pwf = 163.900 bars

DEPTH(m)	P(BAR)	Vel(f)	Ffactor	D(cm)	DPWAT.	DPPOT	DPFRIC	FLOW(kg/s)	TEMP(C)	PFLASH
2600.000	163.900	0.884	0.019	15.940	0.000	0.000	0.000	12.00	319.0	105.415
2500.000	157.191	0.884	0.019	15.940	-6.709	-6.676	-0.032	12.00	319.0	105.415
2400.000	150.483	0.884	0.019	15.940	-6.709	-6.676	-0.032	12.00	319.0	105.415
2300.000	143.774	0.884	0.019	15.940	-6.709	-6.676	-0.032	12.00	319.0	105.415
2200.000	137.066	0.884	0.019	15.940	-6.709	-6.676	-0.032	12.00	319.0	105.415
2100.000	130.357	0.884	0.019	15.940	-6.709	-6.676	-0.032	12.00	319.0	105.415
2000.000	123.648	0.884	0.019	15.940	-6.709	-6.676	-0.032	12.00	319.0	105.415
1900.000	116.940	0.884	0.019	15.940	-6.709	-6.676	-0.032	12.00	319.0	105.415
1800.000	110.231	0.884	0.019	15.940	-6.709	-6.676	-0.032	12.00	319.0	105.415

TWO-PHASE SECTION
Wt = 13.20 kg/s
Pwf = 163.90 bars
H = 1420.7 J/gm
PFLASH = 105.41 bars

DEPTH(m)	P(bar)	TEMP(C)	D(cm)	DRNS	DPT	DPPOT	DPACC	DPFRIC	H(J/g)	W(kg/s)	Ff	SLIP	VOID	TYPE
1728.203	105.415	313.6	15.940	0.000	0.0000	0.0000	0.0000	0.0000	1420.7	13.2	0.0193	1.000	0.000	BUBBLY
1700.000	103.545	312.3	15.940	0.005	-0.6524	-0.6425	-0.0001	-0.0039	1420.5	13.2	0.0193	1.081	0.059	BUBBLY
1600.000	97.586	307.7	15.940	0.022	-0.5553	-0.5472	-0.0001	-0.0039	1419.5	13.2	0.0193	1.100	0.220	SLUG
1500.000	92.429	303.6	15.940	0.036	-0.4866	-0.4794	-0.0001	-0.0041	1418.5	13.2	0.0193	1.120	0.333	SLUG
1400.000	87.859	299.9	15.940	0.049	-0.4349	-0.4283	-0.0001	-0.0042	1417.5	13.2	0.0193	1.141	0.416	SLUG
1308.000	84.056	296.6	15.940	0.059	-0.0791	-0.0782	0.0000	-0.0009	1416.6	13.2	0.0193	1.162	0.476	SLUG
1308.000	84.059	296.6	22.100	0.059	0.0027	0.0000	0.0027	0.0000	1416.6	13.2	0.0150	1.161	0.476	SLUG
1300.000	83.747	296.4	22.100	0.060	-0.3121	-0.3104	0.0000	-0.0005	1416.5	13.2	0.0150	1.163	0.480	SLUG
1200.000	80.027	293.1	22.100	0.070	-0.3578	-0.3556	0.0000	-0.0007	1415.6	13.2	0.0150	1.187	0.531	SLUG
1100.000	76.602	289.9	22.100	0.079	-0.3306	-0.3287	0.0000	-0.0007	1414.6	13.2	0.0150	1.212	0.573	SLUG
1000.000	73.425	286.9	22.100	0.088	-0.3077	-0.3058	0.0000	-0.0007	1413.6	13.2	0.0150	1.239	0.608	SLUG
900.000	70.459	284.0	22.100	0.096	-0.2880	-0.2863	0.0000	-0.0008	1412.6	13.2	0.0150	1.267	0.638	SLUG
800.000	67.675	281.2	22.100	0.103	-0.2709	-0.2693	0.0000	-0.0008	1411.6	13.2	0.0150	1.297	0.663	SLUG
700.000	65.050	278.5	22.100	0.110	-0.2559	-0.2543	0.0000	-0.0008	1410.6	13.2	0.0150	1.329	0.685	SLUG
600.000	62.566	275.8	22.100	0.117	-0.2426	-0.2411	0.0000	-0.0009	1409.7	13.2	0.0150	1.363	0.704	SLUG
500.000	60.205	273.2	22.100	0.123	-0.2309	-0.2294	0.0000	-0.0009	1408.7	13.2	0.0150	1.399	0.721	SLUG
400.000	57.956	270.7	22.100	0.130	-0.2203	-0.2188	0.0000	-0.0010	1407.7	13.2	0.0150	1.438	0.736	SLUG
300.000	55.806	268.1	22.100	0.136	-0.2108	-0.2093	0.0000	-0.0010	1406.7	13.2	0.0150	1.480	0.749	SLUG
200.000	53.746	265.7	22.100	0.141	-0.2022	-0.2007	0.0000	-0.0011	1405.7	13.2	0.0150	1.524	0.761	SLUG
100.000	51.768	263.2	22.100	0.147	-0.1943	-0.1928	0.0000	-0.0011	1404.8	13.2	0.0150	1.572	0.772	SLUG
0.000	49.865	260.8	22.100	0.152	-0.1872	-0.1857	0.0000	-0.0012	1403.8	13.2	0.0150	1.623	0.782	SLUG

D.6 Nasuji-Sogongon area as a single well with rw = 1100 m.

$S = 1.483E\text{-}6$ m/Pa., $T = 1.483E\text{-}6$ m ^{3}/Pa.s

NAME OF FIELD: Nasuji-Sogongon, Palinpinon II
WELL NAME: Nasuji-Sogongon
DATE CALC: Sept 17, 1983

SINGLE-PHASE(WATER) SECTION:

Pa = 120.700 bars
(dP)turb = 0.000 bars
Pwf = 120.700 bars

DEPTH(m)	P(BAR)	Vel(f)	Ffactor	D(cm)	DPWAT.	DPPOT	DPFRIC	FLOW(kg/s)	TEMP(C)	PFLASH
2600.000	120.700	0.000	0.017	11000.000	0.000	0.000	0.000	1100.00	296.0	76.450
2500.000	113.614	0.000	0.017	11000.000	-7.086	-7.086	0.000	1100.00	296.0	76.450
2400.000	106.529	0.000	0.017	11000.000	-7.086	-7.086	0.000	1100.00	296.0	76.450
2300.000	99.443	0.000	0.017	11000.000	-7.086	-7.086	0.000	1100.00	296.0	76.450
2200.000	92.357	0.000	0.017	11000.000	-7.086	-7.086	0.000	1100.00	296.0	76.450
2100.000	85.272	0.000	0.017	11000.000	-7.086	-7.086	0.000	1100.00	296.0	76.450
2000.000	78.186	0.000	0.017	11000.000	-7.086	-7.086	0.000	1100.00	296.0	76.450

TWO-PHASE SECTION

Wt = 1164.00 kg/s
Pwf = 120.70 bars
H = 1299.0 J/gm
PFLASH = 76.45 bars

DEPTH(m)	P(bar)	TEMP(C)	D(cm)	DRNS	DPT	DPPOT	DPACC	DPFRIC	H(J/g)	W(kg/s)	Ff	SLIP	VOID	TYPE
1975.493	76.450	291.8	11000.0	0.000	0.0000	0.0000	0.0000	0.0000	1299.0	1164.0	0.0166	1.000	0.000	BUBBLY
1900.000	71.610	287.8	11000.0	0.015	-0.5857	-0.5785	0.0000	0.0000	1298.2	1164.0	0.0166	1.104	0.211	SLUG
1800.000	66.411	282.2	11000.0	0.030	-0.4746	-0.4703	0.0000	0.0000	1297.3	1164.0	0.0166	1.138	0.375	SLUG
1700.000	62.077	277.7	11000.0	0.044	-0.4038	-0.4009	0.0000	0.0000	1296.3	1164.0	0.0166	1.174	0.478	SLUG
1600.000	58.326	273.6	11000.0	0.055	-0.3540	-0.3519	0.0000	0.0000	1295.3	1164.0	0.0166	1.212	0.550	SLUG
1500.000	54.999	269.8	11000.0	0.065	-0.3167	-0.3151	0.0000	0.0000	1294.3	1164.0	0.0166	1.253	0.603	SLUG
1400.000	51.997	266.2	11000.0	0.074	-0.2875	-0.2862	0.0000	0.0000	1293.3	1164.0	0.0166	1.296	0.645	SLUG
1300.000	49.255	262.8	11000.0	0.083	-0.2640	-0.2630	0.0000	0.0000	1292.4	1164.0	0.0166	1.343	0.677	SLUG
1265.000	48.348	261.7	11000.0	0.086	-0.1282	-0.1279	0.0000	0.0000	1292.0	1164.0	0.0166	1.360	0.687	SLUG
1265.000	48.348	261.7	11000.0	0.086	0.0000	0.0000	0.0000	0.0000	1292.0	1164.0	0.0169	1.360	0.687	SLUG
1200.000	46.725	259.5	11000.0	0.091	-0.2446	-0.2438	0.0000	0.0000	1291.4	1164.0	0.0169	1.393	0.704	SLUG
1100.000	44.370	256.4	11000.0	0.098	-0.2284	-0.2276	0.0000	0.0000	1290.4	1164.0	0.0169	1.448	0.726	SLUG
1000.000	42.165	253.3	11000.0	0.106	-0.2145	-0.2138	0.0000	0.0000	1289.4	1164.0	0.0169	1.508	0.745	SLUG
900.000	40.087	250.3	11000.0	0.112	-0.2025	-0.2020	0.0000	0.0000	1288.4	1164.0	0.0169	1.572	0.761	SLUG
800.000	38.121	247.3	11000.0	0.119	-0.1921	-0.1916	0.0000	0.0000	1287.4	1164.0	0.0169	1.643	0.775	SLUG
700.000	36.251	244.4	11000.0	0.125	-0.1830	-0.1825	0.0000	0.0000	1286.5	1164.0	0.0169	1.720	0.787	SLUG
600.000	34.466	241.5	11000.0	0.132	-0.1749	-0.1745	0.0000	0.0000	1285.5	1164.0	0.0169	1.804	0.798	SLUG
500.000	32.757	238.6	11000.0	0.138	-0.1677	-0.1674	0.0000	0.0000	1284.5	1164.0	0.0169	1.897	0.807	SLUG
400.000	31.116	235.7	11000.0	0.144	-0.1614	-0.1611	0.0000	0.0000	1283.5	1164.0	0.0169	2.000	0.815	SLUG
300.000	29.534	232.8	11000.0	0.149	-0.1557	-0.1554	0.0000	0.0000	1282.5	1164.0	0.0169	2.113	0.823	SLUG
200.000	28.006	229.9	11000.0	0.155	-0.1506	-0.1503	0.0000	0.0000	1281.6	1164.0	0.0169	2.240	0.829	SLUG
100.000	26.526	227.0	11000.0	0.161	-0.1460	-0.1458	0.0000	0.0000	1280.6	1164.0	0.0169	2.382	0.835	SLUG
0.000	25.089	224.0	11000.0	0.167	-0.1419	-0.1417	0.0000	0.0000	1279.6	1164.0	0.0169	2.540	0.840	SLUG

THE PRINTED PRESSURE DROPS (DPT,DPPOT,DPACC,DPFRIC) ARE FOR A SECTION OF 10 m
NEAREST TO THE PRINTED DEPTH.

APPENDIX E. STEAM TABLE CORRELATIONS PROGRAM AND RESULTS

E.1 Program Listings

```
OPEN(UNIT=1,FILE='RUG.DAT',STATUS='NEW',CARRIAGECONTROL='LIST')
        WRITE (6,10)
10      FORMAT (' ENTER T(deg. C) or P(MPaa)')
11      READ(5,19) X
19      FORMAT(F11.7)
        IF(X.GT.1.0)GO TO 20
        WRITE(1,'(A,/)')'      P(MPaa) TEMP(C)  Hf      Hv      ρf
     -      ρv     μf       μv      τ'
        P=X
        GO TO 22
20      WRITE(1,'(A,/)')'      T,C    P(MPaa)   Hf      Hv      ρf
     -      ρv     μf       μv      τ'
        TC=X
21      TC=TC+273.
        PC=SQRT(4.8628E-4**2-4*9.9586E-6*(1./TC-2.20781E-3))
        P=10**((PC-4.8628E-4)/(2*9.9586E-6))
        GO TO 30
22      T=(2.20781E-3-4.8628E-4*ALOG10(P)-9.9586E-6*(ALOG10(P))**2)**-1
        TC=T
30      HG=(-5.96035E-12)*TC**6 + (16.9688E-9)*TC**5
     -     -(20.1099E-6)*TC**4 + (12.67339E-3)*TC**3
     -     -(4.47807*TC**2) + (842.947*TC) - 63599.7
        HF=(44.85E-9*TC**4 - 72.848E-6*TC**3 + 45.601E-3*TC**2
     -     -8.726*TC + 241.75)
        DG=((P/TC)**2*54.94 + (P/TC)*2.212 - 8.93E-6)*1E3
        TC=TC-273.
        VF=(1.81E-8*TC**3-4.06E-6*TC**2+1.05E-3*TC+0.96)*1E-3
        DF=1./VF
        VG=1.0/DG
        VISF=(30.904+12538.2/TC+1934503.1/TC**2-6.6941E7/TC**3)
        VISG=(495.8E-15*TC**3-256.3E-12*TC**2+76.42E-9*TC+6.622E-6)*1E6
        SURFT=(4.33E-10*TC**3-3.55E-7*TC**2-13.57E-5*TC+.075565)*1E3
        IF(X.LT.1.0)GO TO 41
40      WRITE (1,'(T5,F5.1,1X,F8.5,3(1X,F6.1),4(1X,F8.4))')
     -  TC,P,HF,HG,DF,DG,
     -  VISF,VISG,SURFT
        TC=TC+1.0
        IF (TC.LE.330.)GO TO 21
        GO TO 42
41      WRITE(1,'(T5,F8.5,4(1X,F6.1),4(1X,F8.4))')P,TC,HF,HG,DF,DG,
     -  VISF,VISG,SURFT
        P=P+0.05
        IF(P.LT.12.78)GO TO 22
42      WRITE(1,'(A,/)')'------------------------------------------ '
45      WRITE(1,'(A,/)')' Hf,Hv in kJ/kg;   ρf,ρv in kg/m3 ;
     -  μf,μv in kg/ms;      τ in N/m '
        CLOSE (1)
50      STOP
        END
```

E.2 PRESSURE AS A FUNCTION OF TEMPERATURE, P(T)

TEMP(C)	P(MPaa)	Hf	Hv	ρf	ρv	μf(E-6)	μv(E-6)	τ(E-3)
70.0	0.03152	294.7	2615.4	980.6	0.1948	409.6545	10.8856	64.4750
71.0	0.03290	298.8	2617.9	979.9	0.2031	404.2197	10.9333	64.2957
72.0	0.03433	302.9	2620.3	979.1	0.2117	398.8665	10.9806	64.1159
73.0	0.03581	307.0	2622.8	978.4	0.2206	393.5971	11.0277	63.9356
74.0	0.03734	311.1	2625.3	977.7	0.2297	388.4135	11.0745	63.7547
75.0	0.03892	315.2	2627.6	977.0	0.2392	383.3167	11.1210	63.5733
76.0	0.04057	319.3	2630.0	976.3	0.2489	378.3077	11.1672	63.3914
77.0	0.04227	323.4	2632.3	975.6	0.2590	373.3869	11.2131	63.2090
78.0	0.04403	327.6	2634.5	974.9	0.2694	368.5544	11.2587	63.0261
79.0	0.04585	331.7	2636.7	974.2	0.2802	363.8101	11.3041	62.8426
80.0	0.04774	335.8	2639.0	973.4	0.2912	359.1535	11.3491	62.6587
81.0	0.04969	339.9	2641.1	972.7	0.3026	354.5841	11.3939	62.4743
82.0	0.05171	344.1	2643.3	972.0	0.3144	350.1012	11.4384	62.2893
83.0	0.05379	348.2	2645.3	971.3	0.3266	345.7038	11.4827	62.1039
84.0	0.05595	352.3	2647.4	970.6	0.3391	341.3909	11.5267	61.9180
85.0	0.05818	356.5	2649.5	969.9	0.3520	337.1613	11.5704	61.7315
86.0	0.06048	360.6	2651.4	969.2	0.3653	333.0139	11.6139	61.5446
87.0	0.06285	364.8	2653.4	968.5	0.3789	328.9473	11.6571	61.3572
88.0	0.06531	368.9	2655.4	967.8	0.3930	324.9603	11.7000	61.1694
89.0	0.06784	373.1	2657.3	967.1	0.4075	321.0513	11.7428	60.9810
90.0	0.07046	377.3	2659.4	966.4	0.4225	317.2191	11.7852	60.7922
91.0	0.07316	381.4	2661.2	965.7	0.4379	313.4622	11.8274	60.6028
92.0	0.07594	385.6	2663.0	964.9	0.4537	309.7790	11.8694	60.4131
93.0	0.07882	389.8	2664.8	964.2	0.4700	306.1682	11.9111	60.2228
94.0	0.08178	394.0	2666.7	963.5	0.4867	302.6283	11.9526	60.0321
95.0	0.08483	398.1	2668.5	962.8	0.5039	299.1577	11.9939	59.8409
96.0	0.08798	402.3	2670.3	962.1	0.5216	295.7552	12.0349	59.6492
97.0	0.09123	406.5	2672.1	961.4	0.5398	292.4191	12.0757	59.4571
98.0	0.09458	410.7	2673.8	960.7	0.5585	289.1480	12.1163	59.2645
99.0	0.09802	414.9	2675.5	960.0	0.5778	285.9406	12.1567	59.0715
100.0	0.10158	419.1	2677.2	959.2	0.5975	282.7953	12.1968	58.8780
101.0	0.10523	423.3	2678.9	958.5	0.6178	279.7109	12.2367	58.6841
102.0	0.10900	427.5	2680.6	957.8	0.6387	276.6859	12.2764	58.4897
103.0	0.11287	431.7	2682.3	957.1	0.6601	273.7191	12.3159	58.2949
104.0	0.11687	435.9	2683.9	956.3	0.6820	270.8090	12.3552	58.0996
105.0	0.12097	440.1	2685.6	955.6	0.7046	267.9544	12.3943	57.9039
106.0	0.12520	444.3	2687.1	954.9	0.7278	265.1541	12.4332	57.7077
107.0	0.12954	448.5	2688.7	954.2	0.7515	262.4066	12.4719	57.5112
108.0	0.13401	452.7	2690.3	953.4	0.7759	259.7110	12.5104	57.3141
109.0	0.13861	457.0	2691.9	952.7	0.8009	257.0659	12.5488	57.1167
110.0	0.14334	461.2	2693.5	952.0	0.8266	254.4702	12.5869	56.9188
111.0	0.14820	465.4	2695.1	951.2	0.8529	251.9227	12.6248	56.7205
112.0	0.15319	469.6	2696.5	950.5	0.8799	249.4224	12.6626	56.5218
113.0	0.15832	473.9	2698.1	949.7	0.9076	246.9680	12.7002	56.3227

TEMP(C)	P(MPaa)	Hf	Hv	ρf	ρv	μf(E-6)	μv(E-6)	τ(E-3)
114.0	0.16360	478.1	2699.6	949.0	0.9360	244.5587	12.7376	56.1231
115.0	0.16901	482.3	2701.1	948.2	0.9650	242.1933	12.7748	55.9232
116.0	0.17458	486.6	2702.6	947.5	0.9948	239.8708	12.8118	55.7228
117.0	0.18029	490.8	2704.1	946.7	1.0254	237.5902	12.8487	55.5220
118.0	0.18616	495.1	2705.6	946.0	1.0567	235.3506	12.8855	55.3208
119.0	0.19218	499.3	2707.1	945.2	1.0887	233.1510	12.9220	55.1192
120.0	0.19836	503.6	2708.5	944.5	1.1215	230.9905	12.9584	54.9172
121.0	0.20470	507.8	2710.0	943.7	1.1551	228.8682	12.9947	54.7148
122.0	0.21121	512.1	2711.4	942.9	1.1896	226.7833	13.0308	54.5120
123.0	0.21789	516.3	2712.8	942.1	1.2248	224.7348	13.0667	54.3089
124.0	0.22474	520.6	2714.2	941.4	1.2609	222.7220	13.1025	54.1053
125.0	0.23176	524.9	2715.6	940.6	1.2978	220.7440	13.1382	53.9013
126.0	0.23896	529.1	2717.0	939.8	1.3356	218.8001	13.1737	53.6970
127.0	0.24635	533.4	2718.4	939.0	1.3742	216.8895	13.2091	53.4923
128.0	0.25392	537.7	2719.7	938.2	1.4138	215.0114	13.2443	53.2872
129.0	0.26168	541.9	2721.1	937.4	1.4542	213.1652	13.2794	53.0817
130.0	0.26963	546.2	2722.6	936.6	1.4956	211.3501	13.3144	52.8758
131.0	0.27778	550.5	2723.9	935.8	1.5379	209.5653	13.3493	52.6696
132.0	0.28612	554.8	2725.2	935.0	1.5812	207.8104	13.3840	52.4630
133.0	0.29467	559.1	2726.6	934.2	1.6255	206.0845	13.4186	52.2560
134.0	0.30343	563.3	2727.9	933.4	1.6707	204.3871	13.4531	52.0487
135.0	0.31240	567.6	2729.1	932.6	1.7170	202.7175	13.4875	51.8410
136.0	0.32158	571.9	2730.5	931.8	1.7642	201.0751	13.5218	51.6329
137.0	0.33098	576.2	2731.9	930.9	1.8126	199.4594	13.5559	51.4245
138.0	0.34060	580.5	2733.1	930.1	1.8619	197.8697	13.5900	51.2157
139.0	0.35045	584.8	2734.4	929.3	1.9124	196.3055	13.6239	51.0066
140.0	0.36053	589.1	2735.8	928.4	1.9639	194.7663	13.6578	50.7972
141.0	0.37084	593.4	2737.0	927.6	2.0165	193.2515	13.6916	50.5873
142.0	0.38139	597.7	2738.3	926.7	2.0703	191.7606	13.7252	50.3772
143.0	0.39218	602.0	2739.5	925.9	2.1252	190.2931	13.7588	50.1667
144.0	0.40321	606.3	2740.8	925.0	2.1813	188.8484	13.7923	49.9559
145.0	0.41450	610.6	2742.0	924.2	2.2386	187.4262	13.8257	49.7447
146.0	0.42604	615.0	2743.3	923.3	2.2970	186.0260	13.8590	49.5332
147.0	0.43784	619.3	2744.5	922.4	2.3567	184.6472	13.8923	49.3213
148.0	0.44990	623.6	2745.7	921.5	2.4176	183.2895	13.9254	49.1092
149.0	0.46222	627.9	2747.0	920.7	2.4798	181.9525	13.9585	48.8967
150.0	0.47482	632.2	2748.2	919.8	2.5433	180.6356	13.9916	48.6839
151.0	0.48769	636.6	2749.3	918.9	2.6080	179.3384	14.0245	48.4707
152.0	0.50084	640.9	2750.5	918.0	2.6741	178.0607	14.0574	48.2573
153.0	0.51428	645.2	2751.7	917.1	2.7415	176.8019	14.0903	48.0435
154.0	0.52800	649.6	2752.8	916.2	2.8103	175.5618	14.1231	47.8295
155.0	0.54202	653.9	2754.1	915.2	2.8805	174.3399	14.1558	47.6151
156.0	0.55633	658.3	2755.3	914.3	2.9520	173.1358	14.1885	47.4004
157.0	0.57095	662.6	2756.3	913.4	3.0250	171.9493	14.2211	47.1854
158.0	0.58587	666.9	2757.5	912.5	3.0994	170.7799	14.2537	46.9701
159.0	0.60111	671.3	2758.6	911.5	3.1753	169.6273	14.2862	46.7545
160.0	0.61666	675.7	2759.7	910.6	3.2527	168.4913	14.3187	46.5386
161.0	0.63253	680.0	2760.8	909.6	3.3316	167.3714	14.3512	46.3224
162.0	0.64872	684.4	2762.0	908.7	3.4120	166.2673	14.3836	46.1059
163.0	0.66525	688.7	2763.1	907.7	3.4940	165.1789	14.4160	45.8891
164.0	0.68211	693.1	2764.3	906.7	3.5776	164.1056	14.4484	45.6721
165.0	0.69931	697.5	2765.3	905.8	3.6628	163.0474	14.4807	45.4547

TEMP(C)	P(MPaa)	Hf	Hv	ρf	ρv	μf(E-6)	μv(E-6)	τ(E-3)
166.0	0.71685	701.8	2766.3	904.8	3.7496	162.0038	14.5131	45.2371
167.0	0.73474	706.2	2767.2	903.8	3.8380	160.9746	14.5454	45.0192
168.0	0.75299	710.6	2768.2	902.8	3.9281	159.9595	14.5776	44.8010
169.0	0.77160	715.0	2769.4	901.8	4.0200	158.9583	14.6099	44.5826
170.0	0.79057	719.3	2770.3	900.8	4.1135	157.9707	14.6422	44.3638
171.0	0.80991	723.7	2771.4	899.8	4.2088	156.9964	14.6745	44.1448
172.0	0.82962	728.1	2772.4	898.8	4.3059	156.0352	14.7067	43.9256
173.0	0.84972	732.5	2773.3	897.8	4.4048	155.0869	14.7390	43.7061
174.0	0.87020	736.9	2774.4	896.8	4.5055	154.1512	14.7712	43.4863
175.0	0.89107	741.3	2775.3	895.7	4.6081	153.2279	14.8035	43.2662
176.0	0.91233	745.7	2776.1	894.7	4.7125	152.3167	14.8358	43.0459
177.0	0.93399	750.1	2777.1	893.6	4.8188	151.4175	14.8680	42.8254
178.0	0.95607	754.5	2778.0	892.6	4.9271	150.5300	14.9003	42.6046
179.0	0.97855	758.9	2779.1	891.5	5.0374	149.6540	14.9327	42.3835
180.0	1.00144	763.3	2779.9	890.5	5.1496	148.7893	14.9650	42.1623
181.0	1.02476	767.8	2780.9	889.4	5.2639	147.9358	14.9973	41.9407
182.0	1.04851	772.2	2781.6	888.3	5.3802	147.0931	15.0297	41.7190
183.0	1.07269	776.6	2782.5	887.2	5.4986	146.2612	15.0621	41.4969
184.0	1.09730	781.1	2783.5	886.1	5.6191	145.4397	15.0946	41.2747
185.0	1.12236	785.5	2784.4	885.0	5.7417	144.6287	15.1271	41.0522
186.0	1.14788	789.9	2785.0	883.9	5.8665	143.8278	15.1596	40.8295
187.0	1.17384	794.4	2785.9	882.8	5.9935	143.0368	15.1921	40.6066
188.0	1.20026	798.8	2786.7	881.7	6.1227	142.2557	15.2247	40.3834
189.0	1.22715	803.3	2787.4	880.6	6.2541	141.4843	15.2574	40.1600
190.0	1.25451	807.7	2788.2	879.4	6.3879	140.7223	15.2901	39.9365
191.0	1.28235	812.2	2789.0	878.3	6.5240	139.9696	15.3228	39.7126
192.0	1.31067	816.6	2789.7	877.2	6.6624	139.2261	15.3556	39.4886
193.0	1.33949	821.1	2790.5	876.0	6.8032	138.4916	15.3885	39.2644
194.0	1.36879	825.6	2791.2	874.9	6.9465	137.7660	15.4214	39.0399
195.0	1.39859	830.1	2792.0	873.7	7.0922	137.0490	15.4544	38.8153
196.0	1.42890	834.5	2792.6	872.5	7.2403	136.3407	15.4874	38.5904
197.0	1.45973	839.0	2793.2	871.3	7.3911	135.6407	15.5206	38.3654
198.0	1.49106	843.5	2793.9	870.1	7.5443	134.9490	15.5538	38.1401
199.0	1.52293	848.0	2794.6	869.0	7.7001	134.2655	15.5870	37.9146
200.0	1.55532	852.5	2795.2	867.8	7.8586	133.5900	15.6204	37.6890
201.0	1.58826	857.0	2795.8	866.5	8.0198	132.9223	15.6538	37.4632
202.0	1.62173	861.5	2796.4	865.3	8.1836	132.2624	15.6874	37.2371
203.0	1.65574	866.0	2797.1	864.1	8.3502	131.6101	15.7210	37.0109
204.0	1.69032	870.6	2797.6	862.9	8.5195	130.9654	15.7547	36.7845
205.0	1.72545	875.1	2798.2	861.7	8.6917	130.3280	15.7885	36.5580
206.0	1.76115	879.6	2798.7	860.4	8.8667	129.6979	15.8224	36.3312
207.0	1.79742	884.2	2799.1	859.2	9.0446	129.0749	15.8564	36.1043
208.0	1.83428	888.7	2799.7	857.9	9.2254	128.4590	15.8905	35.8772
209.0	1.87171	893.2	2800.1	856.6	9.4092	127.8499	15.9247	35.6499
210.0	1.90972	897.8	2800.6	855.4	9.5959	127.2477	15.9590	35.4225
211.0	1.94835	902.4	2801.1	854.1	9.7858	126.6522	15.9934	35.1949
212.0	1.98756	906.9	2801.6	852.8	9.9787	126.0634	16.0279	34.9672
213.0	2.02740	911.5	2802.1	851.5	10.1747	125.4810	16.0626	34.7392
214.0	2.06785	916.1	2802.4	850.2	10.3740	124.9050	16.0974	34.5112
215.0	2.10892	920.6	2802.6	848.9	10.5764	124.3353	16.1323	34.2829
216.0	2.15062	925.2	2803.1	847.6	10.7821	123.7719	16.1673	34.0546
217.0	2.19296	929.8	2803.5	846.3	10.9911	123.2145	16.2025	33.8260

TEMP(C)	P(MPaa)	Hf	Hv	ρf	ρv	μf(E-6)	μv(E-6)	τ(E-3)
218.0	2.23592	934.4	2803.7	845.0	11.2034	122.6632	16.2378	33.5974
219.0	2.27955	939.0	2804.2	843.6	11.4192	122.1178	16.2732	33.3685
220.0	2.32382	943.6	2804.4	842.3	11.6383	121.5782	16.3088	33.1396
221.0	2.36875	948.3	2804.7	841.0	11.8609	121.0444	16.3445	32.9105
222.0	2.41436	952.9	2805.0	839.6	12.0871	120.5162	16.3803	32.6813
223.0	2.46063	957.5	2805.1	838.2	12.3168	119.9936	16.4163	32.4519
224.0	2.50760	962.2	2805.4	836.9	12.5502	119.4766	16.4525	32.2224
225.0	2.55522	966.8	2805.6	835.5	12.7872	118.9649	16.4888	31.9928
226.0	2.60356	971.5	2805.6	834.1	13.0279	118.4586	16.5252	31.7630
227.0	2.65260	976.1	2805.8	832.7	13.2725	117.9575	16.5619	31.5331
228.0	2.70233	980.8	2806.1	831.3	13.5207	117.4616	16.5987	31.3031
229.0	2.75278	985.5	2806.3	829.9	13.7729	116.9709	16.6356	31.0730
230.0	2.80395	990.1	2806.3	828.5	14.0290	116.4851	16.6727	30.8428
231.0	2.85585	994.8	2806.3	827.1	14.2891	116.0043	16.7100	30.6125
232.0	2.90846	999.5	2806.4	825.7	14.5531	115.5285	16.7475	30.3820
233.0	2.96185	1004.2	2806.6	824.3	14.8213	115.0574	16.7851	30.1515
234.0	3.01595	1009.0	2806.5	822.8	15.0935	114.5911	16.8230	29.9208
235.0	3.07082	1013.7	2806.5	821.4	15.3700	114.1294	16.8610	29.6901
236.0	3.12645	1018.4	2806.6	820.0	15.6507	113.6724	16.8992	29.4592
237.0	3.18283	1023.1	2806.4	818.5	15.9356	113.2200	16.9375	29.2282
238.0	3.23999	1027.9	2806.5	817.0	16.2249	112.7720	16.9761	28.9972
239.0	3.29793	1032.6	2806.4	815.6	16.5186	112.3284	17.0149	28.7660
240.0	3.35665	1037.4	2806.3	814.1	16.8168	111.8893	17.0539	28.5348
241.0	3.41617	1042.2	2806.2	812.6	17.1194	111.4544	17.0930	28.3035
242.0	3.47649	1047.0	2806.0	811.1	17.4267	111.0237	17.1324	28.0721
243.0	3.53762	1051.7	2805.8	809.6	17.7385	110.5973	17.1720	27.8406
244.0	3.59955	1056.5	2805.8	808.1	18.0550	110.1750	17.2118	27.6090
245.0	3.66231	1061.3	2805.5	806.6	18.3764	109.7567	17.2518	27.3774
246.0	3.72590	1066.2	2805.1	805.1	18.7025	109.3425	17.2920	27.1457
247.0	3.79031	1071.0	2804.7	803.6	19.0335	108.9322	17.3325	26.9139
248.0	3.85558	1075.8	2804.7	802.1	19.3694	108.5258	17.3731	26.6820
249.0	3.92167	1080.7	2804.5	800.5	19.7103	108.1233	17.4140	26.4501
250.0	3.98864	1085.5	2804.0	799.0	20.0563	107.7246	17.4551	26.2181
251.0	4.05647	1090.4	2803.6	797.5	20.4074	107.3297	17.4965	25.9861
252.0	4.12515	1095.3	2803.3	795.9	20.7637	106.9384	17.5381	25.7540
253.0	4.19471	1100.1	2803.1	794.4	21.1252	106.5508	17.5799	25.5218
254.0	4.26516	1105.0	2802.6	792.8	21.4920	106.1669	17.6219	25.2896
255.0	4.33650	1109.9	2802.1	791.2	21.8643	105.7864	17.6642	25.0574
256.0	4.40873	1114.9	2801.6	789.6	22.2420	105.4095	17.7068	24.8251
257.0	4.48187	1119.8	2801.3	788.1	22.6253	105.0361	17.7496	24.5927
[illegible].0	4.55591	1124.7	2800.7	786.5	23.0141	104.6661	17.7926	24.3603
[illegible]9.0	4.63087	1129.7	2800.1	784.9	23.4086	104.2994	17.8359	24.1279
[illegible]0.0	4.70674	1134.6	2799.6	783.3	23.8087	103.9361	17.8795	23.8954
[illegible]1.0	4.78357	1139.6	2799.1	781.7	24.2148	103.5761	17.9233	23.6629
[illegible]2.0	4.86132	1144.6	2798.3	780.1	24.6268	103.2193	17.9674	23.4304
263.0	4.94000	1149.6	2797.6	778.5	25.0445	102.8657	18.0118	23.1978
264.0	5.01966	1154.6	2797.0	776.8	25.4685	102.5153	18.0564	22.9652
265.0	5.10025	1159.6	2796.4	775.2	25.8984	102.1681	18.1013	22.7326
266.0	5.18182	1164.6	2795.5	773.6	26.3345	101.8239	18.1465	22.5000
267.0	5.26438	1169.6	2795.0	771.9	26.7771	101.4827	18.1919	22.2673
268.0	5.34790	1174.7	2793.9	770.3	27.2257	101.1446	18.2376	22.0346
269.0	5.43241	1179.8	2793.2	768.6	27.6809	100.8094	18.2837	21.8019

TEMP(C)	P(MPaa)	Hf	Hv	ρf	ρv	μf(E-6)	μv(E-6)	τ(E-3)
270.0	5.51789	1184.8	2792.4	767.0	28.1424	100.4772	18.3300	21.5692
271.0	5.60441	1189.9	2791.5	765.3	28.6107	100.1479	18.3766	21.3365
272.0	5.69190	1195.0	2790.7	763.7	29.0854	99.8214	18.4234	21.1038
273.0	5.78045	1200.1	2789.9	762.0	29.5671	99.4978	18.4706	20.8711
274.0	5.86998	1205.3	2788.7	760.3	30.0554	99.1769	18.5181	20.6384
275.0	5.96057	1210.4	2787.8	758.6	30.5507	98.8589	18.5659	20.4057
276.0	6.05216	1215.6	2786.8	757.0	31.0528	98.5435	18.6140	20.1730
277.0	6.14482	1220.7	2785.9	755.3	31.5622	98.2308	18.6624	19.9403
278.0	6.23852	1225.9	2784.6	753.6	32.0786	97.9208	18.7111	19.7076
279.0	6.33331	1231.1	2783.6	751.9	32.6025	97.6134	18.7601	19.4749
280.0	6.42911	1236.3	2782.6	750.2	33.1333	97.3087	18.8095	19.2422
281.0	6.52601	1241.5	2781.5	748.5	33.6717	97.0064	18.8591	19.0096
282.0	6.62397	1246.8	2779.9	746.7	34.2174	96.7067	18.9091	18.7769
283.0	6.72303	1252.0	2778.7	745.0	34.7709	96.4095	18.9594	18.5443
284.0	6.82321	1257.3	2777.6	743.3	35.3323	96.1148	19.0101	18.3118
285.0	6.92442	1262.6	2776.2	741.6	35.9009	95.8226	19.0611	18.0792
286.0	7.02679	1267.9	2774.8	739.8	36.4777	95.5327	19.1124	17.8467
287.0	7.13025	1273.2	2773.5	738.1	37.0624	95.2452	19.1640	17.6142
288.0	7.23484	1278.5	2772.0	736.4	37.6551	94.9601	19.2160	17.3817
289.0	7.34057	1283.8	2770.8	734.6	38.2561	94.6774	19.2684	17.1493
290.0	7.44739	1289.2	2769.2	732.9	38.8650	94.3969	19.3210	16.9169
291.0	7.55542	1294.6	2767.4	731.1	39.4826	94.1187	19.3741	16.6846
292.0	7.66454	1299.9	2766.0	729.4	40.1084	93.8427	19.4275	16.4523
293.0	7.77483	1305.3	2764.6	727.6	40.7427	93.5690	19.4812	16.2201
294.0	7.88627	1310.8	2762.8	725.8	41.3856	93.2975	19.5353	15.9879
295.0	7.99894	1316.2	2761.1	724.1	42.0376	93.0281	19.5898	15.7558
296.0	8.11272	1321.7	2759.5	722.3	42.6980	92.7610	19.6446	15.5237
297.0	8.22768	1327.1	2757.9	720.5	43.3673	92.4959	19.6998	15.2917
298.0	8.34388	1332.6	2755.7	718.7	44.0460	92.2329	19.7553	15.0597
299.0	8.46126	1338.1	2754.0	716.9	44.7336	91.9720	19.8113	14.8278
300.0	8.57983	1343.6	2752.0	715.2	45.4304	91.7132	19.8676	14.5960
301.0	8.69960	1349.2	2750.0	713.4	46.1365	91.4564	19.9243	14.3642
302.0	8.82062	1354.7	2747.8	711.6	46.8522	91.2016	19.9814	14.1326
303.0	8.94284	1360.3	2745.8	709.8	47.5773	90.9488	20.0388	13.9010
304.0	9.06633	1365.9	2744.1	708.0	48.3123	90.6979	20.0967	13.6694
305.0	9.19097	1371.5	2741.8	706.2	49.0565	90.4490	20.1549	13.4380
306.0	9.31694	1377.1	2739.5	704.3	49.8112	90.2020	20.2136	13.2066
307.0	9.44414	1382.8	2737.3	702.5	50.5756	89.9570	20.2726	12.9753
308.0	9.57261	1388.4	2735.1	700.7	51.3503	89.7138	20.3321	12.7441
309.0	9.70232	1394.1	2732.6	698.9	52.1350	89.4724	20.3919	12.5130
310.0	9.83331	1399.8	2730.3	697.1	52.9300	89.2329	20.4521	12.2820
311.0	9.96561	1405.6	2727.7	695.3	53.7357	88.9952	20.5128	12.0511
312.0	10.09915	1411.3	2725.6	693.4	54.5516	88.7593	20.5739	11.8203
313.0	10.23406	1417.1	2723.0	691.6	55.3787	88.5252	20.6354	11.5895
314.0	10.37021	1422.8	2720.2	689.8	56.2163	88.2928	20.6973	11.3589
315.0	10.50768	1428.6	2717.6	687.9	57.0647	88.0622	20.7596	11.1284
316.0	10.64647	1434.5	2714.8	686.1	57.9243	87.8333	20.8223	10.8980
317.0	10.78659	1440.3	2712.2	684.3	58.7950	87.6061	20.8855	10.6677
318.0	10.92796	1446.2	2709.1	682.4	59.6765	87.3807	20.9491	10.4375
319.0	11.07074	1452.1	2706.3	680.6	60.5699	87.1568	21.0132	10.2075
320.0	11.21493	1458.0	2703.1	678.7	61.4753	86.9346	21.0777	9.9775
321.0	11.36039	1463.9	2700.3	676.9	62.3917	86.7141	21.1426	9.7477

TEMP(C)	P(MPaa)	Hf	Hv	ρf	ρv	μf(E-6)	μv(E-6)	τ(E-3)
322.0	11.50719	1469.8	2697.3	675.0	63.3199	86.4951	21.2079	9.5180
323.0	11.65534	1475.8	2694.2	673.2	64.2598	86.2778	21.2737	9.2885
324.0	11.80492	1481.8	2690.7	671.3	65.2121	86.0621	21.3400	9.0590
325.0	11.95585	1487.8	2687.6	669.5	66.1765	85.8479	21.4067	8.8297
326.0	12.10815	1493.8	2684.2	667.6	67.1530	85.6352	21.4739	8.6005
327.0	12.26189	1499.9	2680.5	665.7	68.1423	85.4241	21.5415	8.3715
328.0	12.41691	1506.0	2677.3	663.9	69.1432	85.2145	21.6095	8.1426
329.0	12.57348	1512.1	2673.4	662.0	70.1579	85.0064	21.6781	7.9138
330.0	12.73133	1518.2	2669.7	660.1	71.1844	84.7998	21.7471	7.6852

Hf,Hv in kJ/kg; ρf,ρv in kg/m^3 ; μf,μv in kg/ms; τ in N/m